CORRELATIONS TO PREDICT AND SMOOTH PORE VOLUME COMPRESSIBILITY FROM LABORATORY TEST MEASUREMENTS

by
Mohammad A. J. Ali

ARTHUR LAKES LIBRARY
COLORADO SCHOOL OF MINES
GOLDEN, CO 80401

ProQuest Number: 10794323

All rights reserved

INFORMATION TO ALL USERS
The quality of this reproduction is dependent upon the quality of the copy submitted.

In the unlikely event that the author did not send a complete manuscript
and there are missing pages, these will be noted. Also, if material had to be removed,
a note will indicate the deletion.

ProQuest 10794323

Published by ProQuest LLC (2018). Copyright of the Dissertation is held by the Author.

All rights reserved.
This work is protected against unauthorized copying under Title 17, United States Code
Microform Edition © ProQuest LLC.

ProQuest LLC.
789 East Eisenhower Parkway
P.O. Box 1346
Ann Arbor, MI 48106 – 1346

A thesis submitted to the Faculty and Board of Trustees of the Colorado School of Mines in partial fulfillment of the requirements for the degree of Master of Science (Petroleum Engineering).

Golden, Colorado
Date November 14, 1997

Singed: Mohammad A. J. Ali
Mohammad A. J. Ali

Approved: Ramona M Graves
Dr. Ramona M. Graves
Thesis Advisor

Golden, Colorado
Date November 14, 1997

Craig W. Van Kirk
Dr. Craig W. Van Kirk
Head, Department of
Petroleum Engineering

ABSTRACT

Pore volume compressibility is used in many engineering calculations such as estimating the volume of oil initially in a reservoir, predicting the amount of oil recovery, and calculating subsidence and compaction. This research focused on the pore compressibility for consolidated and unconsolidated sand using uniaxial test data (varying the pore pressure and/or axial stress) and triaxial test data (varying the vertical and lateral stress independently).

The objective of this research was to determine if a correlation exists between pore volume compressibility and other rock parameters so that pore compressibility can be predicted with minimum laboratory measurements. In addition, methods to smooth inconsistency in compressibility data were investigated. Investigated parameters include permeability, porosity, pore pressure, overburden pressure and amount of consolidation.

Four empirical methods were studied in the analysis of pore compressibility and compared with Jones' (1988) method for fifteen consolidated samples and thirteen unconsolidated samples. Two methods are used to predict pore compressibility, one of which requires an initial value of pore compressibility and three porosity values with stress. The other method requires a good correlation between porosity and stress with as few as two porosity values. Two methods are used to smooth inconsistency in compressibility measurements. One method correlates porosity and stress with the cumulative compressibility, and one correlates porosity-permeability and stress with the cumulative compressibility.

Compressibility predictions of unconsolidated samples are more sensitive at high values of stress and failed to work for some of the methods. The predictions for the highly consolidated samples had a better agreement with the actual measured data. Smoothing compressibility data for all samples was good; however, some methods showed better agreement than others. When porosity and stress were used to predict pore compressibility, the results were in good agreement for all samples.

It is recommended to carry on the investigation of another method that involves the prediction of compressibility from porosity, permeability, stress, and flow rate. Due to the lack of data, this method was not included as a part of this thesis. Data available from only three consolidated samples proved such a correlation might exist.

In addition, a correlation between Poisson's ratio and stress was developed for fifteen unconsolidated samples. This correlation can be used to convert lab data to reservoir conditions properly. It is recommended to further investigate if such correlation exists for consolidated sand.

TABLE OF CONTENTS

LIST OF FIGURES

Figure No.	Title	Page
3-5b	Illustration of Jones' Method - Pore Compressibility vs. Net Stress....	35
4-1a	Using different methods to predict and smooth compressibility - Study No.1 - Sample 4..	39
4-1b	Porosity-Stress relationship for sample - Study No.1......................	40
4-1c	Pore void ratio vs. cumulative pore compressibility - Study No.1........	43
4-1d	Prediction of Jm from two points vs. stress - Study No.1................	44
4-1e	Jones' Method of predicting pore volume from two points vs. stress - Study No. 1..	45
4-2	The effect of varying pore volume on pore compressibility...............	50
4-2a	Using different methods to predict and smooth compressibility - Study No.1 - Sample 14920.5	51
4-2b	Porosity - Stress relationship for sample - Study No.2.................	53
4-2c	Pore void ratio vs. cumulative pore compressibility - Study No.2	55
4-2d	Prediction of Jm from two points vs. stress - Study No.2	57
4-2e	Jones' Method of predicting pore volume from two points vs. stress - Study No. 1..	58
4-3a	Using different methods to predict and smooth compressibility - Study No. 3 - Sample CL-5	62
4-3b	Porosity - Stress relationship for sample - Study No.3	63
4-3c	Pore void ratio vs. cumulative pore compressibility - Study No.3	65
4-3d	Jones' Method of predicting pore volume from two points vs. stress - Study No. 1..	66

LIST OF TABLES

AKNOWLEDGEMENTS

I would like to thank my thesis advisor, Dr. Ramona M. Graves, and the members of this thesis committee, Dr. Richard L. Christiensen and Dr. Alfred W. Eustess, for their support throughout this study. I would like to acknowledge the help of Dr. Graves. She gave me the motivation to research this thesis; her knowledge and inspiration are continuous.

Gratitude is extended to the industry support of supplementary data from Marathon Oil Company, Littleton, Colorado, especially Dr. R. D. Barree, and Mr. R.W. Schaller for his technical support. I also thank Core Laboratory, Carrolton , Texas, for support in additional data gathering, especially Dr. R. Oskui, Mr. J. Ross, Mr. R. Harting, and Dr. D. Daneshjou. I would like to thank Mr. Paul Brauer at TEMCO, Inc. and Mr. Robert Bereskin at TerraTek for their literature support in the description and analysis of pore volume compressibility apparatuses. My greatest appreciation to my employer, Kuwait Institute for Scientific Research, for its scholarship and financial support throughout my study, and the Core Analysis Program for its contribution in core preparation and laboratory analysis.

I would also like to thank my family, especially my mother and aunt for their continuous support, and my friends who were with me during my hospitalization this year.

Finally, I must thank god, Allah, for the help and strength he gave me to complete this work.

CHAPTER 1.
INTRODUCTION

"Pore volume compressibility is the measure of the change in pore space which occurs when the rock is stressed and is related to both the physical properties and spatial arrangements of the constituent minerals" (Anderson, 1985). The production of hydrocarbons from a reservoir results in a reduction of pore pressure causing the rock to compact.

Compressibility can be measured in the laboratory under hydrostatic, uniaxial or triaxial test conditions, depending on the data requirements. A hydrostatic test, where three principal stresses are all equal, is rapid, but the results could be twice as much as under reservoir stress conditions. In uniaxial and triaxial loading, the vertical and lateral stresses are different. The uniaxial test measures the axial deformation while preventing the lateral deformation of the sample. The triaxial test measures the axial and lateral deformations of the sample. Both tests, uniaxial and triaxial, are more representative of reservoir conditions than the hydrostatic tests but they are costly and time consuming.

Porosity, permeability, compressibility, and many other rock properties can be obtained from laboratory core analysis. Both conventional and special core analyses furnish valuable information to the subsurface geologist and engineer. Prior to any request for core analysis, it is necessary to determine the objectives of the study. Once the intervals of interest are determined, core properties must be measured and interpreted.

Correlations between core data and log data will maximize the evaluation and interpretation of the study.

Laboratory measurements of rock properties are not always smooth and consistent. Measuring pore compressibility can take several hours or days. In addition, experiments are costly. Predicting pore compressibility data from minimum laboratory measurements, finding ways to avoid laboratory measurements, and smoothing laboratory data systematically are the goals of this thesis.

This thesis is a study of fifteen consolidated samples tested under uniaxial test conditions and thirteen unconsolidated samples tested under triaxial conditions. Five consolidated samples with high clay content were taken from 8,000-12,000 feet. In the laboratory, axial (ram) stress was presented by 5,800 psi. Ten consolidated samples with lower clay content and friable samples were taken from two reservoirs at 2,000-8,000 feet. In the laboratory, axial (ram) stress was presented by 10,000 psi. Two types of triaxial tests were used for the unconsolidated sand samples. Pore pressure and confining stress were varied while axial (ram) stress was kept constant, or pore pressure was kept constant while increasing axial stress. Samples were taken from 14,000-17,300 foot intervals and tested with reservoir pressure of 11,400 psi.

Four methods were used for the analysis of the study and compared with Jones' method. Two methods are used to predict pore compressibility: Method 1 requires initial compressibility data with a good correlation between stress and porosity, and Method 2 requires good correlation between porosity and stress. Since some samples experienced inconsistency in laboratory measurements, there was a need to smooth compressibility data systematically. Two methods were developed to smooth pore volume compressibility with correlations between porosity, permeability, stress, and three data points of compressibility. Method 3 relates pore void ratio to the cumulative pore compressibility with a straight line equation. With as few as three porosity and compressibility points at different stresses a straight line equation can be generated to smooth and predict compressibility data at higher stress. Method 4 related porosity and permeability to pore compressibility with a power law equation. The power law equation can smooth compressibility and predict values at higher stress. Jones (1985) has developed an equation to predict pore compressibility from two-pore volume data at different stress. Jones' method was used for all samples, consolidated and unconsolidated, to compare its results with the newly developed methods. Illustrations for all methods used to predict and smooth compressibility data are explained in Chapter 3. Discussion of results for the five methods, along with Jones' method, are included to show the validity of each method. Sample calculations for all methods are also included in Appendix D.

In addition, a correlation was found between Poisson's ratio and applied net radial and axial stress for fifteen unconsolidated sand samples. This correlation is useful when converting laboratory data to reservoir conditions. The correlation, however, was not included as a part of this thesis due to the lack of data, but a detailed explanation and examples are included in Chapter 7.

A section on core analysis is presented because improper preparation and handling of core samples may have an effect on laboratory measurements. Understanding the effects of stress on rock properties is included as another section to show how different stress conditions can alter the results of pore volume compressibility calculations. In the literature, there are thoughts, interpretations and analyses of measuring pore compressibility, and how these analyses are used in the laboratories.

Tables and figures included within the text usually illustrate one sample. Tables and figures for all samples are then included in the appendices.

CHAPTER 2.
LITERATURE REVIEW

2.0 Introduction

"Pore volume compressibility is the measure of the change in pore space which occurs when the rock is stressed and is related to both the physical properties and spatial arrangements of the constituent minerals" (Anderson, 1985). Pore volume compressibility is thus used by many engineers to estimate the volume of oil initially in a reservoir and to predict the amount of oil recovery.

The following sections are a review of core analysis and preparation, laboratory techniques of measuring pore compressibility, review of pore volume compressibility, the effect of stress on rock properties and finally, the importance of pore compressibility in reservoir calculations.

2.1 Core Analysis and Preparation

Core analysis is a laboratory study to measure and interpret the petrophysical properties of the reservoir rock. Basic data from conventional core analysis yields residual fluid saturation, formation lithology, porosity, and permeability.

A good understanding of rock properties is critical in planning and implementing a successful waterflood, casing design, exploration program, well completion, workover operation and reservoir evaluation. Since it is unusual to core every well in a field and since full core recovery is often not achieved in a given well, there is a need to estimate some parameters in uncored intervals.

Special core analysis is an extension of conventional core analysis and yields more detailed rock property data. It furnishes the knowledge of the initial distribution and quantity of hydrocarbons, permeability to gas, relative permeability, rock wettability, and fluid properties. In addition, electrical and acoustical properties of the rock can be determined to yield data that enhances the down-hole log interpretation. Capillary pressure, mechanical properties (including compressibility), and rock resistivity can be measured.

Core analysis has evolved into different types depending on the size of the selected core for analysis, that is, *conventional* (plug) analysis, *whole core* (full-diameter) analysis, and *sidewall* core analysis. In this thesis, the terms "core" and "plug" are used interchangeably. Usually plug samples are 1 to 1.5 inches in diameter and 1.5 to 3 inches in length.

In order to achieve representative results, core samples must undergo a series of preparation procedures. This of course is a very critical and time-consuming job. It could takes up to five weeks to allocate orientation and depth, slab, plug, clean, dry, and preserve the core. In addition, core samples required for testing should be representative of the interval of interest (Keelan, 1987).

Measurement of permeability, porosity and fluid saturation requires all residual fluids to be removed and cores to be cleaned and dried. Solvents, including toluene, benzene, and some others, are used to remove oil and water from core samples; methanol is used to remove salt, and silver nitrate is used to detect the presence of salt particles. Solvents, however, must not react with the rock. Flushing with solvent at low temperature and pressure may be the best way to treat the sample to prevent further damages. Care must be taken when drying cores and removing cleaning solvents to prevent mineral reaction or microbial formation.

2.2 Laboratory Techniques to Measure Compressibility

Pore compressibility can be measured statically in the laboratory. Static tests measure the volumetric deformation caused by applied stress. There are three basic laboratory techniques to statically measure pore compressibility. All three tests require saturated samples with a single phase fluid, commonly brine. Assume the change in pore volume is equal to the change of expelled fluid from the rock sample. Sampath (1982), however, developed a new, improved, inexpensive and less time-consuming method to accurately measure pore volume compressibility for dry samples in low permeability sandstone samples. The three static laboratory techniques are hydrostatic, unaxial and triaxial.

2.2.1 Hydrostatic Test

The hydrostatic test has been widely used to measure pore volume compressibility of consolidated rock samples. In a hydrostatic test, the stresses are equal in all directions.

The sample is enclosed by a thin jacket (elastomer or metal foil) that fits the core sample tightly, so that no shape problems exists. The measurement is simple and rapid but not representative of reservoir conditions.

2.2.2 Uniaxial Test

In the uniaxial test, the sample is loaded in the vertical direction while a rigid cylinder wall prevents the lateral deformation of the plug sample. This method is more representative to reservoir conditions than the hydrostatic test because it considers the axial deformation to be more dominant. The corresponding change in length represents the total volumetric change. The accuracy of the test is influenced by two factors: (a) the upper and lower surface must be flat and perpendicular to the cylindrical surface, and (b) the sample must fit precisely into the uniaxial cell, otherwise the requirement of zero lateral deformation will not be met. For clay and friable sand, this method produces valid data, but for consolidated rock it is very hard to meet the test criteria, and thus, interpretation of the results in terms of formation compaction becomes uncertain.

2.2.3 Triaxial Test

The triaxial test is used to determine the strength of porous media under various conditions of stress (Bishop, 1962). The vertical and lateral stresses are independently varied. This test is closer to reservoir conditions than hydrostatic and uniaxial tests. The basic assumption is that the two principal horizontal stresses are equal. The sample is enclosed by a flexible sleeve to allow lateral deformation. The accuracy of the test depends on the shape of the sample like the conditions for the unaxial test.

2.2.4 Review of Pore Volume Compressibility Measurements

Since the establishment of the Adams and Williamson (1923) equation of compressibility, several engineers have tried to measure compressibility of different rock samples: sandstone, limestone, consolidated, unconsolidated, and friable; yet very few correlations have been found. In fact, no solid evidence has been found to correlate porosity or permeability to pore volume compressibility.

Van Der Knaap (1958) showed that the three dimensional representation of the volume of a nonlinear porous system is a cylindrical ruled surface, the generating lines of which have a slope according to the solid rock compressibility. It follows that the bulk and pore volume compressibilities depend on the difference between pore fluid and external pressure. He concluded that the average pore volume compressibility falls in the range to the compressibility of the water and that of undersaturated crude oil. "In general, pore compressibility is found to be higher the lower the porosity."

In a reservoir, stress is usually applied from above by the overburden and lateral deformation being prevented by surrounding rocks; thus, only vertical compaction occurs. This is a lesser change than the hydrostatic stress compaction. Compressibility measured in a laboratory under hydrostatic stress can be almost double that occurring under the uniaxial strain conditions believed to exist in the reservoir. Teeuw (1970) presented a simple and inexpensive laboratory testing procedure for simulating realistic reservoir compaction behavior for both cemented and friable rocks. Based on previous work by Geerstma (1957) and others, he developed a new triaxial cell-type compaction measurement for friable rock. Van Der Knaap (1958) has shown that the deformation in reservoir rock is mainly vertical and that the uniaxial compaction is related to the hydrostatic bulk deformation by the formula:

$$\mathrm{Cm} = \frac{1}{3}\frac{(1+\nu)}{(1-\nu)}(1-\beta)c_b \tag{2-1}$$

where: ν = Poisson's ratio

Cm = uniaxial compaction coefficient

β = Cma/c_b , the ratio of the rock matrix to rock bulk compressibility

Anderson (1985) also developed a practical procedure to convert the hydrostatic-stress, pore volume reduction test data into the uniaxial strain compressibility data to resemble reservoir conditions. Static Poisson's ratio is determined by shortening the sample in response to an applied axial load and allowing it to bulge or deflect laterally into the constant pressure-confining media. The ratio is calculated by dividing the fractional change in transverse diameter of the sample by its fractional longitudinal shortening.

2.2.5 Two-Point Pore Volume vs. Net Confining Stress (Jones' Method)

Jones (1985) established a study to predict pore volume compressibility from two points using only a straight line transformation. The purpose of his study was to modify the available techniques to better estimate the decline of permeability and pore volume from basic routine core analysis.

Normalized permeability vs. net stress generates an exponential decline correlation that best fits the coefficients (a_k, k_o, C, and σ *). Equation 2-2 may be rewritten in an equivalent form of Equation 2-3.

$$(k) = ki\ \exp(a_k[\exp(-\sigma/\sigma^*)-1]/(1+C\sigma)) \tag{2-2}$$

$$\ln[k(1+C\sigma)] = \ln(ki) - a_k[1-\exp(-\sigma/\sigma^*)] \tag{2-3}$$

where ki = initial permeability

a_k = point of best fit

σ = net stress

σ^* = empirical value = 3000 psi

C = decay constant arbitrarily set to 3E-6

A semilogarithmic plot of Equation 2-3 results in a straight line with an intercept of k_o and a slope of ($-a_k$). Pore volume can be estimated with the above technique using the following formula:

$$(Vp) = Vpi\ \exp(a_v[\exp(-\sigma/\sigma^*)-1]/(1+C\sigma)) \tag{2-4}$$

$$\ln[Vp(1+C\sigma)] = \ln(Vpi) - a_v[1-\exp(-\sigma/\sigma^*)] \tag{2-5}$$

Permeability and pore volume data from a number of core plugs were best fit by the use of Equation 2-4. For a majority of the cases, the decay constant (σ^*) had values fairly closely clustered about 3,000 psi and the coefficient C varied from 0 to $3*10^{-6}$ psi^{-1}. If these coefficients could be fixed prior to the calculations, then the linear form of the equations suggests that the entire permeability stress and pore volume stress curve could be estimated from measurements at only two stressed points. Pore volume compressibility can be describe as follows:

$$c_f = (a_v^* \exp(-\sigma/\sigma^*))/\sigma^* + \frac{C}{1+C\sigma} \tag{2-6}$$

Jones pointed out that "when the derivative of experimental data is required, these data generally need to be about one order of magnitude better quality than when the derivative is not required."

Nelson (1980) suggested that when a fluid-confining pressure is applied to the outside of a jacketed rock sample in a manner similar to the hydrostatic pressure test, the confining stress remains constant throughout the test while the piston load is gradually increased until either the strength of the material or the piston travel or the load capabilities of the apparatus are exceeded. Triaxial test is most often used to simulate both rock behavior during deformation and rock properties at depth.

2.3 Effect of Stress on Rock Properties

Normally, reservoir rocks are subjected to two types of stresses, internal stress exerted by fluids contained in the pores and external stress exerted by the overlying rocks. When pore pressure depletes from a reservoir during production, the effective external stress increases. The increase of the external stress and the reduction of internal stress causes a structural change in the reservoir volume. For reservoirs that are producing above the bubble point (no free gas existing), the drive mechanism is the expansion of water and oil and the reduction of pore space resulting from pressure decline. Neglecting formation compressibility results in the overestimated values of initial oil-in-place.

Adams and Williamson (1923) measured the decrease in volumes of several sand samples at elevated pressure up to 12,000 psi. From the measured volumes, compressibility data was calculated directly, and then approximate values of the rigidity of the rocks were computed. Adams and Williamson defined compressibility as the fractional change in pore volume per unit change in pressure. Many engineers and researchers have recorded the change in compressibility of reservoir rocks as a function of fluid pressure decline.

$$c = \frac{-1}{V_i}\frac{dV}{dP} \tag{2-7}$$

where V_i = initial volume

dp = pressure change

c = compressibility

Van Tuyl (1926) described several experiments in which various types of unconsolidated sedimentary materials were arranged in a steel cylinder and pressured up to 3,375 psi. He concluded that the pressure imposed by the overburden or diastrophism may be an important factor in causing the migration of oil into reservoir rocks.

A study carried out by Hundall (1934) conjectured that as oil and gas are withdrawn from a reservoir, the potential production or capacity of the wells is reduced because the accompanying reduction in hydrostatic or reservoir pressure causes compaction of the reservoir rock, which in turn reduces the porosity and permeability of the rock. In other words, Hundall considered that the voids in the rocks become smaller when the internal or hydrostatic pressure resisting the downward pressure exerted by the weight of the overburden is decreased.

Botset and Reed (1935) measured the compressibility of unconsolidated sand at pressure up to 3,000 psi. The result of their experiments indicated a decrease of 0.70 in the percentage of porosity of the unconsolidated sand. They concluded that "since the sand used in the experiment was unconsolidated, the compressibility of even a slightly consolidated sand should be much less, and it is apparent that compressibility of sand is, in general, a minor factor in oil production."

Since 1918, some evidence of subsidence of the ground surface over a few production oil fields has been observed (Carpenter and Spencer, 1940). This observation led the engineers and geologist to believe that the weight of the earth crust overlying an oil-bearing reservoir causes a compression and compaction of the reservoir sands and rocks as oil and gas are withdrawn from them. Subsidence of the Goose Creek oil field, Harris County, Texas, was observed to be about three feet and the effected area was about 2 ½ miles long and 1 ½ miles wide. This incident led scientists and engineers to seriously study the compaction of the reservoir formation and to study how and when compaction occurs.

Several engineers tried to find if a correlation exists between porosity and stress. Hall (1953) pointed out the importance of including pore volume compressibility of the reservoir rock in certain reservoir engineering calculations. He showed that in calculating the hydrocarbon volume of an undersaturated reservoir from the production per unit change in reservoir pressure, the neglect of pore compressibility could, in the extreme case of low porosity rock, lead to results in error by a factor of two. He stated that, "as reservoir pressure declines, pore compressibility of any reservoir rock is a result of two separate factors: expansion of the individual rock grains and the additional formation compaction." Both of these factors tend to decrease porosity values.

Most limestone and sandstone formations have pore volume compressibilities in the order of 10^{-6} to $25*10^{-6}$ psi^{-1}. Hawkins (1955) and Hobson (1956) showed that both rock and interstitial water compressibilities must be included to achieve satisfactory calculations.

Other engineers tried to develop correlations between pore volume and stress conditions and directions. Geertsma (1957) was the first engineer to develop a set of practical pressure-volume relationships explaining pore and rock bulk volume variation in petroleum reservoirs. He derived the following expression:

$$\frac{dV_p}{V_p} = c_f * dPp + \frac{1}{\phi}(c_b - c_f)d(\sigma - Pp) \tag{2-8}$$

where: Pp = pore pressure

c_f = pore compressibility

c_b = bulk compressibility

V_p = pore volume

σ = net stress (Axial Stress - Confining stress) - (Axial Stress - Pore Pressure)

ϕ = porosity

Geertsma explained that the decline of fluid pressure in connection with the withdrawal of fluid from an underground reservoir gives rise to a change in volume of reservoir rock and fluids. The variation of reservoir rock is the result of a decrease of both the pore volume and the total volume of the fluid-filled formation. Geertsma concluded that in a porous structure three kinds of compressibility must be distinguished:

(1) Rock Matrix Compressibility: the fractional changes in grain volume of the solid rock material (without pores) per unit change in uniform pressure.

(2) Rock Bulk Compressibility: the fractional change in total or bulk volume of the porous rock per unit change in uniform pressure.

(3) Pore Volume Compressibility: the fractional changes in pore volume per unit changes in uniform pressure.

In addition, he also derived another expression showing that in petroleum reservoirs, only the vertical component of hydrostatic stress is constant and that the stress component in the horizontal plan is characterized by the boundary condition. For this boundary condition, he developed the following approximation for sandstones:

$$C_f = \frac{2}{V_p} * \frac{dV_p}{dPp} \tag{2-9}$$

This means compressibility of sandstones obtained by using triaxial apparatus is about twice as high as those obtained in a uniaxial test. Fatt (1958) reported results of experimental tests on a limited number of consolidated rock samples and sand-packs. Plots of pore volume compressibilities of poorly sorted unconsolidated sand as a function of net overburden pressure are shown in Figure 2-1a. These compressibilities are higher than well-sorted sandstones grains (Figure 2-1b). Fatt's results show the absence of correlation between compressibility and porosity data.

Dobrynin (1962) carried out experiments to investigate the effect of overburden stress on permeability, porosity, and pore compressibility of sandstone. He concluded that pore compressibility was the major factor that affects the change in these parameters. Chierici (1967) and Dobrynin concluded the following results from experimental tests:

(1) When dealing with undersaturated reservoirs, it is necessary to include the effect of shale on pore volume compressibility.
(2) Formation resistivity factor and permeability of clean sandstone are affected by stress. The lower the porosity, the higher the sensitivitiy to stress.

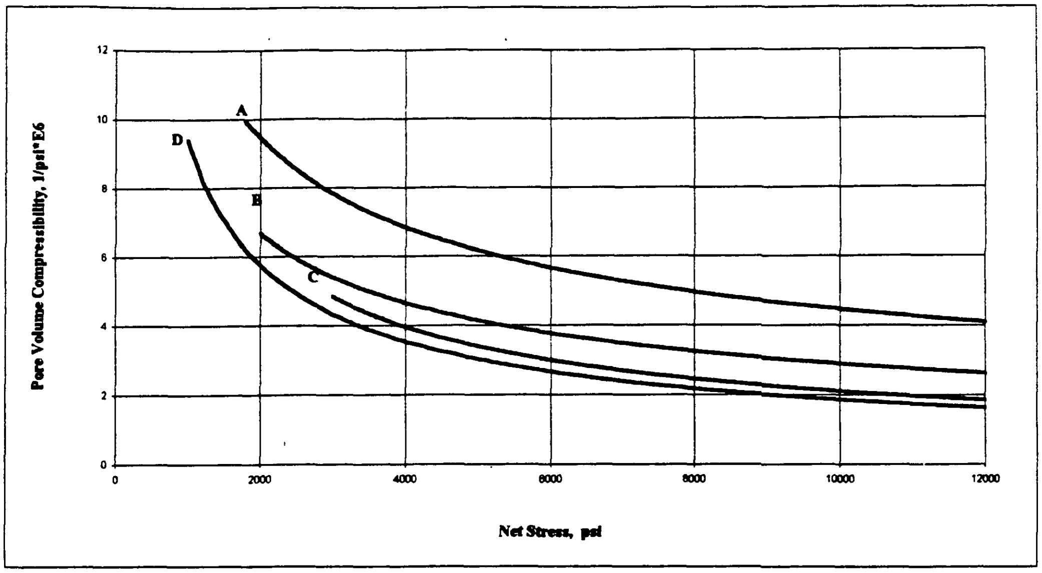

Figure 2-1a: Influence of overburden pressure on pore volume compressibility for poorly sorted unconsolidated sand.
Porosity values of curve A(f = 0.36), B(f = 0.13), C(f = 0.15) and D(f = 0.12), (Fatt, 1958).

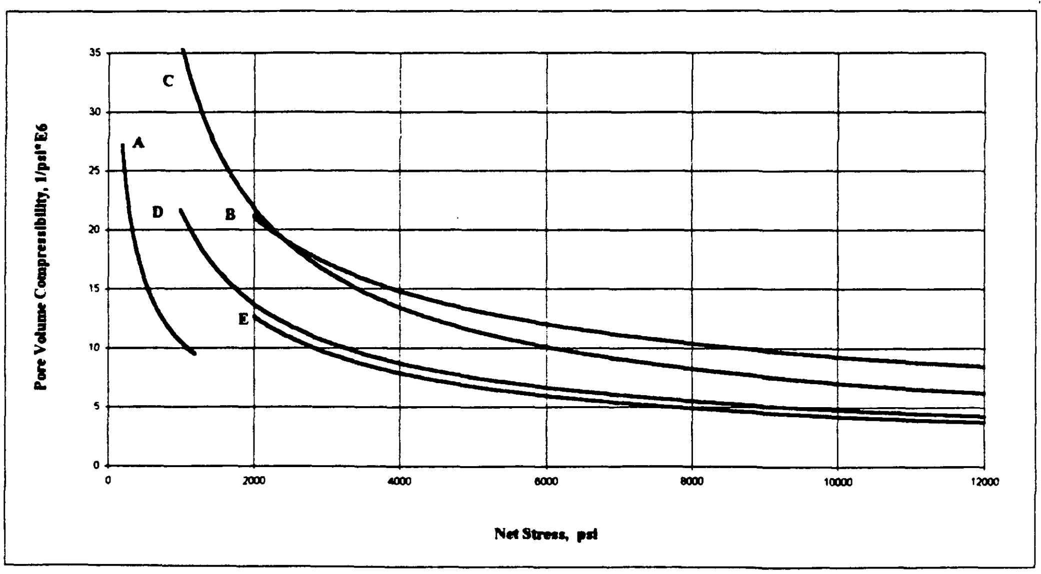

Figure 2-1b: Influence of overburden pressure on pore volume compressibility for well sorted consolidated sandstone grains.
(Fatt, 1958).

(3) Permeability anisotropy is slightly affected by overburden pressure.

(4) Capillary pressure curves are greatly affected by stress tensor at the lower values of pressure, whereas the irreducible water saturation is only slightly influenced by the overburden stress.

Andersen (1985) concluded that pore volume compressibility can account for almost one-fourth of a system compressibility. Difference in direction and magnitude of the applied confined stress is a concern when comparing laboratory measured data to reservoir values. Vertical compaction occurs typically in the reservoir, with stress applied from above by the overburden and lateral deformation prevented by surrounded rock.

The studies of Geertsma and Fatt were carried on, summarized, and elaborated upon by Zimmerman (1986), under the assumption that the solid rock-forming material is microscopically homogeneous and isotropic. Zimmerman's analysis along with Hooke's equation states that "for any bulk volumetric strain that occurs in an externally pressurized porous rock, over and above that which would occur in a similarly shaped non-porous rock composed of the same minerals, must exactly equal the total change in pore volume." This result can also be applied to tests in which a rock that contains a single fracture is loaded by normal stress. In this case, the excess volume change of the rock, due to the existence of the fracture, is exactly equal to the reduction in void volume within the fracture. This result should be useful in developing models for fracture compressibility and fracture permeability.

Experimental data generated by Ruddy (1988), Jones (1988), and Dobrynin on a large number of sandstone samples showed that with the increase of the net overburden pressure, porosity and permeability reduce at different rates. A normalized porosity was defined as the ratio of the initial porosity to the stressed porosity, and normalized permeability was defined as the initial permeability to the stressed permeability. When the normalized ratio was taken the following results were observed:

(1) Highly cemented samples with a lower porosity range had a small reduction in the normalized porosity and permeability values.
(2) Normalized porosity usually reduced sharply for friable core samples.
(3) Unconsolidated samples with high porosity values showed a larger decline in normalized porosity, and a very sharp decline in normalized permeability.
(4) High permeability values had a lesser rate of decline than the lower permeability values, whereas high porosity values had a larger rate of decline.
(5) Overall, permeability was more sensitive to stress than porosity.

Hence, several engineers have tried to correlate compressibility and stress based on the quantity and types of the cementing materials.

2.4 Predicting Pore Volume Compressibility from Porosity for Consolidated, Friable, and Unconsolidated Sand.

Several correlations in reservoir engineering have been developed by Hall (1953) and Van Der Knaap (1958) for sandstone and limestone samples from single wells, and their correlations seem very promising for all type of reservoirs. Newman (1973) applied several samples from different reservoirs and formations and the results were disappointing. These data showed no correlation between porosity and pore compressibility exists.

Consolidated Sand consists of hard rock which is well cemented, cannot be broken off by hand, and can resist high stress. Most samples tends to be in the elastic region, yet compressibility data tend to define trends for sandstone and limestone sample from similar lithology (Figure 2-2).

Friable Sand consists of somewhat hard rock that can be cut into core plug samples but cannot resist high stress and it can be broken by hand. Friable samples tend to be in the elastic region. There is no correlation between compressibility and initial porosity values (Figure 2-3).

Unconsolidated Sand consists of sand that falls apart under its own weight and cannot be plugged (unless they are frozen). Rearrangement of grains tends to provide a looser packing, which results in higher pore volume compressibility value during the laboratory test. The unconsolidated samples also have the tendency to be in the inelastic region, meaning permanent volume reduction with pressurization, resulting from internal grain failure (Figure 2-4).

In conclusion, there is no correlation between porosity and pore compressibility for any of the sand samples.

2.5 The Effect of Pore Compressibility On Reservoir Calculations

Estimating initial oil-in-place is one of the first and most important calculations to a reservoir engineer. Hall stated that the most common method used to determine oil-in-place from the pressure decline data in an undersaturated reservoir above the bubble point is :

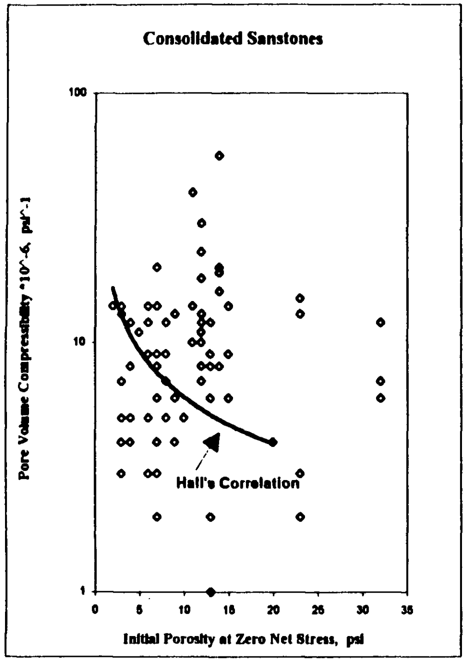

Figure. 2-2: Pore Volume Compressibility vs. Initial Sample Porosity for Consolidated Sandstones. (Newman, 1973)

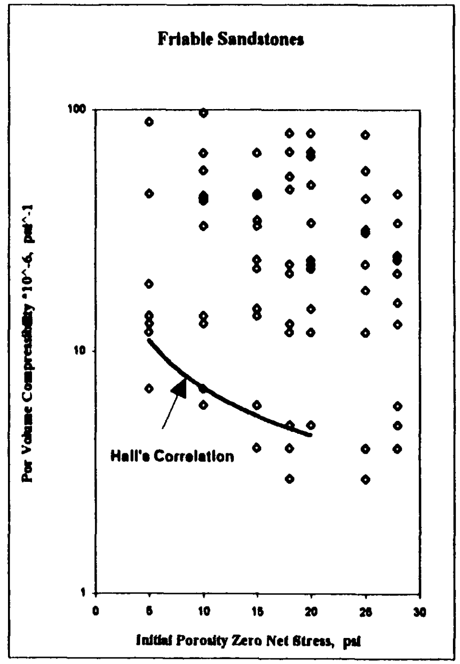

Figure. 2-3: Pore Volume Compressibility vs. Initial Sample Porosity for Friable Sandstones.

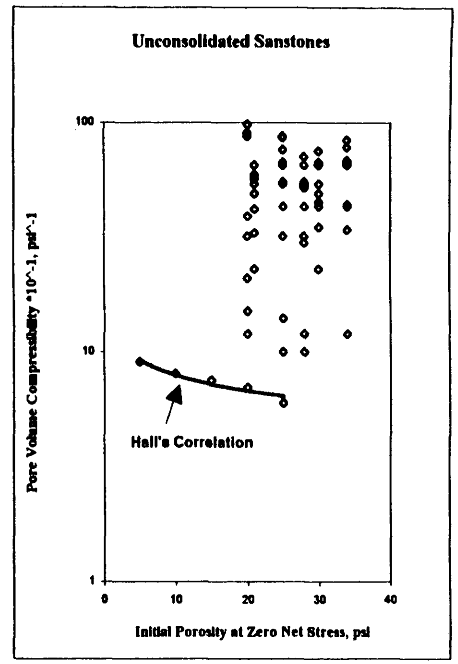

Figure. 2-4: Pore Volume Compressibility vs. Initial Sample Porosity for Unconsolidated Sanstones.

$$N = \frac{N_p}{c_e \Delta P} \tag{2-10}$$

where: N = initial oil in place, bbl.

N_p = oil production during the pressure decline, bbl.

c_e = effective compressibility of the reservoir psi^{-1}.

ΔP = change in reservoir pressure draw-dawn.

where c_e expressed as follows:

$$c_e = c_t / S_o \tag{2-11}$$

$$c_t = c_o S_o + c_g S_g + c_w S_w + cr$$

where :c_o, c_g, c_w are oil, gas and water compressibilities, and S_o, S_g, S_w, are the saturation of oil, gas, and water.

Ignoring pore volume compressibility may result in 100% overestimation of reservoir fluids. Fluid compressibility, on the other hand, is done by PVT analysis.

CHAPTER 3.
METHODS OF PREDICTING AND SMOOTHING PORE VOLUME COMPRESSIBILITY

3.0 Introduction

As stated in the literature review, many methods of predicting pore volume compressibility have been developed. In this thesis, new methods were developed to minimumize the amount of time and lab data required to predict and smooth compressibility. When porosity or pore volume is measured at different stresses, such correlations can be valuable in predicting pore volume compressibility.

Laboratory measurement is the best way to determine pore volume compressibility of rocks. Depending on the requirements (hydrostatic, uniaxial, triaxial), every apparatus has its own way of loading and unloading core samples, maintaining and changing stress, controlling the sample's deformation limits, and stressing the sample to reservoir conditions. Theoretically, pore volume compressibility decreases with the increase of net stress and a smooth decline curve is obtained. Experimentally, this is not always the case. As you will see later in the discussion of results, rock deformation can be altered due to either human errors during sample preparation, loading, or pressure control, or to mechanical instability in the rock itself; thus, inconsistency in pore compressibility exists with some samples. Therefore, there is a need to smooth compressibility data by careful study of permeability, porosity, and stress relationship.

3.1 Method No. 1

This method is used to predict compressibility at different stresses from an initial value of compressibility and a good correlation between porosity and stress. It is empirically found that when porosity is plotted against net stress, a power law equation can be established (Figure 3-1a). Net stress for all methods is defined as:

Net Stress = (Net Radial Stress) - (Net Axial Stress)

Net stress = (Axial stress - Radial Stress) - (Axial Stress - Pore Pressure)

Figure 3-1a illustrates a power law equation that describes the relationship between the porosity and net stress as follows:

$$y = a\,(x)^b$$

$$\phi = a\,(\text{Net Stress})^b \tag{3-1}$$

where y = porosity

x = net stress

a and b are best fit of equation

It is empirically found that pore compressibility is also a function of the normalized porosity and the exponent (b) from the power law equation (Figure 3-1b). Normalized porosity is defined as:

$$\phi_n = \phi/\phi i \tag{3-2}$$

$$c_f = c_{fi}\,(\phi_n)^{(-1/b)} \tag{3-3}$$

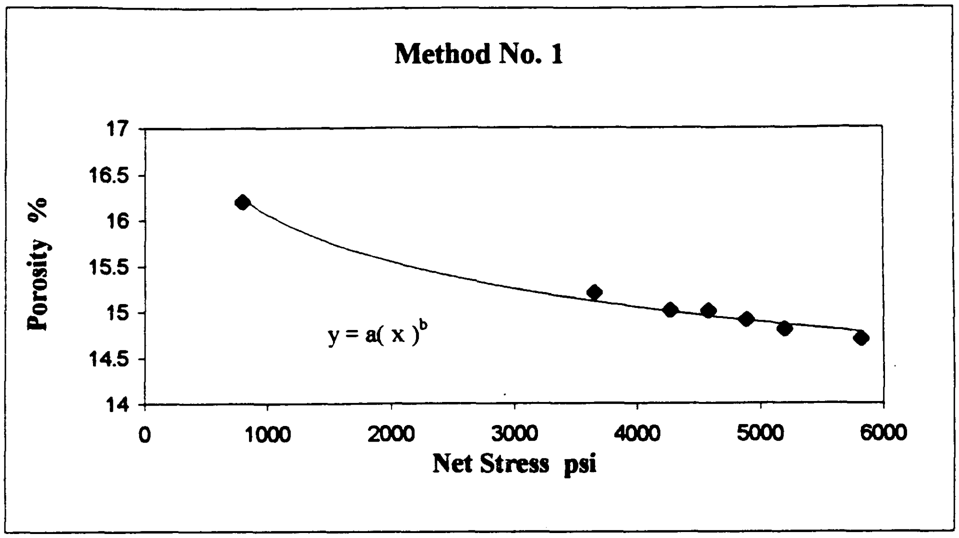

Figure. 3-1a: Illustration of Method 1-Porosity vs.Net Stress(power law fit)

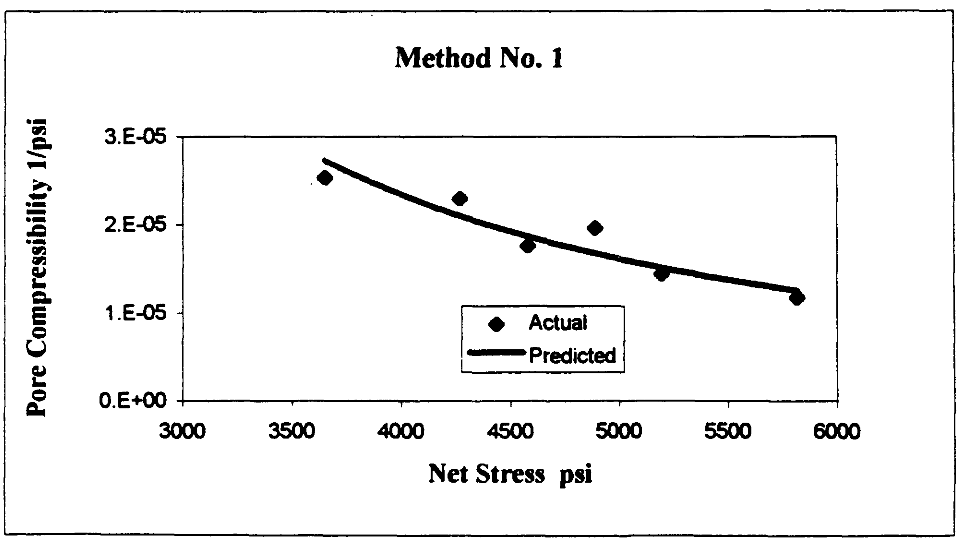

Figure 3-1b: Illustration of Method 1 - Pore Compressibility vs. Net Stress

where ϕ = stressed porosity

ϕ_n = normalized porosity

i = initial conditions

c_f = pore volume compressibility

The advantage of this method is that by knowing one compressibility point, preferably the initial data, and 3 to 4 porosity points, good predictions and smoothing of pore compressibility can be obtained. A limitation of this theory exists when a poor correlation between stress and porosity exists. If there is a poor correlation between stress and porosity, the power law equation could result in predicting compressibility up to one order of magnitude higher. See sample calculation (Appendix D-1).

3.2 Method No. 2

This method is used to predict compressibility from correlations between porosity and stress. It requires the measurement of as few as two porosity points, preferably three, in order to predict pore volume compressibility at higher stress. From the definition of porosity, the following can be obtained:

$$\phi = \frac{V_p}{V_b} \tag{3–4}$$

$$\phi = \frac{V_p}{V_p + V_g} \tag{3-5}$$

where V_p, V_b, and V_g are the pore, bulk, and grain volume respectively.

$$V_p + V_g = V_p(\frac{1}{\phi}) \tag{3-6}$$

$$V_g = V_p(\frac{1}{\phi} - 1) \tag{3-7}$$

$$V_p = V_g\left(\frac{1}{\frac{1}{\phi} - 1}\right) \tag{3-8}$$

multiply Eq. (3-8) by $(\frac{\phi}{\phi})$ to simplify it to Eq. (3-9):

$$V_p = -\frac{\phi}{\phi - 1} * V_g \tag{3-9}$$

Pore compressibility is defined in literature as:

$$c_f = \frac{1}{V_p}\frac{dV_p}{dP} \tag{3-10}$$

substituting Eq. (3-9) into Eq. (3-10)

$$c_f = -\frac{\phi - 1}{\phi * V_g} * \frac{d(\frac{-\phi}{\phi - 1}V_g)}{dP} \tag{3-11}$$

Assuming the change in grain volume is much lower than the change in pore volume, ΔV_g will be negligible. This means that V_g will be a constant value outside the integral and Eq. (3-11) can be rewritten as:

$$c_f = -\left(\frac{\phi - 1}{\phi * V_g}\right) * (V_g) * \frac{d\left(\frac{-\phi}{\phi - 1}\right)}{dP} \qquad \text{from Eq. (3-11)}$$

$$c_f = -\frac{\phi - 1}{\phi} * \frac{d\left(\frac{-\phi}{\phi - 1}\right)}{dP} \qquad (3\text{-}12)$$

Integration of porosity values can be achieved by a best fit equation, power law equation or polynomial, in order to achieve successful predicted results (Figure 3-2a). Using this relationship can predict compressibility data properly (Figure 3-2b).

3.3 Method No. 3

This method is used to smooth inconsistencies in compressibility data by correlating the void ratio to the cumulative pore volume compressibility (cc_f), which is the total compressibility starting from the first test point. When void ratio is plotted against the cumulative compressibility, a straight line equation is established (Figure 3-3a). Void ratio is defined as:

$$\text{Void Ratio} = \frac{\phi_i - \phi}{\phi_i} \qquad (3\text{-}13)$$

If the fractional change in bulk volume is considerably smaller than the fractional change in porosity, then from the straight line relationship in Figure 3-3a, the cumulative compressibility can be described as:

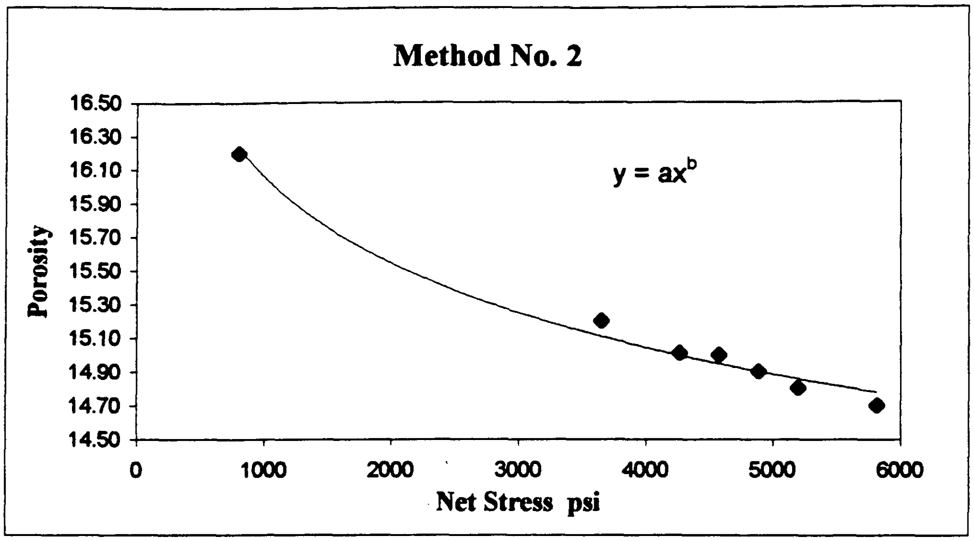

Figure 3-2a: Illustration of Method 2 - Porosity vs. Net Stress

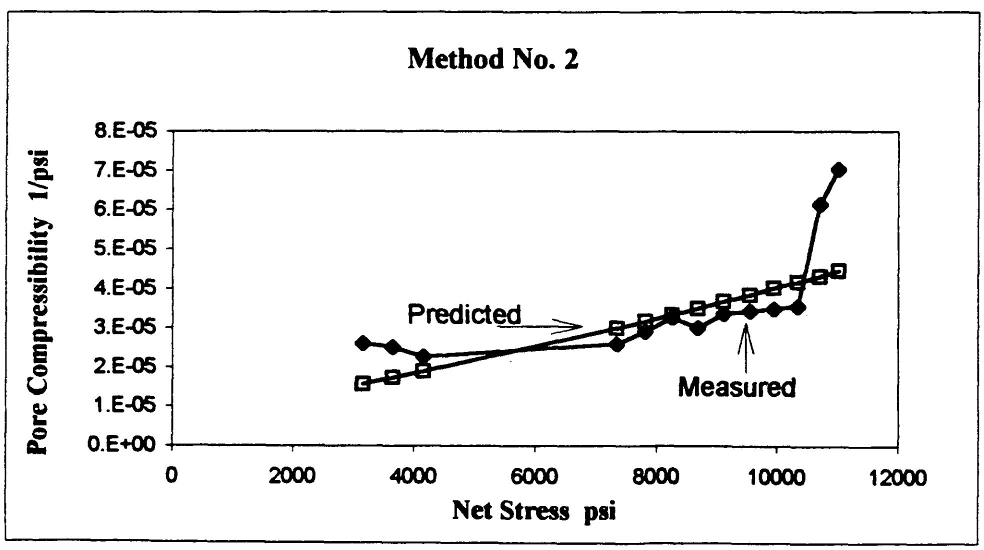

Figure 3-2b: Illustration of Method 2 - Pore Compressibility vs. Net Stress

ARTHUR LAKES LIBRARY
COLORADO SCHOOL OF MINES
GOLDEN, CO 80401

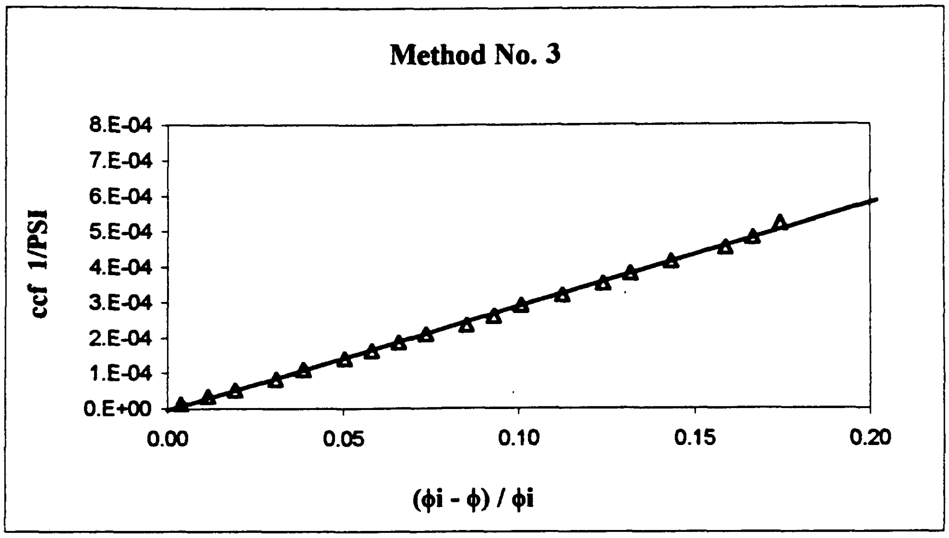

Figure 3-3a: Illustration of Method 3 - Pore Void Ratio vs. ccf

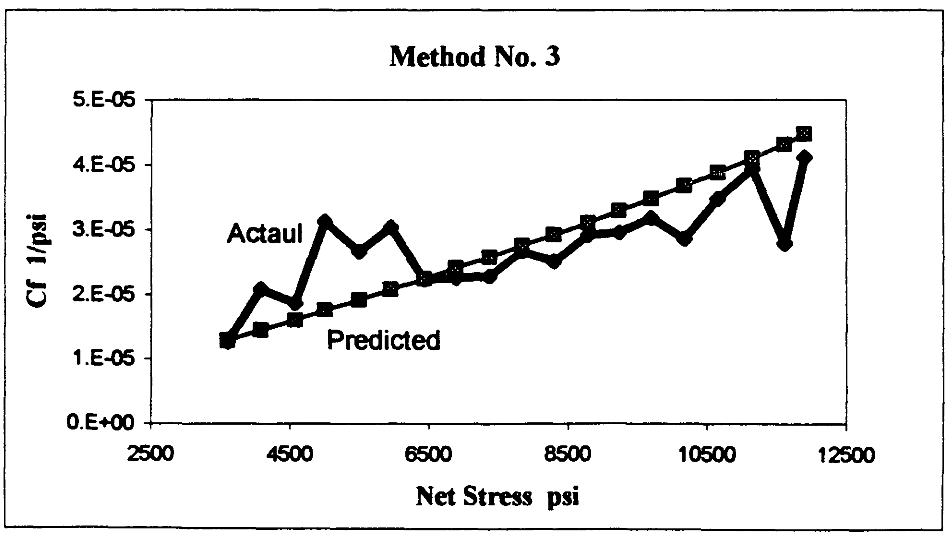

Figure 3-3b: Illustration of Method 3 - Pore Compressibility vs. Net Stress

$$CC_f = \frac{1}{V_{p\bullet}} * \frac{dV_{p\bullet}}{dP} = \frac{1}{V_{pi}} * \frac{d(V_{pi} - V_p)}{dP}$$

$$CC_f = m * \frac{\phi_i - \phi}{\phi_i} + b \qquad (3\text{-}14)$$

where m is the slope of the line, b is the intercepts and i is initial conditions.

With three porosity and pore compressibility values measured, a smooth correlation is established (Figure. 3-3b). Compressibility can be smoothed systematically, and prediction can be extended to forecast values at higher stress with minimum laboratory requirements.

3.4 Method No. 4

It is empirically found that when plotting Jm against a stress function defined by Jones (1988) in a semi-log plot, a straight line relationship is established (Figure 3-4a). Jm is the ratio between the normalized permeability over normalized porosity, where normalized permeability is the ratio between permeability at different stress to the permeability value when the sample is not stressed.

$$k_n = k/k_i \qquad (3\text{-}15)$$

$$Jm = \frac{k_n}{\phi_n} \quad \text{in the y axis} \qquad (3\text{-}16)$$

As mentioned in the literature review, Jones developed a function to use with net stress in a semi-log when describing the change in pore volume, porosity, or permeability at different stress.

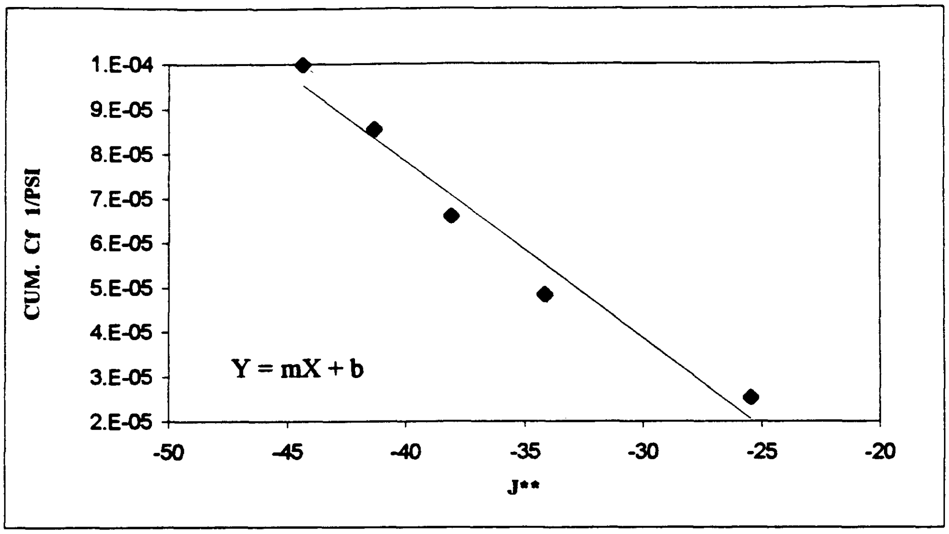

Figure 3-4a: Illustration of Method 4 - J** vs. ccf

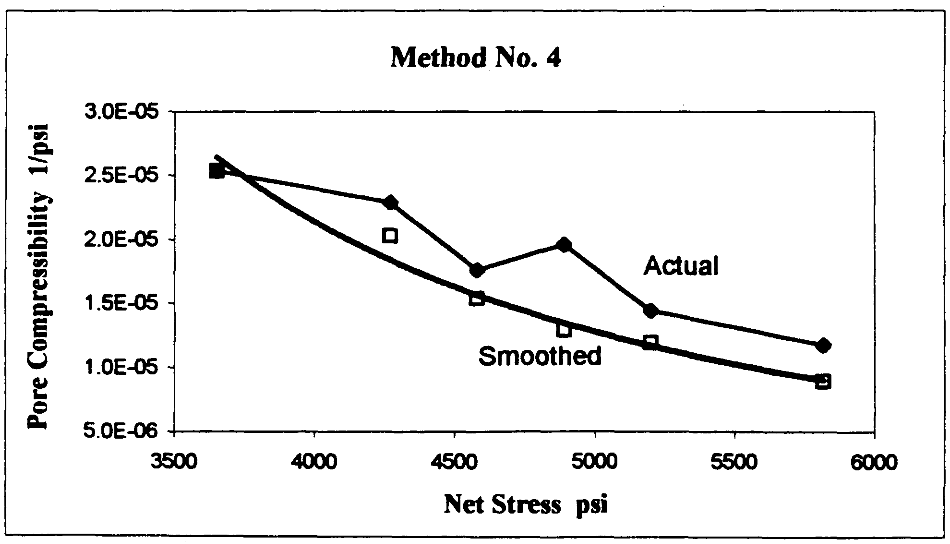

Figure 3-4b: Illustration of Method 4 - Pore Compressibility vs. Net Stress

1-exp(-stress/3000) in the x axis (Jones)

From the straight line equation of Jm and stress, with two values of Jm, values at higher stress ranges can be obtained. Once Jm values are known, then Jm vs. c_f can be plotted to best fit the data (Figure 3-4b). With only three values of pore compressibility, data can be smoothed, and prediction at higher stress can also be obtained. The advantage of this theory is that it considers the effects of permeability, porosity, and stress on pore compressibility.

3.5 Jones' Method

Jones (1988) developed a correlation to determine the change in permeability and pore volume using only two data points. This method is used in this thesis as a comparison to the newly developed methods. When plotting the normalized pore volume over net stress, the data will be best fitted by the equation:

$$V_p = V_{pi}\, \mathrm{EXP}\{av\, [\exp(-\sigma / \sigma^*)-1]\}/(1+C\sigma) \tag{2-4}$$

where av = (- slope) of the straight line transformation from Figure. 3-5a

σ = net stress

σ^* = decay constant arbitrarily set to 3000 psi, for two point fit

C = constant in equation, which is arbitrarily set to (3E-6) for two point fit.

The linear transformation of Eq.(2-4) is a semi-log plot of pore volume and stress, (Figure 3-5a) in the following form:

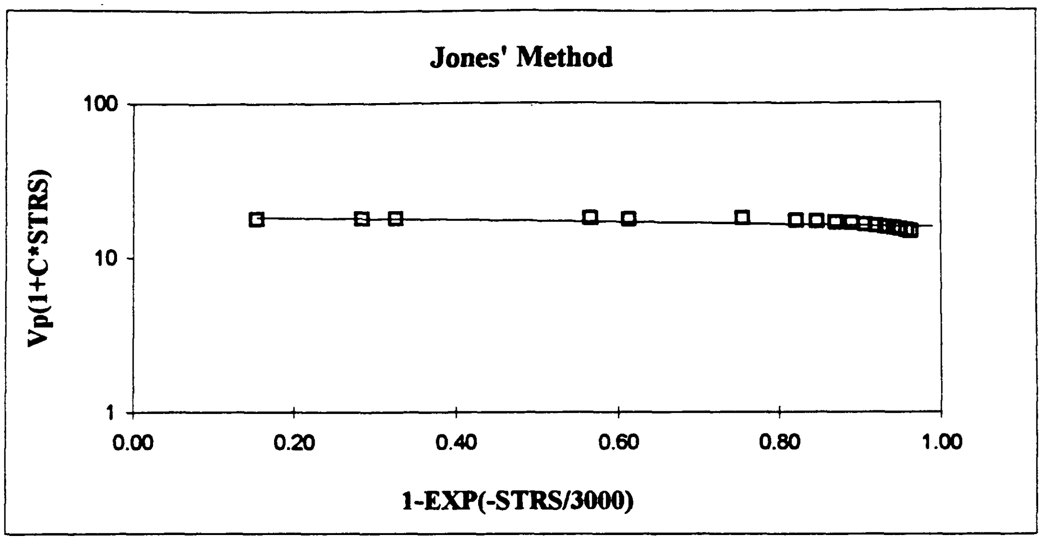

Figure 3-5a: Illustration of Jones' method - Pore Volume vs. Stress

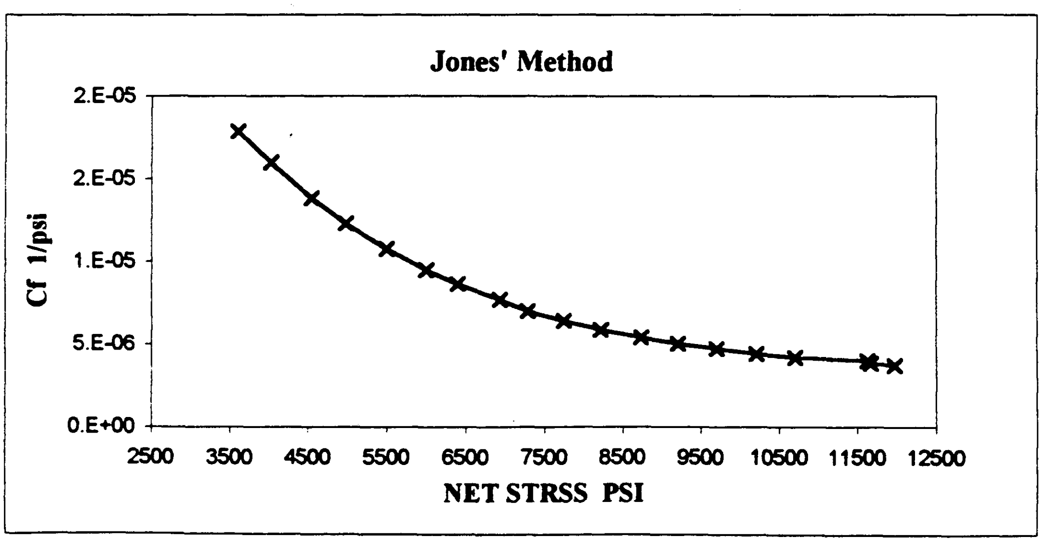

Figure 3-5b: Illustration of Jones' method - Pore Compressibility vs. Net Stress

$Vp(1+C\sigma)$ in the Y axis vs. $[1-\exp(-\sigma/\sigma^*)]$ in the X axis

The abscissa ranges from zero to one. The zero corresponds to a net stress of zero, and one corresponds to infinite stress. The constants C = 3E-6 and σ^* = 3000 psi are empirically found to be suitable numbers to best fit the equation. It was found that a rock sample is usually less sensitive to stress of 3000 psi and higher. Jones modified the classic equation of pore compressibility to the new idealized pore volume-stress relationship:

$$c_f = \frac{a_v * EXP(-\sigma/\sigma^*)}{\sigma^*} + \frac{C}{1+C\sigma} \tag{2-6}$$

Figure 3-5b shows Jones' prediction of pore volume compressibility. The accuracy of the predicted values also depends on the constants C and σ^*, even though they are insensitive to higher stress. A complete pore volume compressibility curve can be obtained from two-point pore volume-stress measurements, but more points are recommended.

CHAPTER 4.
DISCUSSION OF RESULTS

4.0 Introduction

Laboratory data from twenty eight samples were analyzed. There were five consolidated sand samples with large a mount of calcite cement, ten consolidated and friable sand samples with less quantity of calcite, and thirteen unconsolidated samples. All consolidated and friable samples were measured under uniaxial test measurements while unconsolidated sand samples were tested under triaxial test cell. All samples were placed in a vacuum to remove excess air which may have become entrapped in the cores and core holder, and cores were saturated with brine and stressed to reservoir conditions. Samples were taken from different reservoirs at varied depths and reservoir pressures.

The analysis was based on different rock properties, high and low values of porosity, permeability, and stress to make sure that the analysis was valid for all types of reservoirs. The predictions using the developed results methods are usually up to $\pm 20\%$ different from the actual measured data. As stated by many engineers, including Jones, a compressibility value with one order of a magnitude different from the actual measured data is still acceptable within the laboratory experimental errors. Therefore, it was decided that a $\pm 20\%$ difference from the actual results was in the acceptable range of prediction and smoothing. The discussion of the results was categorized by a field study number and subcategorized by the method number. There are four studies and six methods in the following discussion. Table 4-5 is a summary of the discussed methods.

4.1 Study No. 1

Five consolidated samples with large amount of calcite cement were used for the study. Samples were tested under uniaxial conditions. Pore pressure was decreased while axial stress was increased. Since a uniaxial test cell was used, spacing between the core sample and the core holder became critical, and thus, care was taken during core preparation to eliminate spacing problems. No detailed SEM tests were performed for the samples except for the determination of calcite presence; therefore, the detailed lithology is unknown. Table 4-1 lists initial values of basic rock properties.

Samples were saturated with brine and put in a test cell, and axial stress was increased to 5,800 psi. All samples were recovered from the compressibility test without damages. Compressibility values for all samples ranged between 10.2E-6 to 25.3E-6. Sample 4 will be used as an illustration for all methods (Figure 4-1a). See appendix B-1 for figures and appendix D-1 for data calculations for Study 1.

4.1.1 Method 1.

This method was used to predict compressibility from initial compressibility value and correlation between porosity and stress. All five samples showed a good correlation between net stress and porosity using a power law equation (Figure 4-1b). When the exponent from the power law equation was used to estimate compressibility, two samples were in good agreement with the actual measured data and three samples were one order of a magnitude higher (see sample calculation appendix E-1). The samples that showed higher values of prediction, Samples 3, 15, and16, were taken from approximately

Table 4-1: Initial rock properties for consolidated sand - Study No.1

SAMPLE ID #	INITIAL POROSITY %	INITIAL PERMEABILITY, md	INITIAL COMPRESSIBILITY 1/PSI	INITIAL NET STRESS, PSI
2	16.2	14.9	2.53E-05	800
3	26.1	4.96	1.02E-05	800
4	20.2	24.9	1.92E-05	800
15	30.2	2041	1.40E-05	800
16	33.1	5950	1.85E-05	800

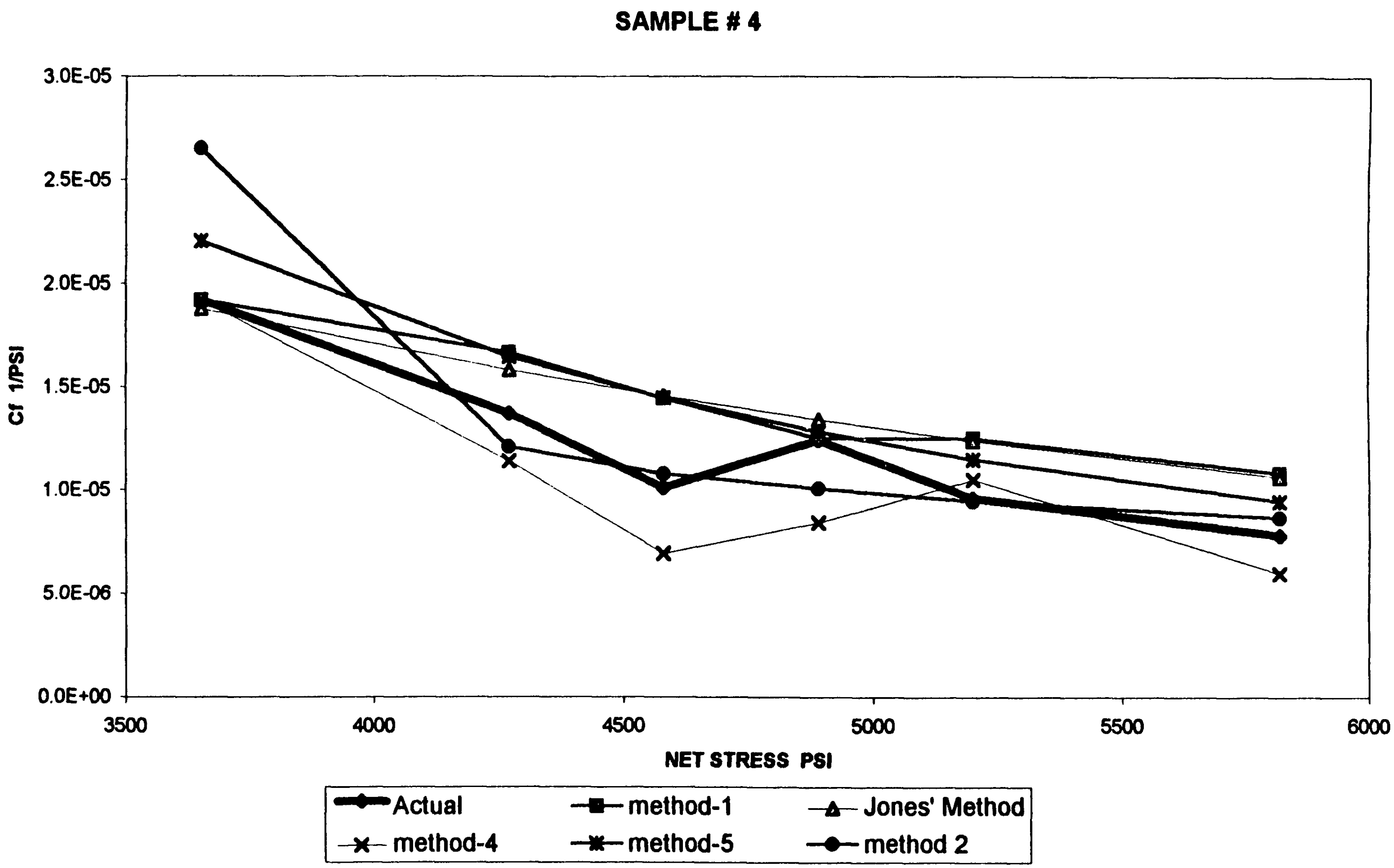

Figure. 4-1a: Using different methods to predict and smooth compressibility-Study No.1 - Sample 4.

STUDY NO.1

THE EFFECT OF STRESS ON POROSITY

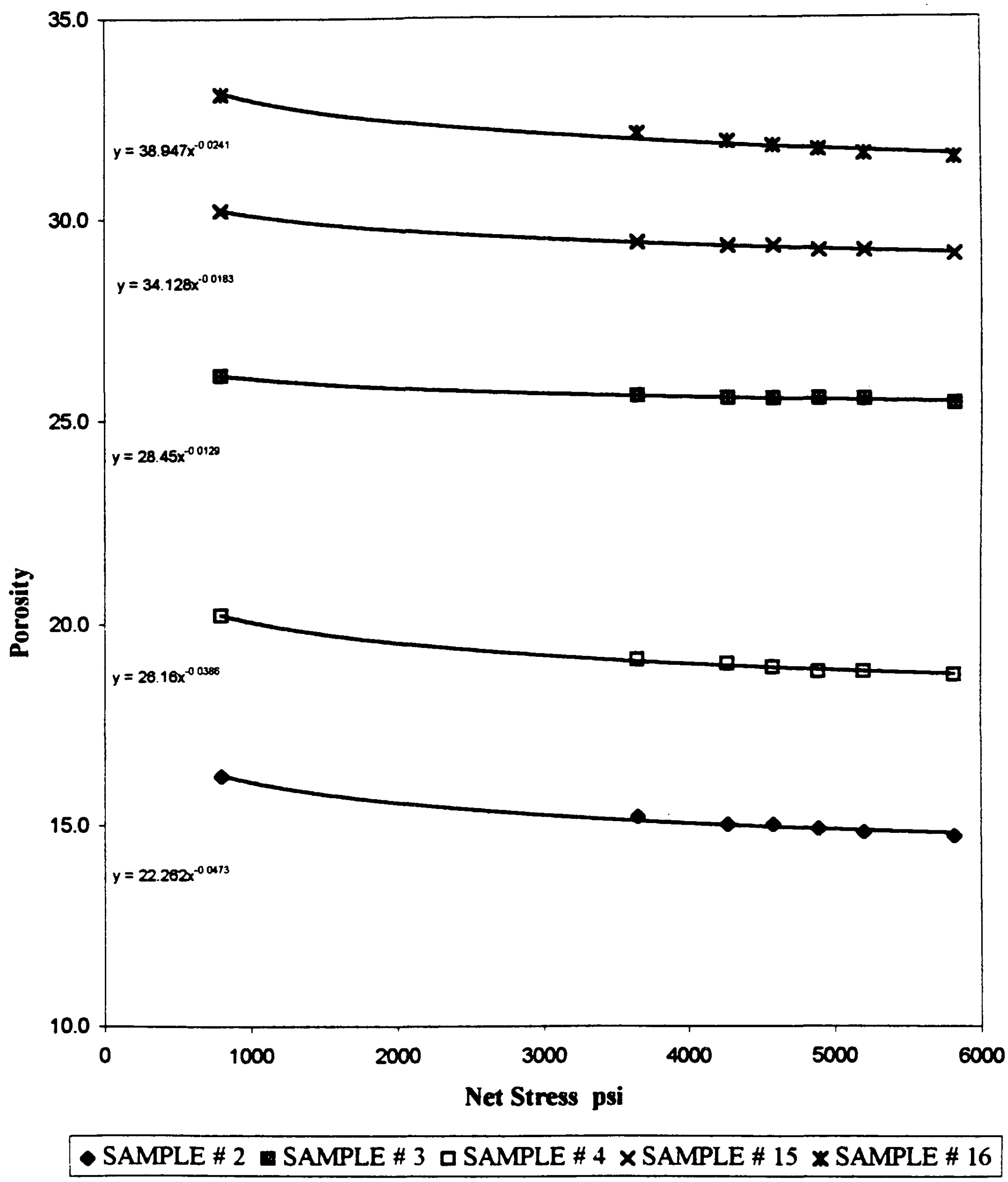

Figure. 4-1b: Porosity - Stress realtionship for samples - Study No.1

12,000 feet whereas samples 2 and 4 were taken from 8,000 feet. The higher predictions of the three samples could be due to many factors:

- Samples 2 and 4 had porosity and permeability values lower than samples 3, 15, and 16. Since this method has an indirect relation with porosity and stress, samples with higher porosity values were less sensitive to stress than samples with lower porosity values, as stated in the literature review (Fatt, 1958).
- Hysteresis was another factor that could alter the predictions. Cement material could be stronger in the lower intervals than samples from higher intervals due to late crystallization of minerals and depositional environment (Djebaar and Erle, 1996).
- Mechanical problems in the test procedure itself were a possibility. Since pore pressure and axial stress were adjusted manually, maintaining a constant stress was difficult.

4.1.2 Method 2.

This method was used to predict compressibility from porosity-stress correlation. Using the power law equation from Figure 4-1b to predict pore volume compressibility resulted in good compressibility predictions for all samples (see sample calculation in appendix E-2). The assumption of negligible change in grain volume is valid for the consolidated samples (no grain crushing and the change in pore volume is equal to the amount of fluid expelled from the core sample).

4.1.3 Method 3.

This method was used to smooth compressibility data and to predict values at higher stress from three values of compressibility and porosity. All five samples showed good correlations between void ratio and the cumulative compressibility with a straight line equation (Figure 4-1c). Even though straight line correlations were established, and the cumulative prediction agreed with the cumulative measured compressibility, when back calculating compressibility values all samples failed to be smoothed. Using a slope from two initial compressibility points did not seem suitable to smooth compressibility data and predict values at higher stress. Figures and results were discarded (sample calculation included in appendix E-3).

4.1.4 Method 4.

Figure 4-1d illustrates straight line correlations between Jm and the stress function defined by Jones (1988), {1-EXP(-strs/3000)}. Using this correlation to predict Jm values at higher stresses resulted in a power equation (Figure C-1). Two compressibility points were used to smooth compressibility values at higher stress, and all five samples smoothed very well when converted to the actual measured compressibilities (sample calculation included in appendix E-4).

4.1.5 Jones' Method

Figure 4-1e illustrates a straight line correlation between pore volume and the stress function established by Jones. When transforming the straight line correlation to

STUDY NO. 1

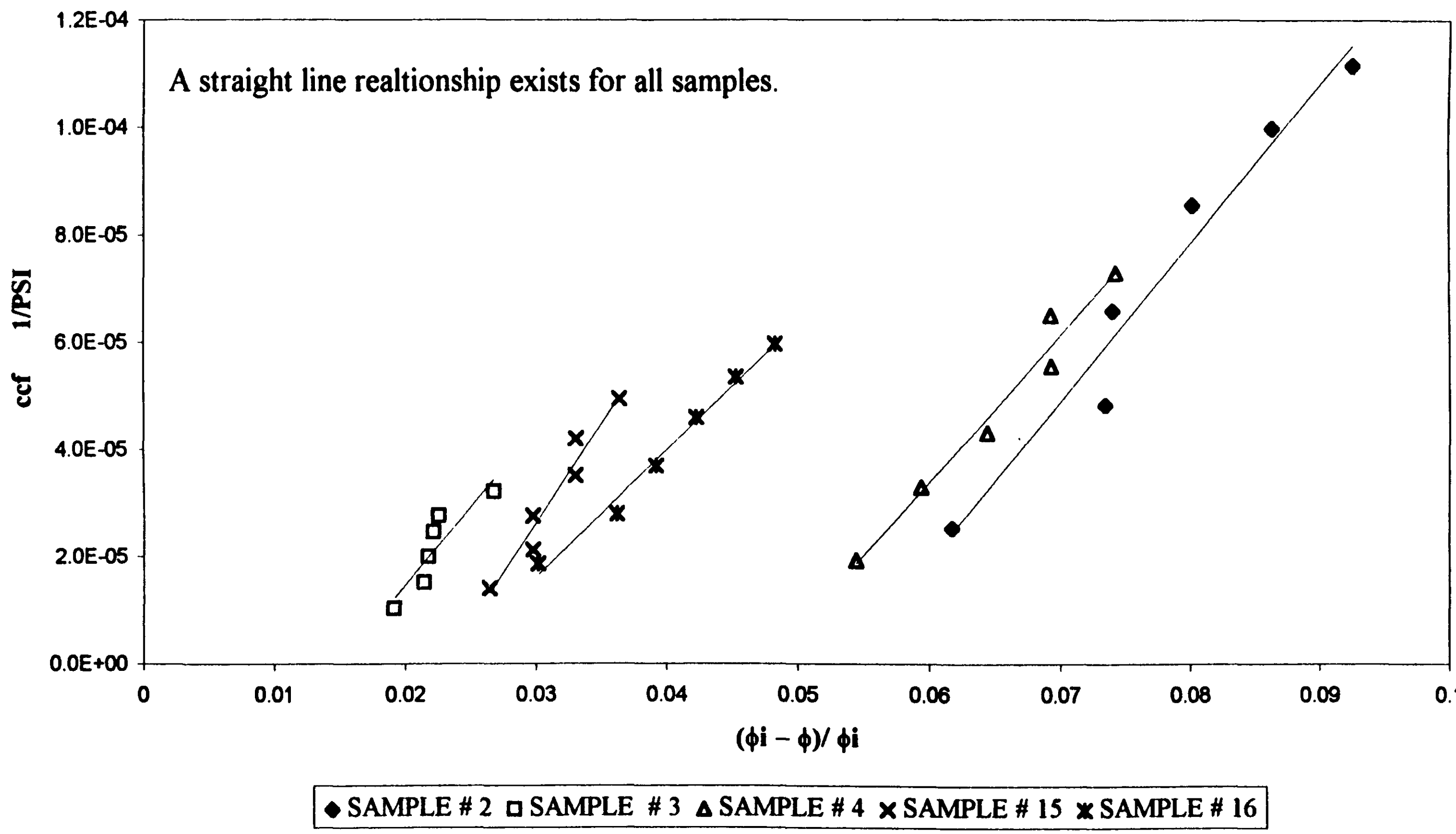

Figure. 4-1c: Pore void ratio vs. cumulative pore compressibility for samples - Study No. 1

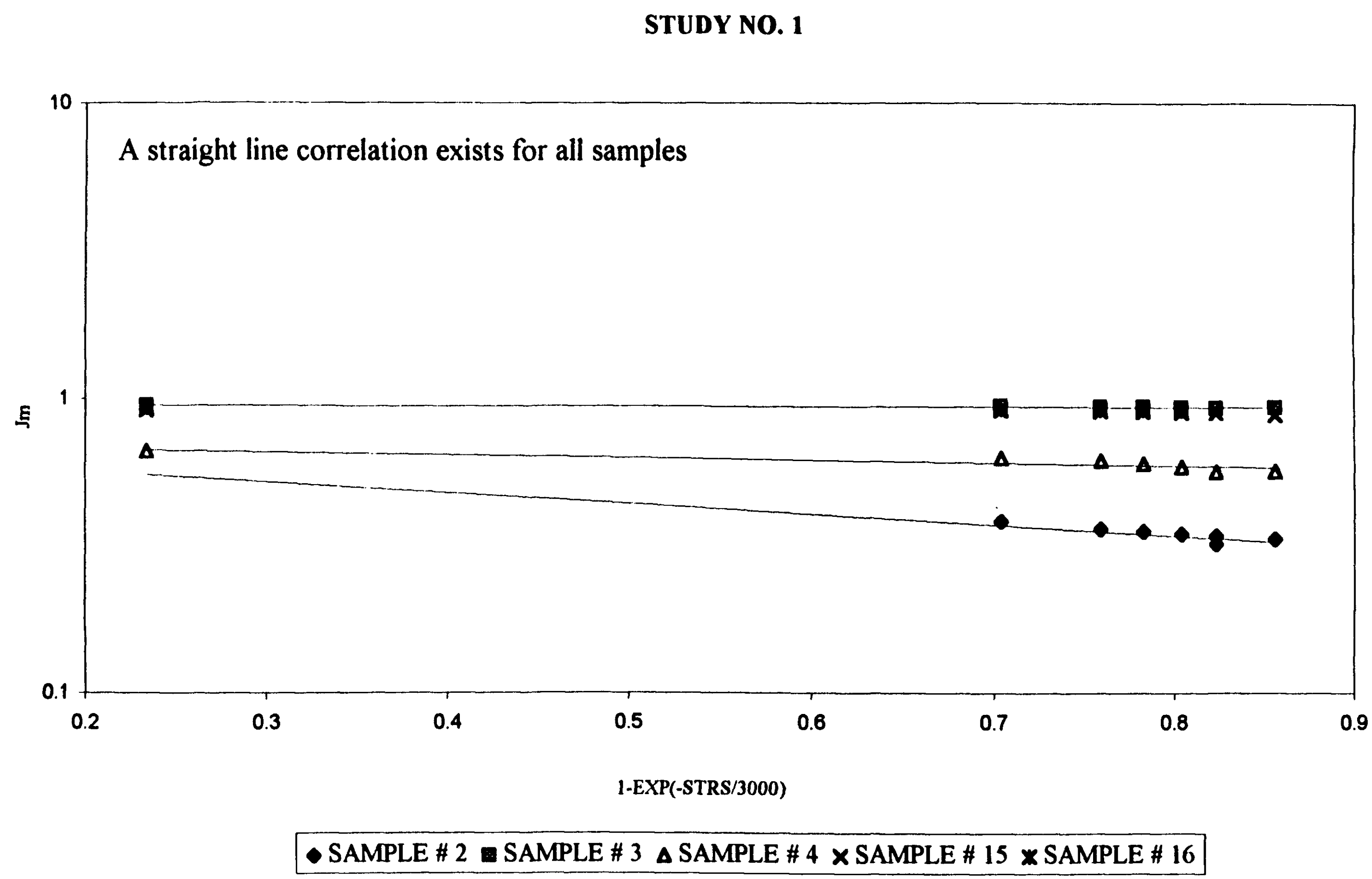

Figure. 4-1d: Prediction of Jm from two points vs. stress for samples - Study No. 1

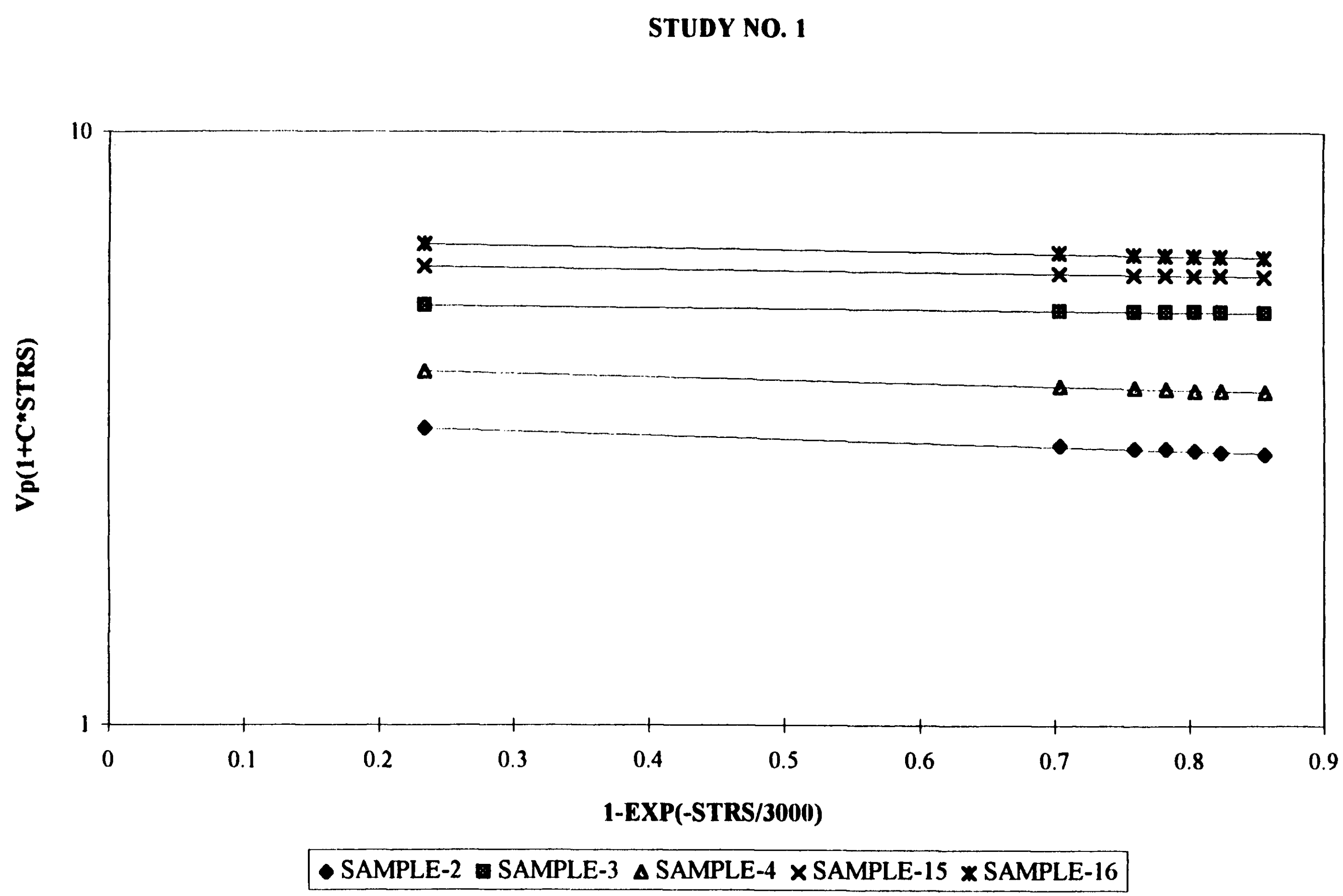

Figure. 4-1e: Jones' Method of predicting pore volume from two points vs. stress for Study No. 1

predict compressibility data, all samples showed agreements to the actual data which were either close or up to 20% higher. Samples 3 and 15 were one order of magnitude higher. As mentioned earlier in the literature review, permeability and pore volume are more sensitive to stress than porosity, and thus the decrease in pore volume and permeability is most evident. Therefore, prediction of compressibility from two pore volume points is only valid when a straight line can be generated. If a sample tends to have sharp change in pore volume and a curve is obtained instead of a straight line, predictions will be wrong.

4.1.6 Conclusions and Recommendations

Method 2 best predicted compressibility data and agreed well with the actual values. Method 1 predicted values close to the actual or in the acceptable range of experimental error, ±20% different from the actual values. When permeability and porosity were used to smooth compressibility, Method 4 related porosity and permeability to smooth and predict compressibility. In Method 3, the straight line correlation between the cumulative compressibility and pore void ratio failed to smooth data for all samples. Depending on the requirements and available data, if one compressibility point is known and a good correlation between porosity and stress exists, then Method 1 will give good predictions. If no compressibility data is available but porosity and stress profile is available, then Method 2 will give good predictions. If samples show inconsistency in laboratory measurements, then Method 4 will smooth the data properly. In conclusion, instead of measuring several compressibility points at elevated stress, three values of compressibility are enough to smooth and predict values at higher stress. In addition, if porosity is measured at different stress, there is no need to perform compressibility experiments. The use of these methods will consume less time and money than the methods currently used in the industry.

4.2 Study No. 2

Seven unconsolidated samples were tested with a triaxial test cell. Samples were initially frozen with liquid nitrogen during core preparation and saturated and pressurized to reservoir conditions of approximated 11,400 psi. Initial porosity values ranged between 22% to 28%, permeability ranged between 130 to 3600 md, and compressibility ranged between 1.19E-6 to 3.03E-6 (see Table 4-2a). During the test, pore pressure and confining stress were varied while keeping a constant axial (ram) stress. This was not exactly representative to reservoir conditions. Usually, the axial stress (overburden) is more dominant than the lateral stress in a reservoir. The deformation in the axial direction caused by the overlaying rocks in a reservoir is greater than the lateral deformation.

SEM tests showed clay particles in some samples. Clay presence can alter porosity and permeability when samples are saturated with fresh water (Djebaar and Erle, 1996). Cores were put in a humidity oven to stabilize clay. If clay particles dehydrate, fine migration might occur and damage the sample. In unconsolidated sand, grains tend to crush, causing the compressibility to increase with the increase of stress as opposed to the consolidated sand. Even though pore volume (V_p) decreased with the increase of net stress, the change of pore volume (dV_p) increased at greater rate. Table 4-2b and Figure 4-2a illustrate how (dV_p) can effect pore compressibility.

Table 4-2a: Initial rock properties for unconsolidated sand - Study No.2

SAMPLE ID #	INITIAL POROSITY %	INITIAL PERMEABILITY, md	INITIAL COMPRESSIBILITY 1/PSI	INITIAL NET STRESS, PSI
14915.5	26.8	1389	2.60E-05	3158
14916.5	26.9	878.38	3.03E-05	3060
14020.5	25.7	961.1	1.26E+05	3060
14927	28	3624.18	2.25E-05	3060
17305.3	22	130.58	9.23E-06	980
17135.65	22.2	420.88	3.66E-06	1062
17322.4	23.4	293.69	1.19E-06	826

Table. 4-2b: The effect of varying pore volume on the measurements of pore compressibility.

	Net Stress psi	Pore Volume cc	d(Vp) cc	cf 1/psi
Materials other than rock. d(Vp) is constant causing compressibility to increase.	500	10	---	---
	1000	9	1	2.22E-04
	1500	8	1	2.50E-04
	2000	7	1	2.86E-04
	2500	6	1	3.33E-04
	3000	5	1	4.00E-04
	3500	4	1	5.00E-04
	4000	3	1	6.67E-04
	4600	2	1	8.33E-04
	5000	1	1	2.50E-03
Consolidated sand. d(Vp) decreases causing compressibility to decrease.	500	10	---	---
	1000	7	3	8.57E-04
	1500	5	2	8.00E-04
	2000	4	1	5.00E-04
	2500	3.5	0.5	2.86E-04
	3000	3.2	0.3	1.88E-04
	3500	3.1	0.1	6.45E-05
	4000	3.07	0.03	1.95E-05
	4600	3.05	0.02	1.09E-05
	5000	3.04	0.01	8.22E-06
Unconsolidated sand. d(Vp) increases causing compressibility to increase.	500	10	---	---
	1000	9.8	0.2	4.08E-05
	1500	9.5	0.3	6.32E-05
	2000	9.1	0.4	8.79E-05
	2500	8.5	0.6	1.41E-04
	3000	7.3	1.2	3.29E-04
	3500	6	1.3	4.33E-04
	4000	4.5	1.5	6.67E-04
	4600	2.8	1.7	1.01E-03
	5000	1	1.8	4.50E-03

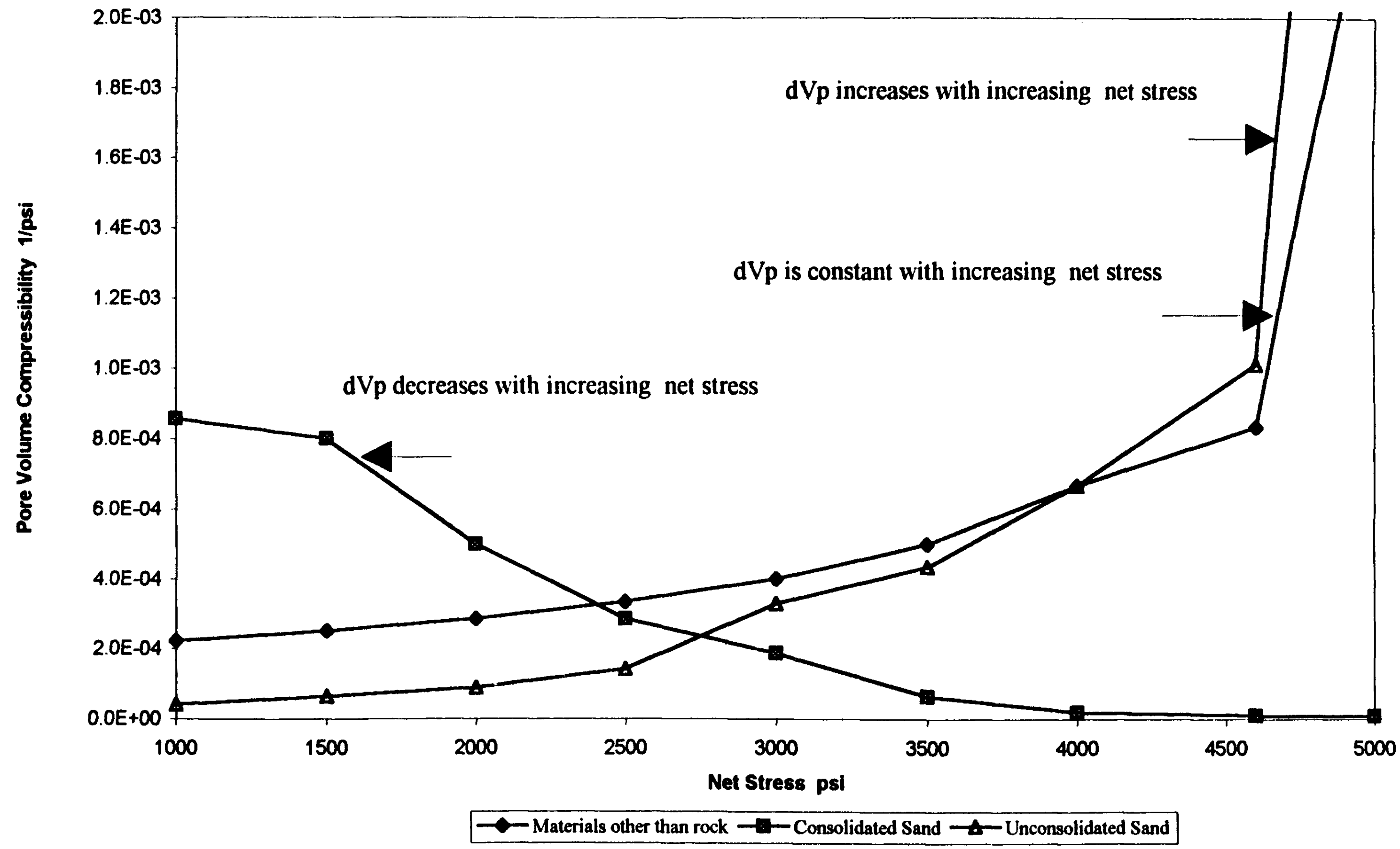

Figure. 4-2: The effect of varing the change in pore volume on the measurement of pore compressibility.

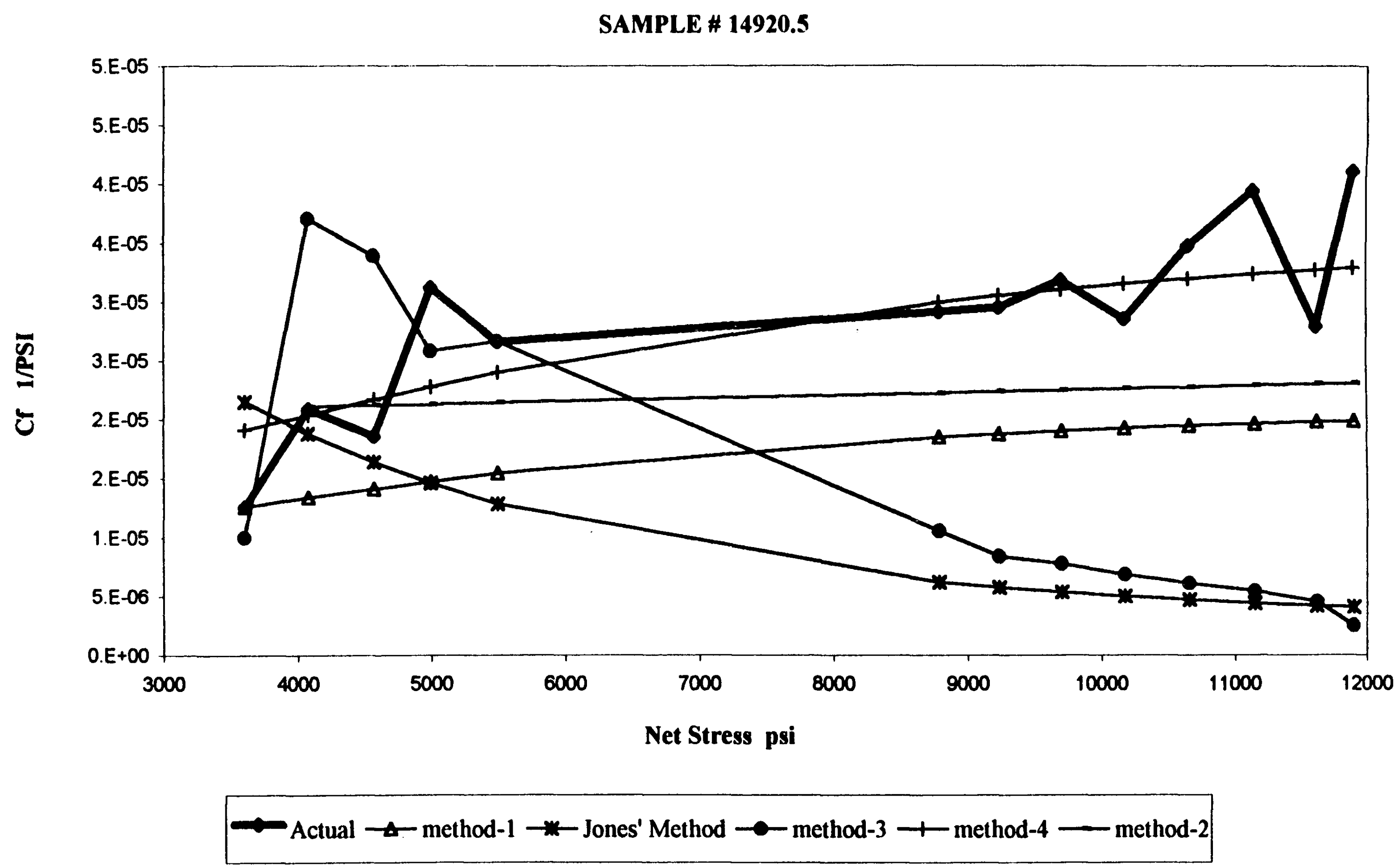

Figure. 4-2a: Using different methods to predict and smooth compressibility - Study No.2 - Sample 14920.5.

SEM analyses of the samples were as follows: Samples 17305.3 and 17322.4 contained illite, fine particles that can break, block pores, and then reduces permeability. Sample 17315.65 had mechanical test problems. Sample 14916.5 contained chlorite which is rich in iron and sensitive to HCL in brine. The chlorite caused clay swelling and a reduction in pore volume due to expansion of grains, and increased in compressibility. Sample 14920.5 contained kaolinite where migration of particles was large; other samples contained little clay. Figure 4-2a illustrates sample 14920.5 which is used as an example for this study. Figures for all samples are included in Appendix B-2 while data calculations appears in Appendix D-2.

4.2.1 Method 1.

All samples containing large amounts of clay had poor agreement with the power law equation (Figure 4-2b). It appears, though, that a polynomial equation might fit the data better (see Appendix A-1).

When using the power law equation to estimate compressibility, all samples showed $\pm$ 20% different from the actual data. Samples 17322.4, 17315.65, and 14920.5. showed lower predictions while Samples 14916.5 and 17305.3 predicted values higher than the actual results. Samples that agreed with the actual data were Samples 14915.5 and 14927. The predicted compressibility values were different from the actual due to poor power law equation correlation. Data from only 2 or 3 porosity points can be used to estimate porosity and compressibility values at different stress. It also appears that samples containing illite predicted values lower than actual while samples containing chlorite predicted values higher than actual. Samples that contained very little clay agreed well with the actual data.

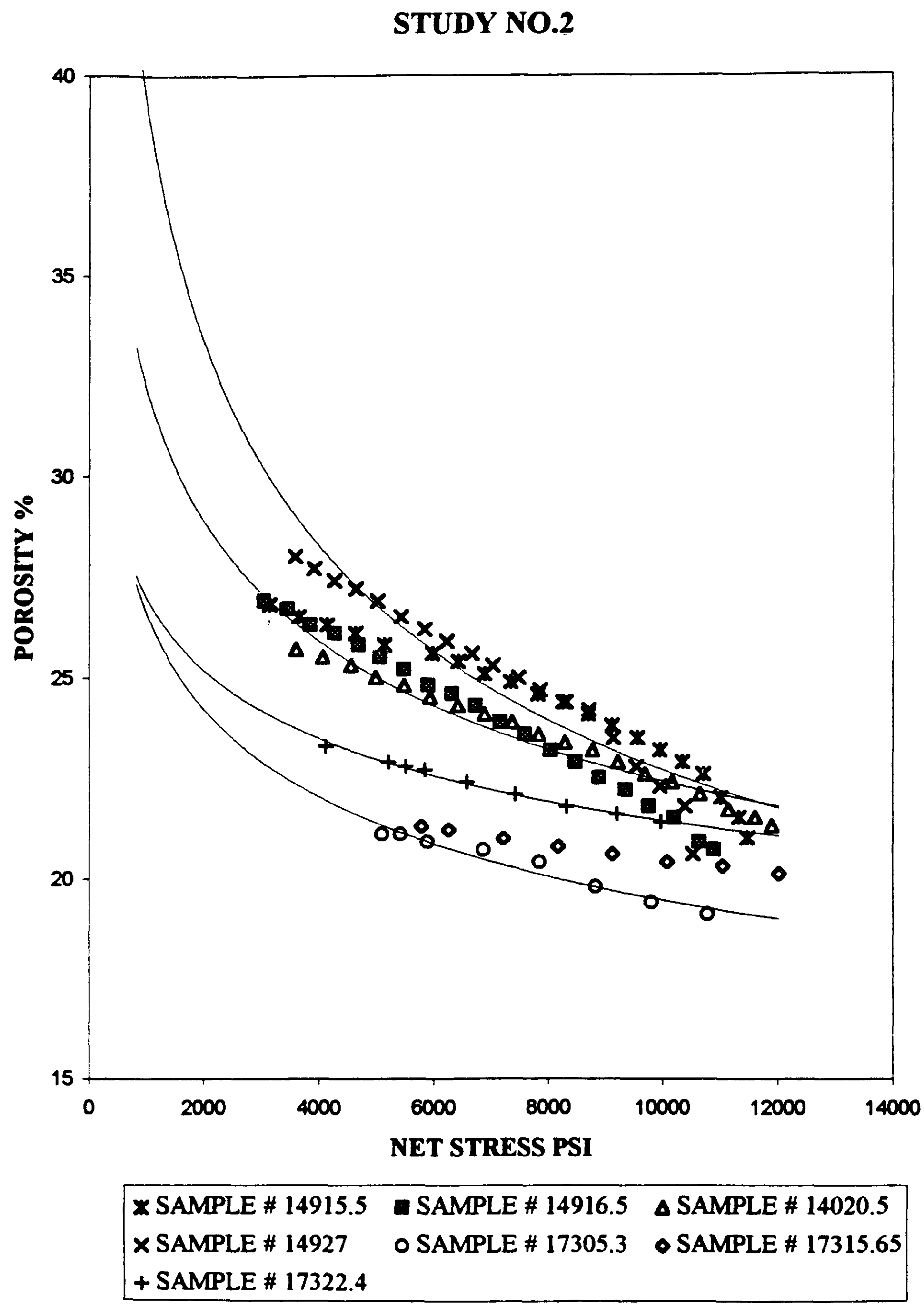

Figure. 4-2b: Porosity-Stress relationship for sample Study No. 2

ARTHUR LAKES LIBRARY
COLORADO SCHOOL OF MINES
GOLDEN, CO 80401

4.2.2 Method 2.

Because accurate correlations between porosity and stress are essential for this method, a polynomial equation would best fit the data (see Appendix A-1). When a pore void ratio was used to predict compressibility, all samples predicted values ± 20% different from the actual results. Grain crushing and/or rearrangements could be the reason for the difference in the predicted values. The effect of grain crushing though was not evident when porosity was used for the correlation. When pore volume was used in Jones' method, the error was more evident.

4.2.3 Method 3.

Some samples showed good straight-line equations with the actual cumulative compressibility data. Samples 17315.65, 17305.3 and 17322.4 showed poorer fits (Figure 4-2c). The result of Sample 17315.65 was poor due to mechanical problems, and the poor predictions of Samples 17305.3 and 17322.4 were due to the presence of illite.

Even though a straight-line correlation was established between void ratio and the cumulative compressibility, all samples failed to predict compressibility close to the actual results. All predicted compressibility values decreased with the increase of net stress, which is not the case for unconsolidated sand. As mentioned earlier, even though porosity and pore volume decreased with the increase of net stress, it was (dV_p) that increased, causing compressibility to increase. Hence, even though this method accounts for the reduction in porosity, a straight line is not valid. This was proved differently in Study 4 when pore pressure was kept constant while axial stress was increased.

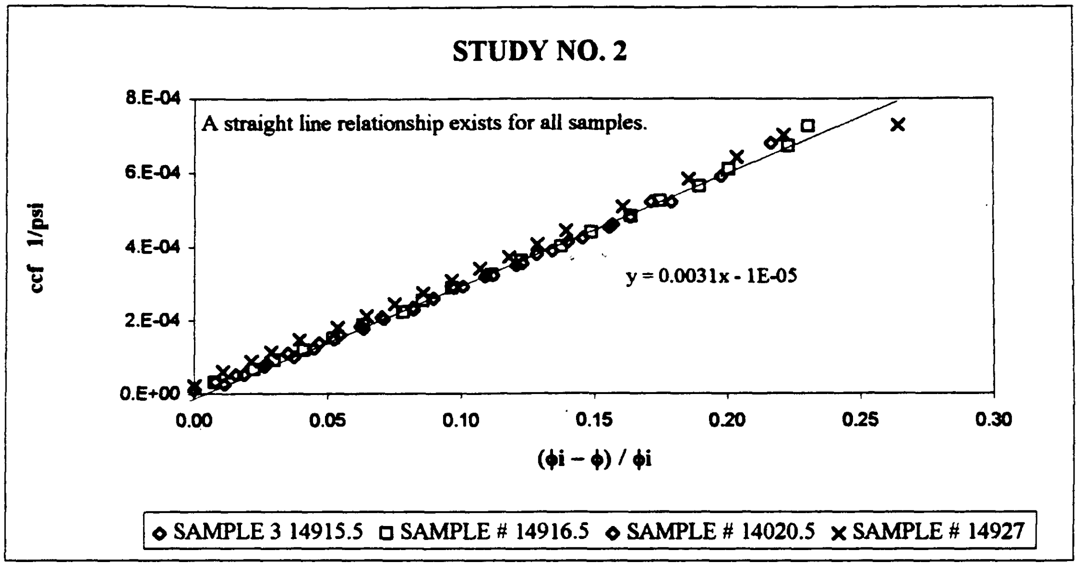

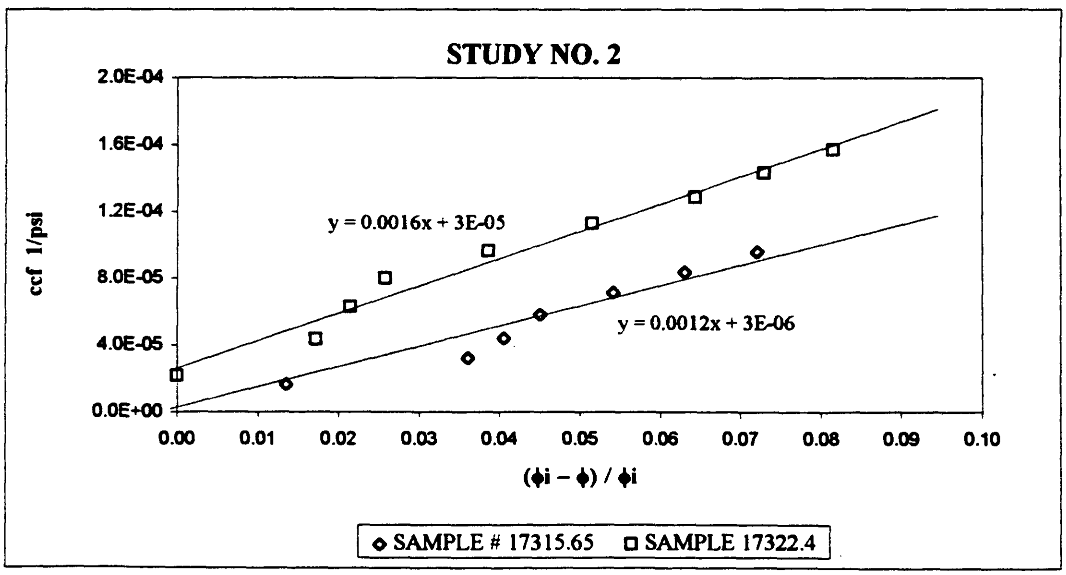

Figure 4-2c: Pore void ratio vs. cumulative compressibility for samples - Study No. 2

4.2.4 Method 4.

Most data showed a straight-line correlation between Jm and stress (Figure 4-2d). Using this relationship to predict data at higher values of stress, a good relationship between Jm and c_f was obtained (Figure C-2). Using the power law equation to smooth compressibility data, all samples correlated well with the actual results.

4.2.5 Jones' Method

Most samples showed poor correlations using Jones' method at the high stress value (Figure 4-2e). Pore volumes tended to decrease sharply at higher stresses, and thus, a straight-line correlation predicted higher values. If a slope is used for the lower stress ranges, it will give poor estimates at the higher stress ranges and vice versa. Due to the poor fits, predicted values of compressibility were 30% lower than the actual data when a slope, a_v, was used at the lower stress values. Like Method 3, predicted compressibility values decreased with the increase of net stress while the actual compressibility values were increased. It seems that Jones' method does not work properly for the unconsolidated sand because it assumes dV_p is equal to ΔV_p.

4.2.6 Conclusions and Recommendations

Compressibility of unconsolidated sand tend to increases with the increase of net stress due to either grain expansion, clay swelling, or grain crushing. A good understanding of clay and its effect on compressibility and other rock properties can be

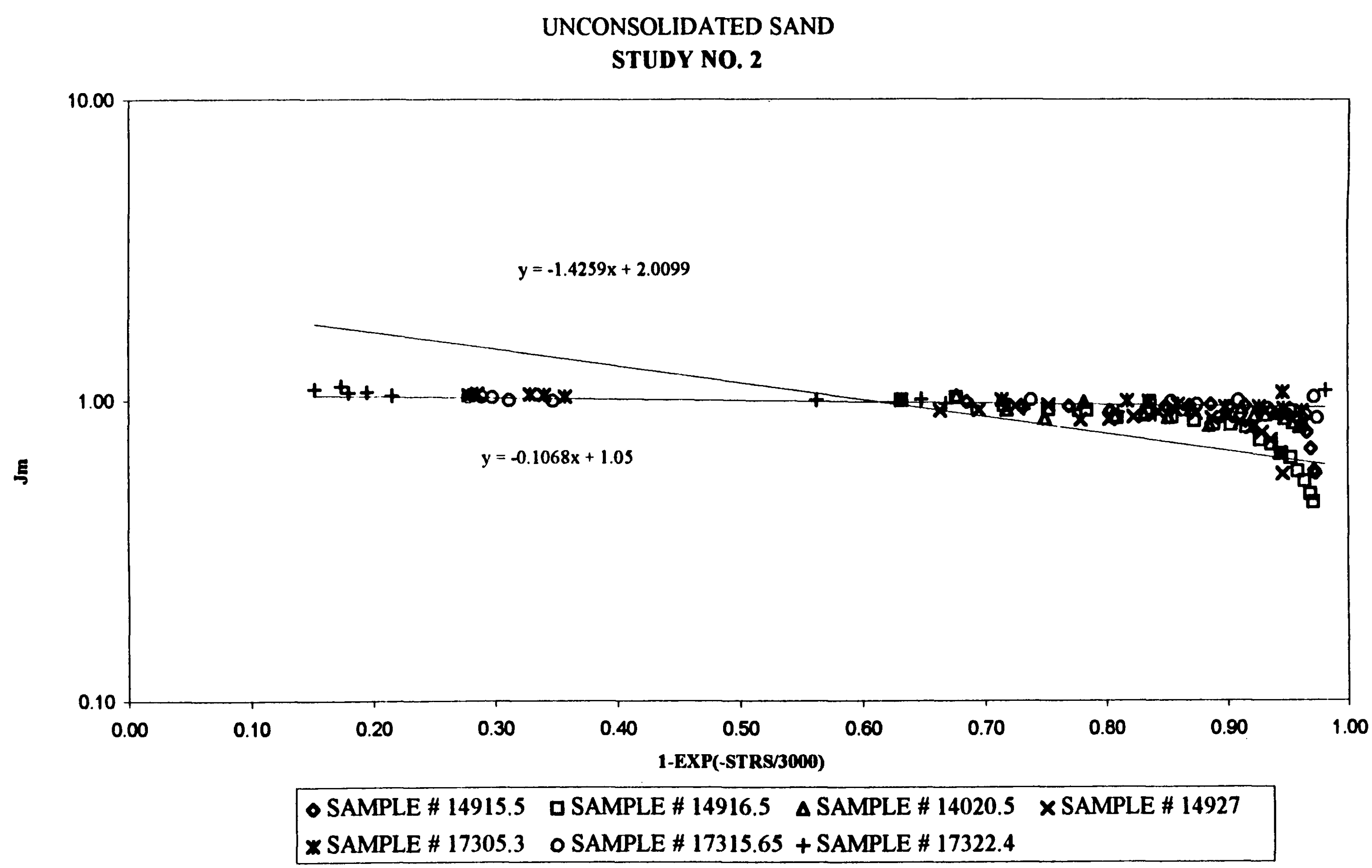

Figure 4-2d: Prediction of Jm from two points vs. stress for samples - Study No. 2

Unconsolidated Sandstones

STUDY NO. 2

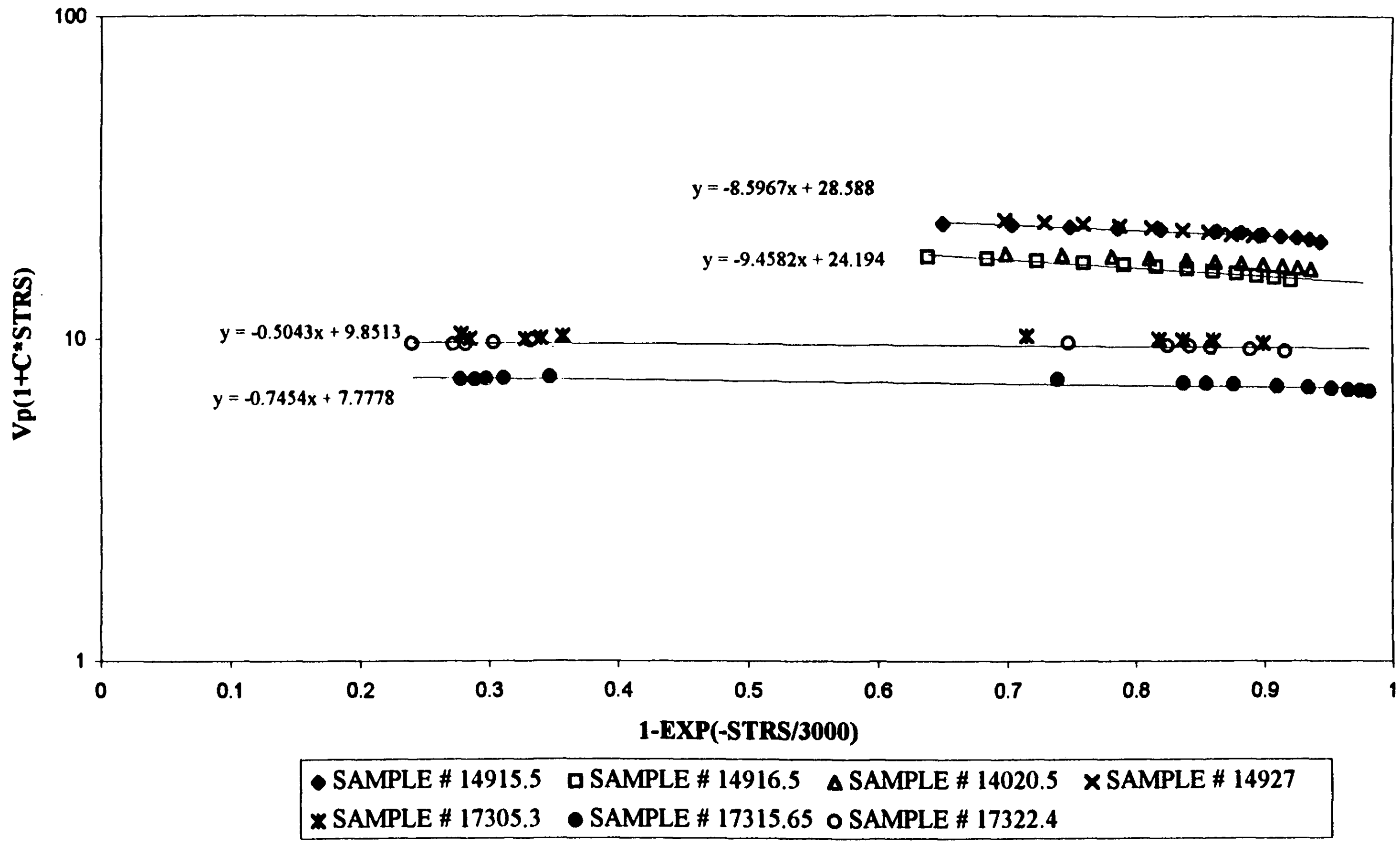

Figure 4-2e: Jones' method of predicting pore volume from two points vs. stress for Study No. 2

useful in reservoir description. From this study, it appears that illite can reduces porosity and permeability and thus predict values lower than the actual. Chlorite is sensitive to HCL in brine, causing swelling of grains and reducing pore volume. This affects the prediction of compressibility values which are higher than the actual. Kaolinite can migrate in pores, but for this study, it did not have much effect on data predictions.

Method 1 predicted values that were 15% lower than the actual. Jones' method and Method 3 predicted compressibilities that decreased with an increase of net stress, which is not the case for unconsolidated sand. Methods 2 and 4 agreed very well with actual data. Method 4 would best smooth compressibility data with minimum compressibility data, while Method 2 would best predict compressibility from a porosity-stress correlation.

4.3 Study No. 3

Ten consolidated and friable samples with calcite cement lower than Study 1 were taken from two different reservoirs and tested under uniaxial conditions. Initial values of porosity ranged from 2% to 20%; compressibility ranged from 2.70E-6 to 303E-6 (see Table 4-3). Permeability was not measured, and thus, Method 4 could not be used.

SEM studies were performed for all samples indicating some calcite content for the consolidated sand and a negligible amount for the friable samples. Friable samples were taken from approximately 2,000 feet, and the consolidated samples were taken from 8,000 feet. The consolidated samples CL-5 and CL-10 contained approximately 40% calcite. The Samples CL-1, CL-8, and CL-9 contained 32% calcite. Samples CL-3, CL-

Table 4-3: Initial rock properties for consolidated sand - Study No.3

SAMPLE ID #	INITIAL POROSITY %	INITIAL PERMEABILITY, md	INITIAL COMPRESSIBILITY 1/PSI	INITIAL NET STRESS, PSI
CL-1	2.83	N/A	3.03E-04	200
CL-2	5.32	N/A	9.60E-05	200
CL-3	8.02	N/A	1.94E-04	500
CL-4	12	N/A	3.50E-05	500
CL-5	2.81	N/A	2.79E-06	200
CL-6	5.26	N/A	1.00E-04	500
CL-7	19.22	N/A	9.23E-05	500
CL-8	20.59	N/A	5.12E-05	500
CL-9	13.58	N/A	2.76E-05	500
CL-10	10.93	N/A	4.25E-05	500

6 , and CL- 7 were classified as friable sand and contained 5% calcite or less. Sample CL- 4 was classified as beach-sand and sample CL-2 was shaley-sand.

Pore compressibility for friable samples tended to decrease dramatically with the increase of net stress. This is due to grain rearrangements, loose grains, or hysteresis of the cementing material. Calcite cement from shallow formations might be less effective as a cementing material than calcite cement from deep formations. Cementing material from deep formations tends to be more effective due to late depositions and crystallization of fluids and minerals. Samples containing small amounts of cement tended to behave like unconsolidated samples where pore volume decreases sharply at higher stresses. Sample CL-5 will be used for the analysis of this study (Figure 4-3a). Appendix B-3 includes figures for all samples. Data calculations are included in Appendix D-3.

4.3.1 Method 1.

Figure 4-3b shows a good correlation between net stress and porosity for all ten samples. When the power law equation was used to predict compressibility, consolidated sand, beach-sand, and shaley-sand agreed within $\pm 16\%$ of the actual data. Friable samples, however, were 10% higher at lower stress values and up to 300% percent higher at the higher stress range.

The poor predictions for the friable sand were due to the fact that compressibility changes dramatically at higher stress where grains are loose. Using the uniaxial test cell is not be the best technique for the friable sands because meeting the test criteria (by not

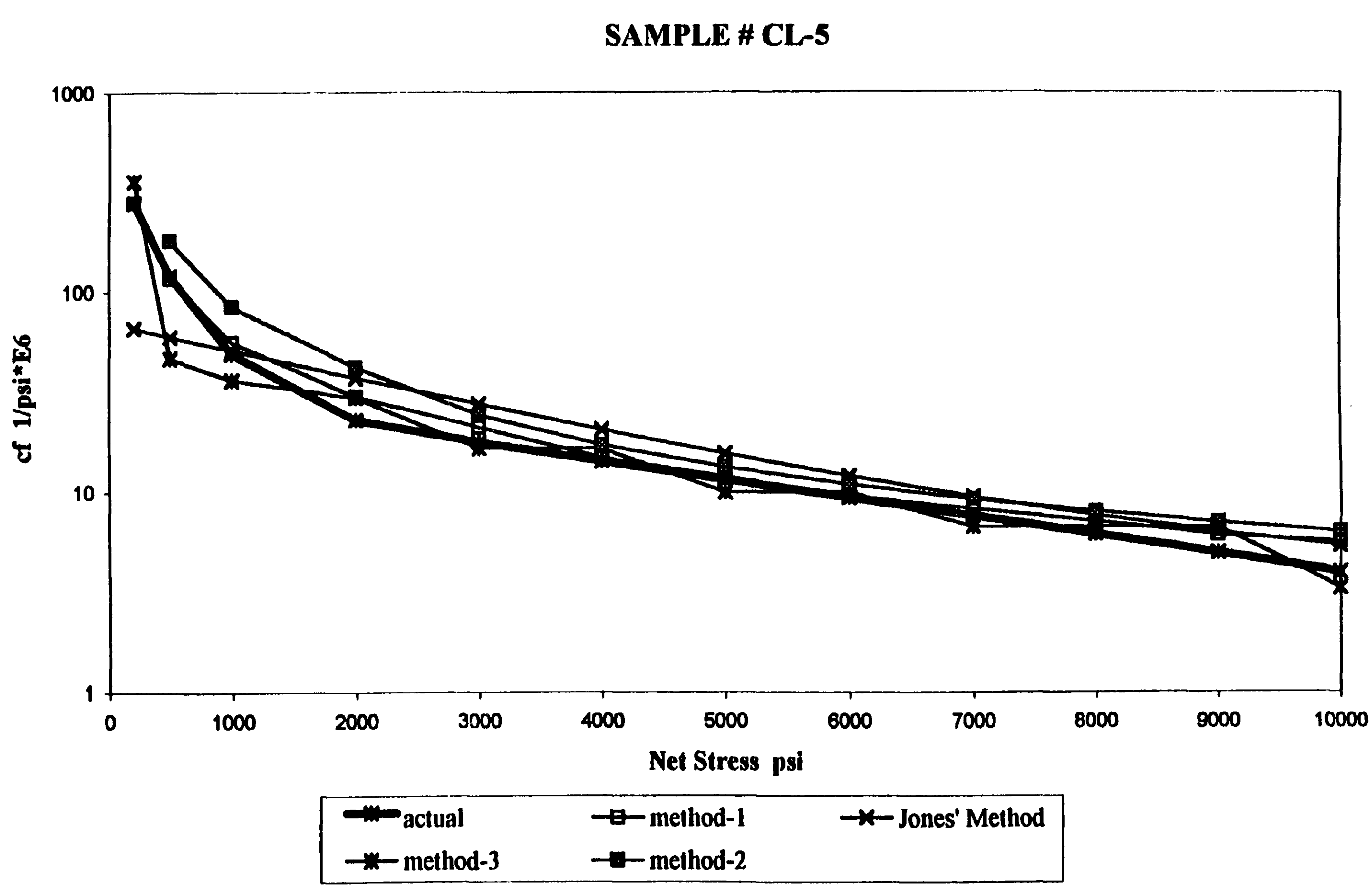

Figure.4-3a: Using different methods to predict and smooth compressibility - Study No. 3 - Sample CL-5

STUDY NO. 3

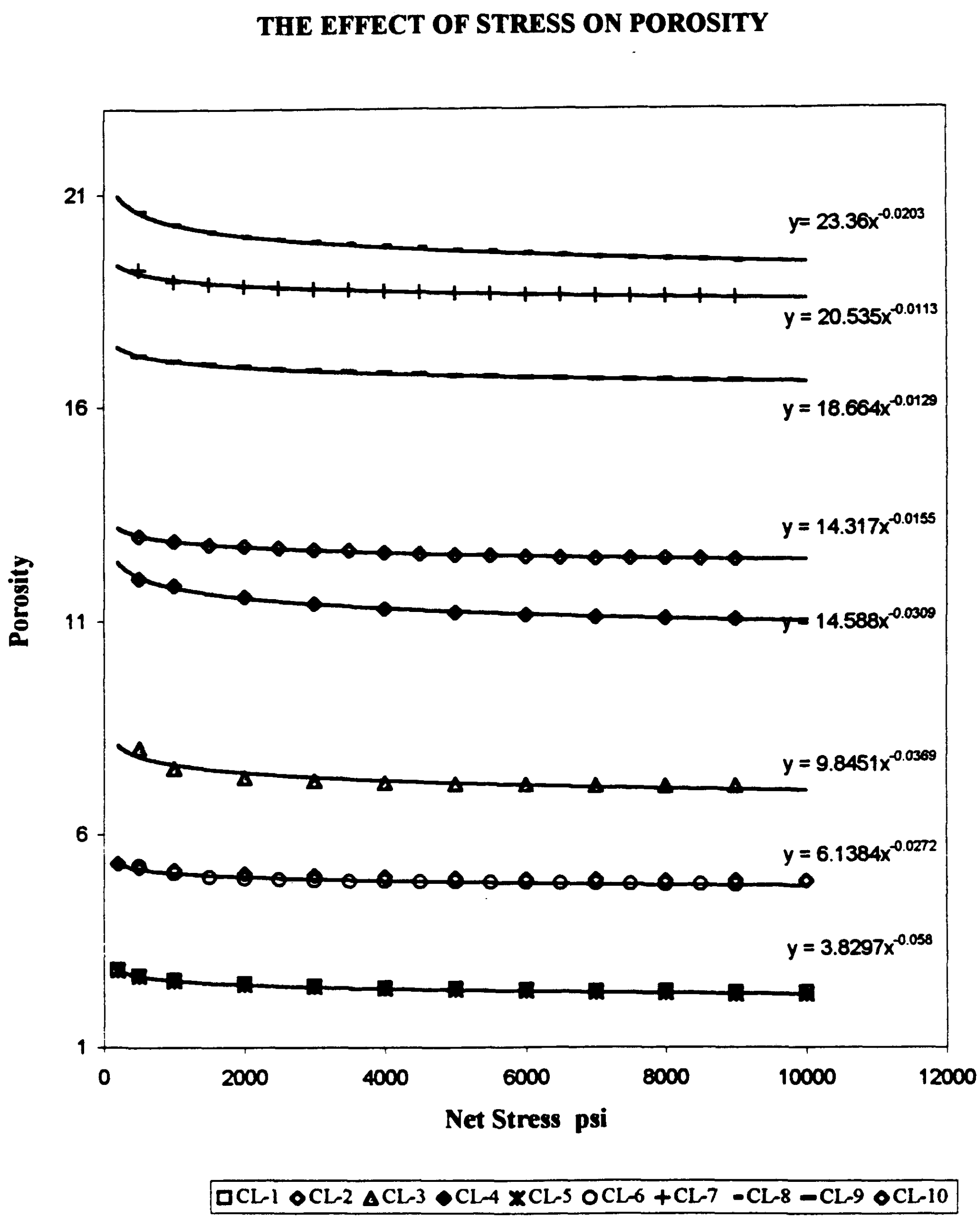

Figure. 4-3b: Porosity-Stress relationship for samples - Study No. 3

having large spaces between the core sample and the inside wall of the core holder) is most likely to happen.

4.3.2 Method 2.

From Figure 4-3b, a good power law correlation for all ten samples was established. When the power law equation was used to predict compressibility, results were 30% higher than the actual results. The higher predictions of samples CL-2 and CL-4 could be due to the presence of shale or loose grains. Since this method integrates porosity from a power law equation, the predicted compressibility values for consolidated sand seemed to be valid and very close to the actual results.

4.3.3 Method 3.

All ten samples showed a straight-line correlation between void ratio and measured compressibilities (Figure 4-3c). Using the straight line relationships to smooth compressibility and predict values at higher stress resulted in an adequately smooth prediction with the actual results. Predictions were $\pm$ 10% from the actual compressibility data.

4.3.4 Jones' Method

All ten samples showed an adequate straight-line correlation between pore volume and the stress function defined by Jones (Figure 4-3d). When transforming the straight-

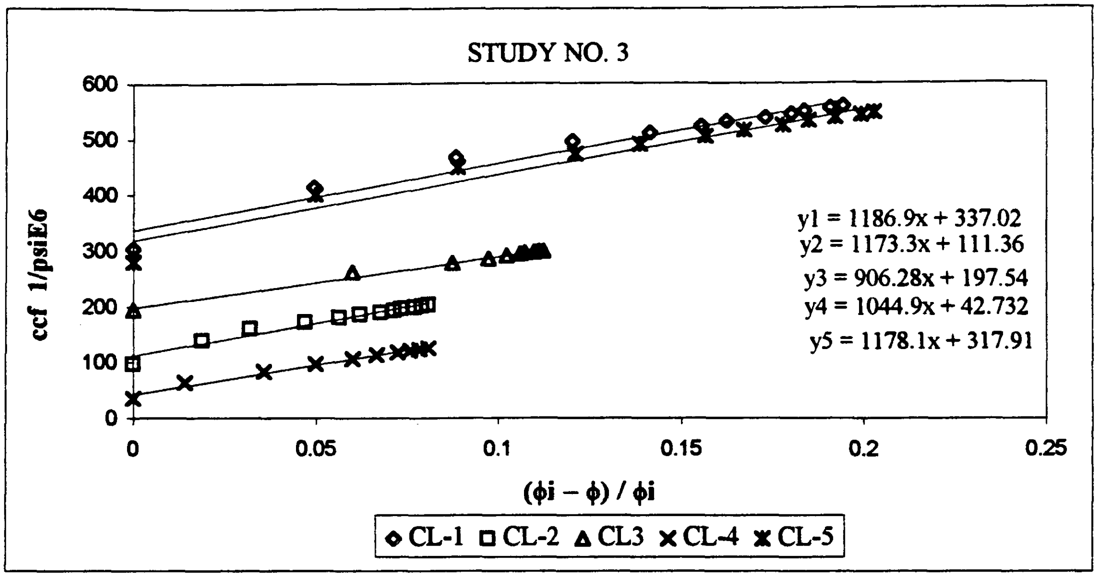

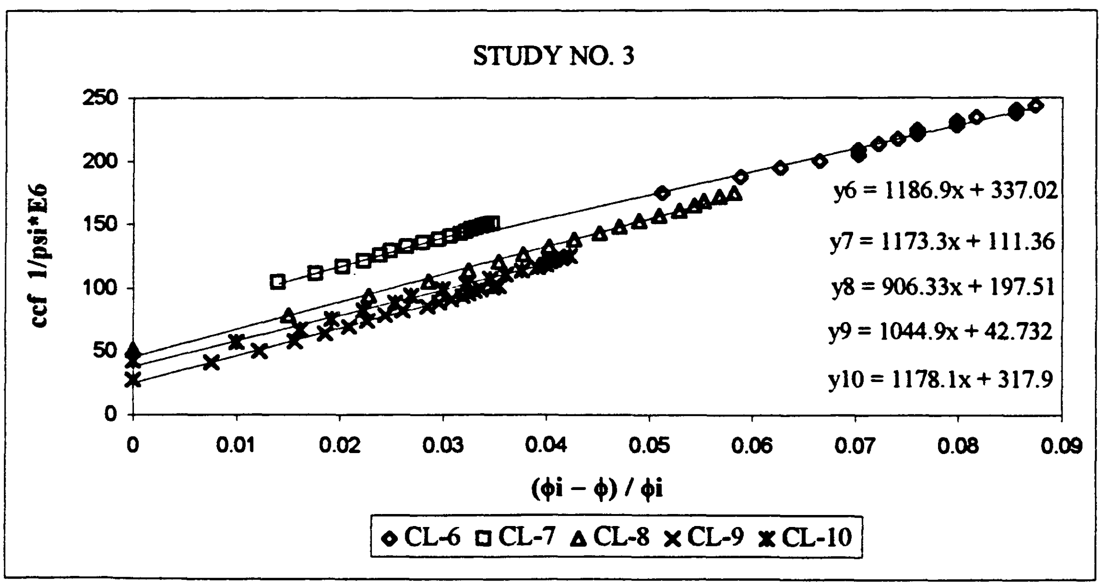

Figure. 4-3c: Pore void ratio vs. cumulative compressibility for samples - Study No. 3

Consolidated Sandstones

STUDY NO. 3

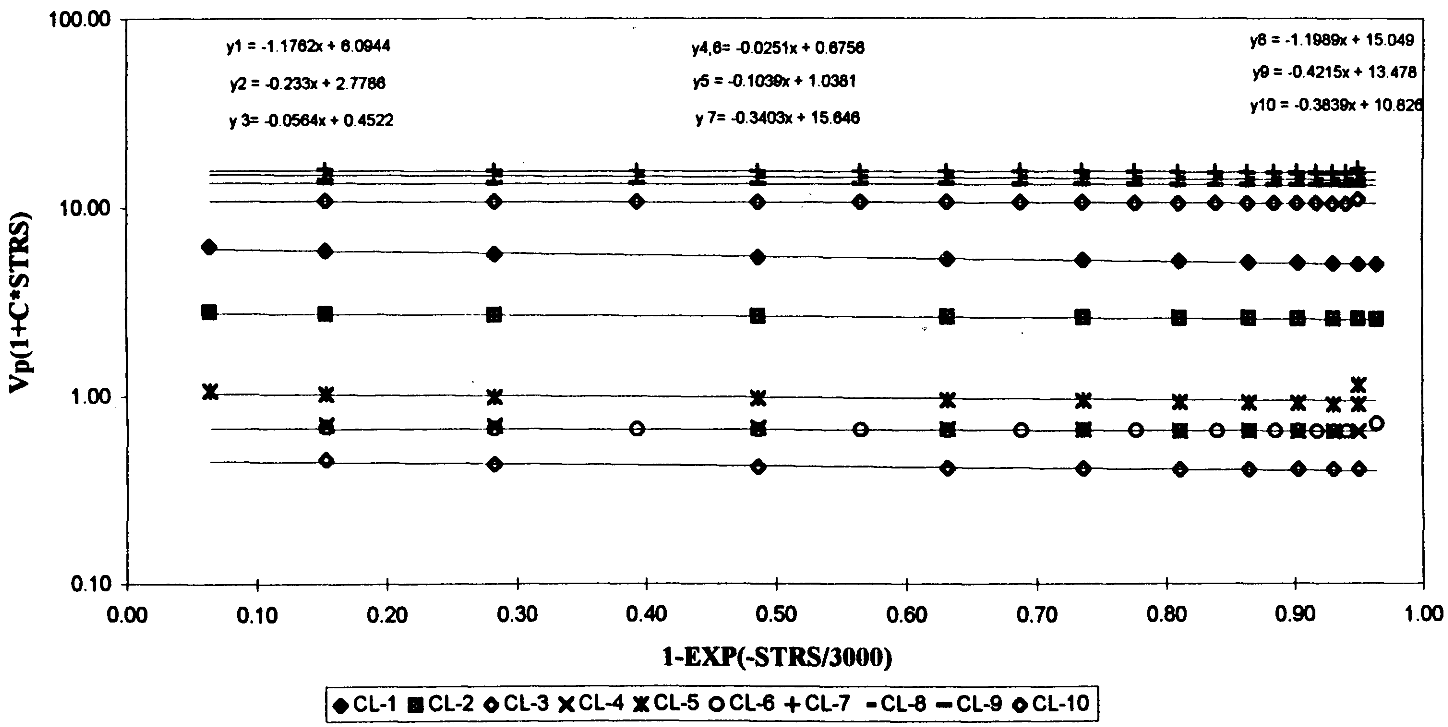

Figure. 4-3d: Jones' method of predicting pore volume from two points vs. stress for Study No. 3

line relationship to predict compressibility, only Samples CL-5 and CL-10 agreed with the actual data; all other samples were up to 50% higher. The poor estimates could be a result of grain crushing, or perhaps the test criteria for the uniaxial test was not met. The assumption that (dV_p) is equal to ΔV_p from the straight line transformation failed to work.

4.3.5 Conclusions and Recommendations

Unlike the unconsolidated sand, compressibility of consolidated and friable sand decreases with increasing net stress. Calcite acts like cement and hold the grains together until it becomes loose and grains becomes more plastic. Compressibility of friable sands tends to reduce sharply with increasing net stress; then it remains almost constant.

Methods 1 and Jones' method failed to work for most samples because test criteria for the uniaxial test was not met and the assumption that (dVp) is equal to ΔV_p failed. Method 1 predicted values that are up to 300% higher while Jones predicted values that are up to 50% higher than the actual. Method 3 will best smooth and predict compressibility data at higher stress while Method 2 will predict data from porosity-stress correlations.

4.4 Study No. 4

All six unconsolidated samples were tested under a triaxial test cell. Pore pressure was kept constant while axial stress was increased. Samples were taken from

ARTHUR LAKES LIBRARY
COLORADO SCHOOL OF MINES
GOLDEN, CO 80401

Table 4-4: Initial rock properties for unconsolidated sand - Study No.4

SAMPLE ID #	INITIAL POROSITY %	INITIAL PERMEABILITY, md	INITIAL COMPRESSIBILITY 1/PSI	INITIAL NET STRESS, PSI
1-KISR	27	1236	2.60E-05	500
2-KISR	27	1177	3.03E-05	500
3-KISR	26	1240	1.26E-05	500
4-KISR	28	3624.18	2.25E-05	500
5-KISR	26	1282.23	2.96E-05	500
6-KISR	22	1052	1.97E-05	500

14,000 feet. Initial values of porosity ranged from 22% to 28%, permeability ranged from 1052 to 3625 md, while pore compressibility ranged from 12.6E-6 to 3.03E-6 (see Table 4-4).

SEM studies showed very little clay present for most samples, but Samples 3-KISR and 4-KISR contained some illite. Sample 5-KISR, however, had some mechanical problems during the test procedure. The rubber sleeve was ruptured and the test was interrupted and then redone. Data from the first test was discarded, and new compressibilities were measured.

Sample KISR-1 will be used for demonstrations (Figure. 4-4a). Figures for other samples are included in Appendix B-4, and data calculations are included in Appendix D-4.

4.4.1 Method 1.

All samples showed a poor power law correlation between porosity and stress as in Study 2 (Figure 4-4b). When this correlation was used to predicted compressibility, the predicted values were -10% than actual results. Samples 3-KISR and 4-KISR, however, showed values up to -30% than the actual. As stated in Study 2, it appears that samples with large amount of illite have prediction values that are lower than the actual. Using more than four porosity points to predict compressibility for Sample 5-KISR provided a good prediction.

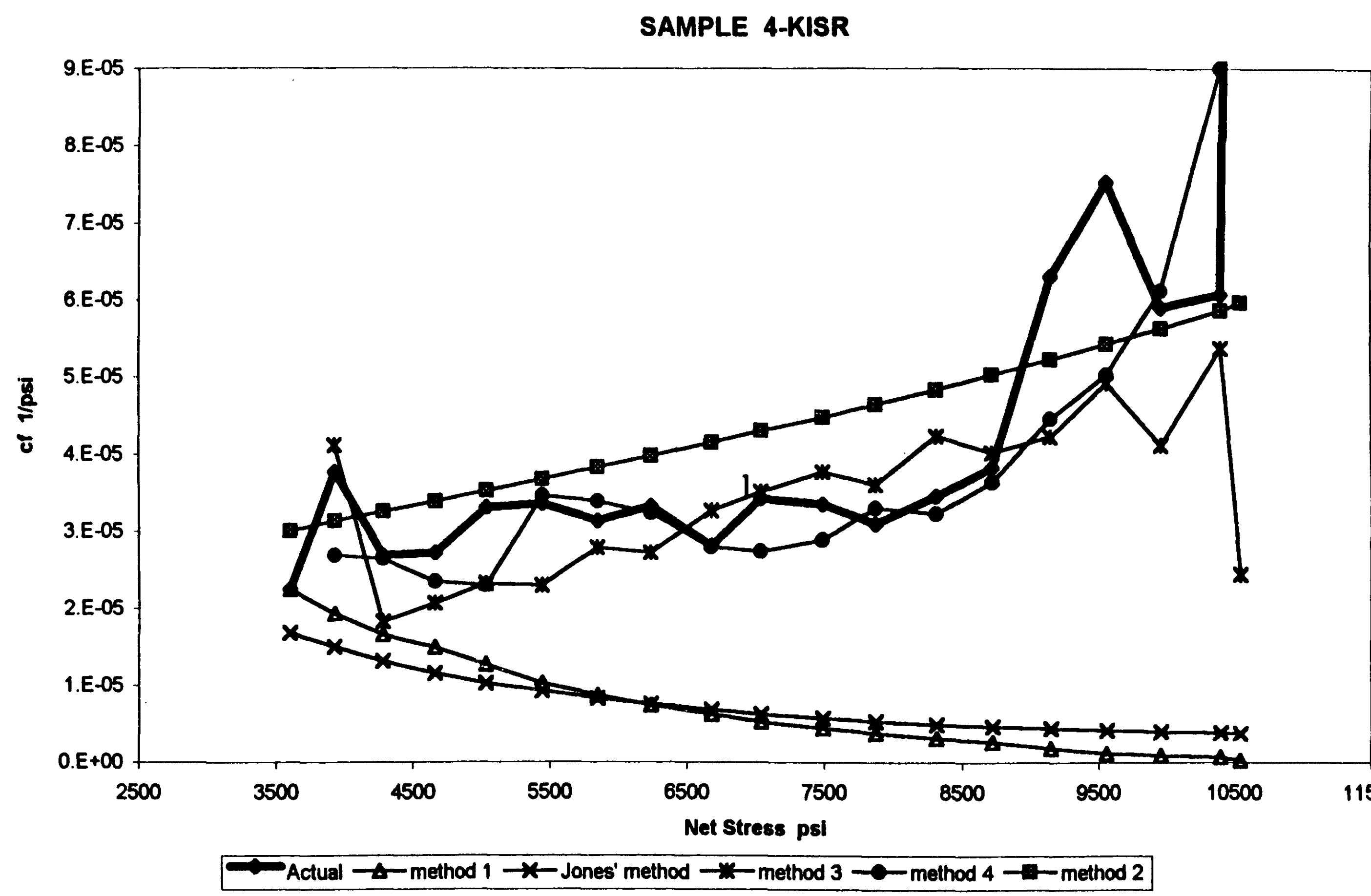

Figure 4-4a: Using different methods to predict and smooth pore compressibility - Study No. 4 - Sample 4-KISR.

STUDY NO. 4

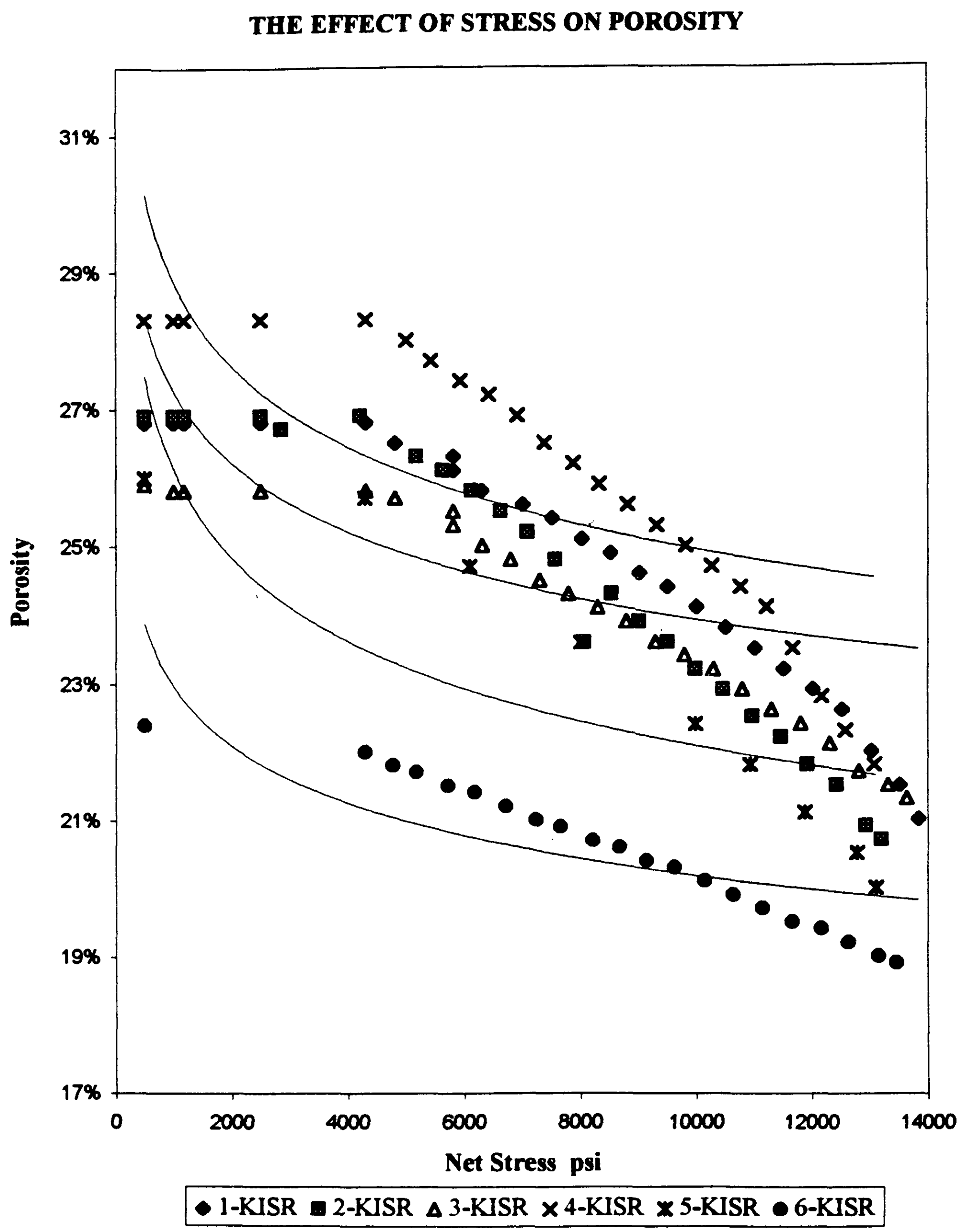

Figure. 4-4b: Porosity - Stres relationship for samples - Study No. 4

4.4.2 Method 2.

The polynomial correlation between porosity and stress from three data points showed a good correlation for all samples (Figure. A-2). Using the polynomial correlation to predict compressibility resulted in a good comparison with the actual data. With only two porosity points used to predict compressibility for sample 5-KISR, the prediction was +20% higher than the actual compressibility.

4.4.3 Method 3.

A straight-line correlation was established between pore void ratio and the cumulative pore compressibility for all samples (Figure 4-4c). Using the straight-line correlation to smooth compressibility data gave good predictions that were only +15% from the actual. The higher estimate for sample 5-KISR was due to the mechanical conditions of the test mentioned earlier.

4.4.4 Method 4.

All samples showed good correlations between Jm and stress (Figure 4-4d). This correlation was used to predict Jm values at higher stresses using a power law correlation fit (Figure C-3). When these correlations were used with only three compressibility points at different stresses to smooth compressibility data, all samples agreed with actual results. It was preferable to use compressibility data from low and high stresses.

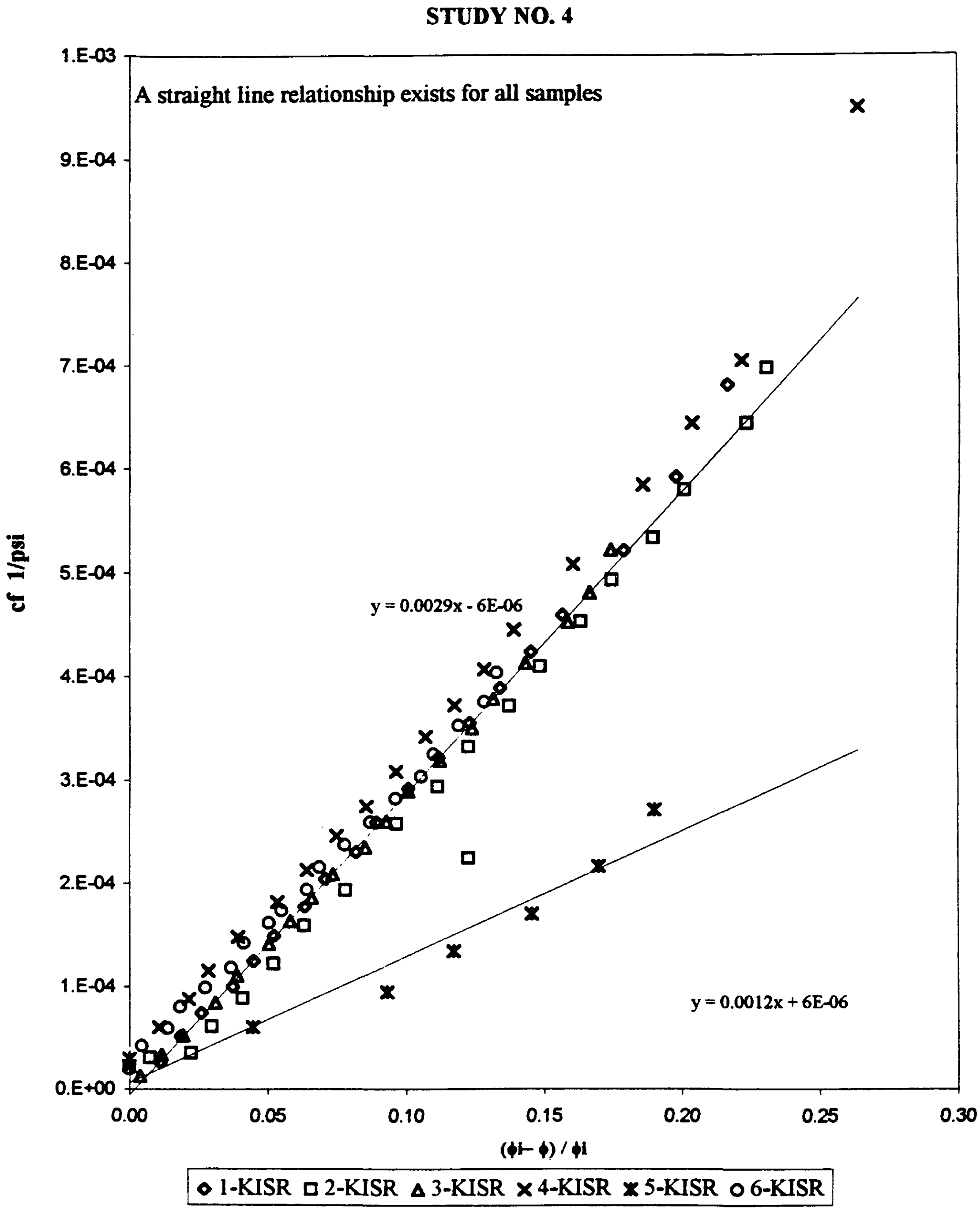

Figure 4-4c: Pore void ratio vs. cumulative compressibility for samples - Study No. 4

Unconsolidated Sandstones

STUDY NO. 4

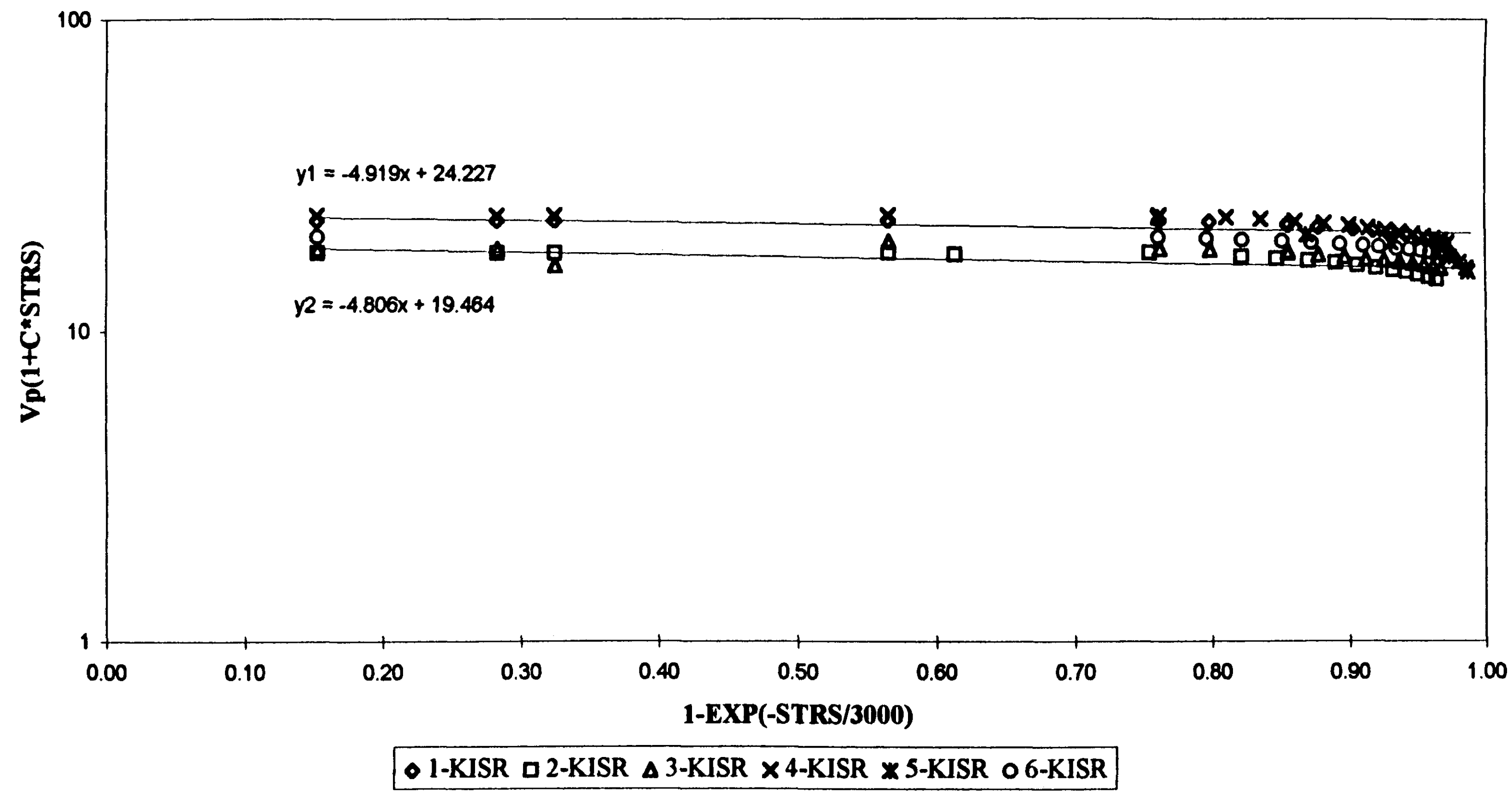

Figure 4-4d: Jones' method of predicting pore volume from two points vs. stress for samples - Study No. 4

4.4.5 Jones' Method

All samples have a good correlation between pore volume and net stress using Jones' method, but the straight-line correlation tended to diverge at higher stress (Figure 4-4e). When using the straight-line correlation to predict compressibility at higher stress, all samples failed to agree with the actual measured data. Samples were up to three orders of magnitude higher than the actual. The same problem is presented in Study 2 for the unconsolidated sand, when compressibility tended to increase with the increase of stress. Jones' theory proved to be invalid for unconsolidated sand when pore compressibility increases with increase of stress.

4.4.6 Conclusions and Recommendations

As in Study 2, unconsolidated sand compressibility tended to increase with the increase of net stress. Illite again proved to lower the estimated prediction when fragments blocked the pores causing a reduction in porosity and permeability. Jones method failed to predict compressibility for the unconsolidated sand in this study.

Methods 2 and 4 agreed well with actual data. Method 4 would best smooth data for unconsolidated sand while Method 2 would predict values that would be very close to the actual compressibility from porosity and stress correlations. Method 3 predicted values within 10% of the actual, while Method 1 and Jones' failed the prediction (the predicted values decreased with stress while the actual values increased).

Table 4-5: Summary of the different methods used to predict and smooth pore compressibility.

Study No.	**Method - 1**	**Method - 2**	**Method -3**	**Method - 4**	**Jones' Method**
1 Consolidated	20%	good	failed	good	20%
2 Unconsolidated	25%	10%	failed (Jones)	good	failed
3 Consolidated	good	good	good	N/A	15%
4 Unconsolidated	failed (Jones)	good	good	good	failed

The percentage values shown above are the difference between the predicted/smoothed methods and the actual data. Methods that failed are marked with (Jones) behaved like Jones' method (compressibility was decreasing for the unconsolidated sand samples).

CHAPTER 5.
TEST PROCEDURE

This thesis is a study of fifteen consolidated samples tested under uniaxial test conditions and thirteen unconsolidated samples tested under triaxial conditions. Five consolidated samples with high clay content were taken from 8,000-12,000 feet intervals with a reservoir pressure of 5,800 psi. Initial values of porosity ranged from 16% to 33%, while permeability ranged from 14.9 md to 5,950 md. Initial values of pore compressibility were tested and ranged between 10.2E-6 to 25.3E-6.

Ten consolidated and friable sand samples with little clay content were taken from two reservoirs at 2,000-8,000 feet. Laboratory stress was presented at 10,000 psi for most samples tested with triaxial test conditions. Initial values of porosity ranged from 2% to 20% and pore compressibility ranged from 2.79E-6 to 303E-6. Permeability was not measured. Two types of triaxial tests were used for the unconsolidated sand samples. Pore pressure and confining stress were varied while axial (ram) stress was kept constant, or pore pressure was kept constant while increasing axial stress.

Seven unconsolidated samples were taken from 14,000-17,300 feet and tested with reservoir pressure of 11,400 psi. Pore pressure and confining stress were varied during the test while ram stress was kept constant. Initial values of porosity ranged from 22% to 28%, permeability ranged from 130 md to 3,600 md, and pore compressibility ranged between 1.19E-6 and 3.03E-6.

Six unconsolidated samples where taken from 14,000 feet and tested with laboratory pressure to approximately 11,000 psi. Initial values of porosity ranged from 22% to 28%, permeability ranged between 1,052 md and 3,625 md, and pore compressibility ranged between 12.6E-6 and 30.3E-6.

All samples, consolidated and unconsolidated, were used to determine the effect of stress changes on sample pore volume, permeability, and pore compressibility. All consolidated and friable samples where cut into plug size samples and the upper and lower surfaces were trimmed flat and perpendicular to the cylinder surface. All unconsolidated samples were frozen with liquid nitrogen and placed in special sleeves. After inserting the samples into the core holder, the plugs were vacuumed to remove excess air which may have become entrapped in the cores and core holder. Core samples were then saturated with brine and stressed to reservoir conditions.

In all fifteen consolidated samples, a uniaxial test cell was used to determine the compaction of the samples. Core samples were put in core holder and placed under a vacuum to insure that no air could occupy the sample's pore space. Samples were then saturated with brine, and 2,000 psi confining stress was applied. Samples were then installed in a rigid cylinder to prevent lateral deformation while axial stress was applied to approximately 14,000 psi. Pore pressure was initially increased to reservoir pressure and then depleted while increasing the axial (ram) stress.

For the unconsolidated samples, a triaxial test cell was used to measure pore compressibility. In the triaxial cell, axial stress was used to simulate vertical overburden stress in the reservoir, and the confining stress (radial) was used to simulate horizontal stresses. To obtain the initial stress conditions, cores were loaded into the triaxial core holder with an applied stress of approximately 100 psi. The axial and radial stresses were then increased together while maintaining a differential of less than 500 psi. When the pore pressure reached the initial reservoir pressure, the sleeve pressure was shut in and the axial stress was increased to reservoir overburden pressure. During the pore pressure depletion, the axial stress was maintained at a nominally constant value to simulate the constant weight of the reservoir overburden. The pore volume of fluid withdrawn and the corresponding decrease in pore pressure were used to calculate pore volume compressibility. In this thesis, net stress is defined by:

Net Stress = (Net Radial Stress) - (Net Axial Stress)

Net Stress = (Axial Stress - Radial Stress) - (Axial Stress - Pore Pressure)

Unlike some of the consolidated samples, SEM examination of the unconsolidated samples revealed moderately sorted, subangular sand grains which were loosely compacted and had very little cement holding the grains together. Normal burial and compaction of samples with clay have resulted not only in close packing of grains, but also in cracking and deformation of detrital micas. Many of the fragments and broken parts were so small that, if they were to break loose and migrate, they could potentially block pore throats and further contribute to the permeability reduction already associated with increased compaction. Because the change in pore volume increased with the increase of stress, pore volume compressibility for the unconsolidated samples tended to increase as rock became more plastic and began to fail. These are the four studies of this thesis:

Study No.1 Consolidated sand at high pressure tested with uniaxial apparatus.

Study No.2 Unconsolidated sand at high pressure tested under triaxial test apparatus. Pore and confining pressure were varied while ram stress was constant.

Study No.3 Consolidated sand at low pressure tested with uniaxial apparatus.

Study No.4 Unconsolidated sand at high pressure tested with triaxial apparatus. Pore pressure was kept constant while ram stress was increased.

CHAPTER 6.
CONCLUSIONS

Based on the analysis of predicting and smoothing compressibility data from the six discussed methods, the following results were observed:

1. New methods have been developed to predict compressibility from minimum laboratory requirements and to smooth inconsistency in laboratory results.

2. From a good correlation between porosity and stress (three points are recommended), pore compressibility can be predicted successfully.

3. From three or four values of pore compressibility, correlations can be established to smooth data and predict values at higher stress.

4. Minimizing the number of pore compressibility data measured in the laboratory will save time and money. For example, instead of measuring pore compressibility at ten stress values, three or four points are enough, with the developed methods.

5. A triaxial test cell seems to be more representative to reservoir conditions and is suitable to use for unconsolidated sand.

6. A uniaxial test cell is suitable to use for consolidated sand if gap and irregular shape do not exist in the plug.

7. Friable sand seems to fail the uniaxial test criteria.

8. Method No. 1 predicts compressibility from initial compressibility when a good correlation exists between porosity and stress. Generally speaking, the predicted values for consolidated samples are within $\pm 20\%$ of the actual measured data. Predictions fail for the friable sand samples.

9. Method No. 2 of predicting compressibility from stress-porosity calculation gave very good predictions for all samples. A power law equation should be used to best fit porosity-stress correlations for the consolidated sand. A polynomial equation should be used to best fit data for the unconsolidated sand.

10. Method No. 3 of smoothing compressibility data from the linear relationship between pore void ratio and the cumulative pore compressibility failed to work for the consolidated sand at low stress with uniaxial test measurement but agreed very well with the consolidated sand measured at high stress using the uniaxial cell. Smoothing compressibility data for unconsolidated sand with high clay content measured at the triaxial cell gave poor correlations for all samples. Unconsolidated sand with no clay content and measured with triaxial cell gave very good smoothing correlations to the actual data.

11. Method No. 4 of smoothing compressibility data by the correlations Jm and pore compressibility gave smooth predictions for all samples, consolidated and unconsolidated sand.

12. Jones' method of predicting compressibility from two pore volume points gave poor estimates for all unconsolidated sand, and 20% of the actual for the consolidated

sand. Part of the failure was that the predicted compressibility was assumed to decrease with increasing net stress, yet the actual unconsolidated compressibilities increased.

13. Compressibility for consolidated sand tended to decrease with the increase of net stress until the sample reached its plastic region and started to fail. Then compressibility increased with increasing net stress. Compressibility of unconsolidated sand tended to increase with the increase of net stress as the loose grains compacted more with higher stress.

14. Clay swelling can reduce porosity and permeability as stress increases and tends to increase compressibility for the unconsolidated sand. Samples with a large amount of illite gave compressibility estimates lower than the clean samples.

15. The thesis also recommends to carry on the investigations in Chapter 7.

CHAPTER 7.
RECOMMENDATIONS FOR FUTURE WORK

Three methods of this thesis are not included due to minimum requirements to establish such conclusions. These sections are (1) the use of porosity, permeability, flow-rate, and stress to predict pore compressibility, (2) the correlation between Poisson's ratio and stress for consolidated and unconsolidated sand samples, and (3) the use of porosity data from well logs to predict compressibility without laboratory measurements.

Three samples were used to test the prediction of compressibility from porosity, permeability, flow rate and stress for consolidated sand samples. Fifteen unconsolidated samples were used to correlate Poisson's ratio to stress, and all samples agreed very well. Five consolidated samples failed the correlation. Finally, equations of porosity from logs are recommended for investigation to determine if they can be used to predict compressibility.

7.1 Predicting Compressibility from Porosity-Permeability and Flow Rate

From the previous work of relating permeability-porosity relationship to pore volume compressibility, Method 4 can be modified to develop a promising method applicable to use without laboratory measurements. A method has been developed to smooth compressibility by relating the effect of permeability and porosity on stress. Rearranging Darcy's equation to the form of Eq. (7-1):

$$k = \frac{Q \mu L}{A(dP)} \tag{7-1}$$

$$k_i = \frac{Q_i \mu L_i}{A_i (dP)_i} \tag{7-2}$$

Normalized permeability is defined as:

$$k_n = k/ki \tag{3-15}$$

substituting Eq. (7-1) and Eq. (7-2)in Eq. (3-15), then normalized permeability can be redefined as:

$$k_n = \frac{Q \mu L}{A\, dP} * \frac{A_i\, dP_i}{Q_i \mu L_i} \tag{7-3}$$

where k = permeability, md

L = length of core

A = cross section area

Q = flow rate

dP = pressure differential

μ = fluid viscosity

i = initial conditions

From the relationship between pore volume and porosity:

$$\phi = \frac{V_p}{V_b} \tag{7-4}$$

$$\phi_i = \frac{V_{p_i}}{V_{b_i}} \tag{7-5}$$

Eq. (3-2) can be rewritten as:

$$\phi_n = \frac{Vp}{Vb} * \frac{Vbi}{Vpi} \tag{7-6}$$

dividing Eq. (7-6) by Eq. (7-3)

$$\frac{k_n}{\phi_n} = \frac{Q\,\mu\,L}{A\,d\,P} * \frac{A_i\,d\,P_i}{Q_i\,\mu\,L_i} * \frac{Vb}{Vp} * \frac{Vpi}{Vbi} \tag{7-7}$$

multiplying Eq. (7-7) by (L/L)*(Li/Li) to cancel the cross section area and bulk volume,

$A = V_b * L$

$A_i = V_{bi} * L_i$

$$\text{Jm} = \frac{L^2 * V_{pi} * dp * Q}{V_p * L_i^2 * dp * Q_i} \tag{7-8}$$

Rearranging Eq. (7-8) to predict pore volume:

$$\text{Vp} = \frac{\phi_n}{k_n}\frac{Q}{d\,P}\frac{d\,P_i}{Q_i}V_{pi} \tag{7-9}$$

Substituting Eq. (7-8) in Eq (3-9) to calculate pore volume compressibility:

$$c_f = \frac{1}{V_p}\frac{dV_p}{dP} \tag{3-10}$$

$$c_f = \frac{k_n}{\phi_n * Q} * d\left(\frac{Q * \phi_n}{k_n dP}\right) \tag{7-10}$$

for a constant flow rate, Eq. (7-10) will be written as:

$$Cf = \frac{k_n}{\phi_n} * d\left(\frac{\phi_n}{kn * dp}\right) \tag{7-11}$$

for a constant *dp* (pressure drop), Eq. (7-11) can be written as:

$$Cf = \frac{k_n}{\phi_n * Q} * d\left(\frac{Q\,\phi_n}{k_n}\right) * \frac{1}{dp} \tag{7-13}$$

Data from three consolidated sand samples were available. Figures 7-1a, b, and c illustrate the correlation between the actual compressibility in the laboratory and the predicted data using the above equations. Two correlations were used: one accounts for the change in length, and the other assumes constant length. Both correlations predicted values very close to the actual data.

When this theory proves to be valid, not only theoretically but also experimentally, it can be used for future calculations of pore volume compressibility. The theory is indeed more practical, useful, easy and less costly, and less time-consuming than current methods.

7.2 Predicting Poisson's Ratio for Unconsolidated Sand from Stress Conditions

Compressibility measured using hydrostatic stress in laboratory tests can be almost double that occurring under the uniaxial strain conditions believed to exist in the reservoir. In the reservoir, with stress applied from above by the overburden and lateral deformation being prevented by the surrounding rock, only vertical compaction occurs, which is a lesser change than the hydrostatic test compaction.

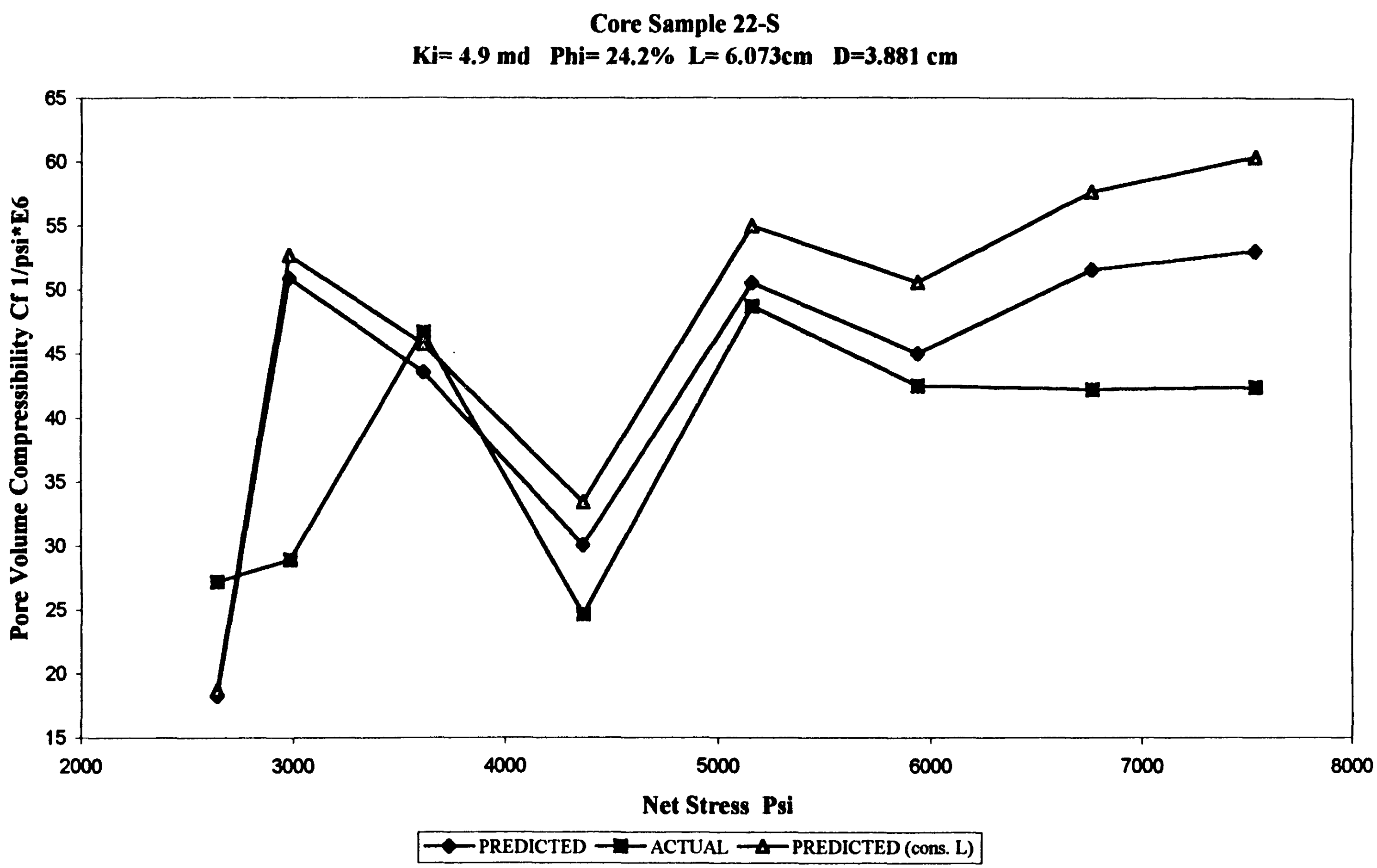

Figure. 7-1a: Predicting compressibility from porosity-permeability-flow rate at different stress - Sample 22-S.

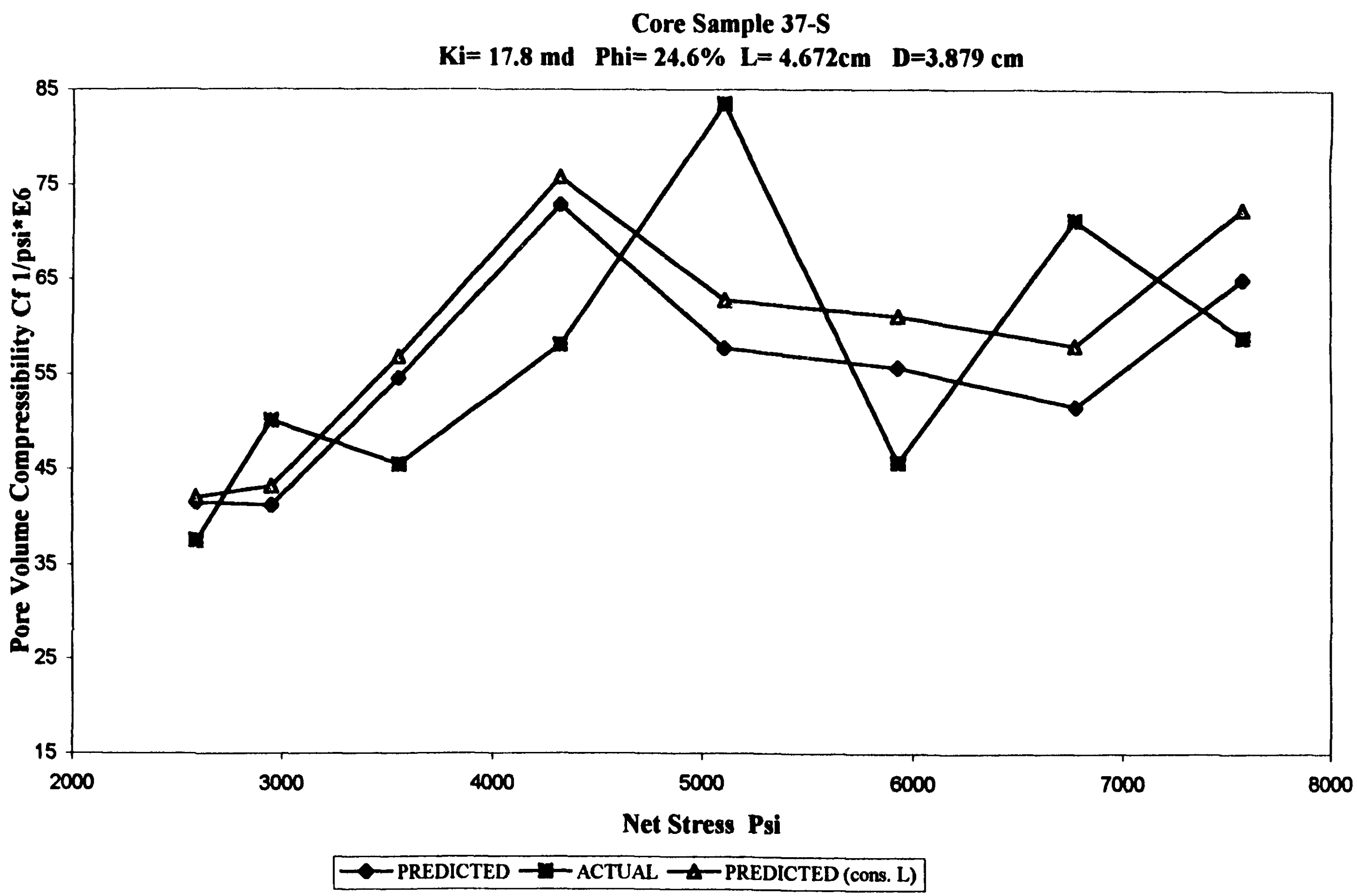

Figure. 7-1b: Predicting compressibility from porosity-permeability-flow rate at different stress - Sample 37-S.

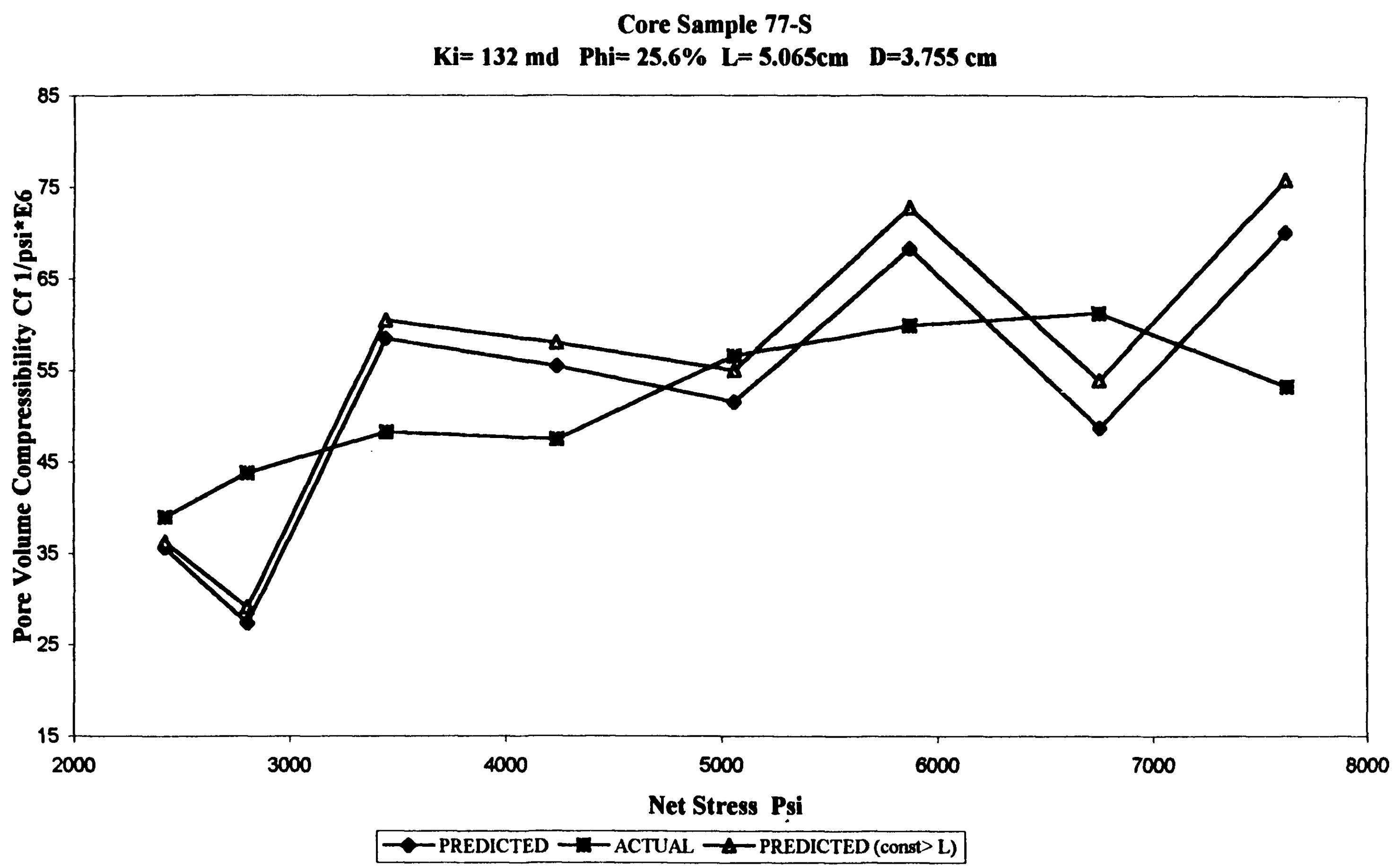

Figure. 7-1c: Predicting compressibility from porosity-permeability-flow rate at different stress - Sample 77-S.

Jones and many engineers have developed correlations to convert laboratory data to reservoir conditions by using Poisson's ratio for translation factor,

$$\frac{\sigma_H}{\sigma_Z} = \left(\frac{\nu}{1-\nu} \right)^{(1/n)} \tag{7-14}$$

Where the exponent n for sandstones and carbonates varies for given rocks. Fifteen unconsolidated samples from different reservoirs were used to predict Poisson's ratio at different stresses. It is empirically found that:

$$\text{Poisson's Ratio } (\nu) = 0.5 * (\text{Net later stress / Net Axial Stress})^{0.55} \tag{7-15}$$

All fifteen samples were run under a triaxial cell and the net ram was almost constant while pore pressure decreased (Figure 7-2a,b). If this correlation exists for most unconsolidated sand then it will furnish valuable information without the need for laboratory measurements.

This relationship failed to work for the consolidated samples tested by Hugues (a graduate student from Colorado School of Mines). Even though a power law equation existed (Figure 7-3), the exponent varied for each sample. More consolidated and unconsolidated samples with more SEM information available are recommended for the analyses and investigations.

The consolidated sand failed to have the same trend as the unconsolidated sand. This could be due to several factors. The test procedure was used on the unconsolidated

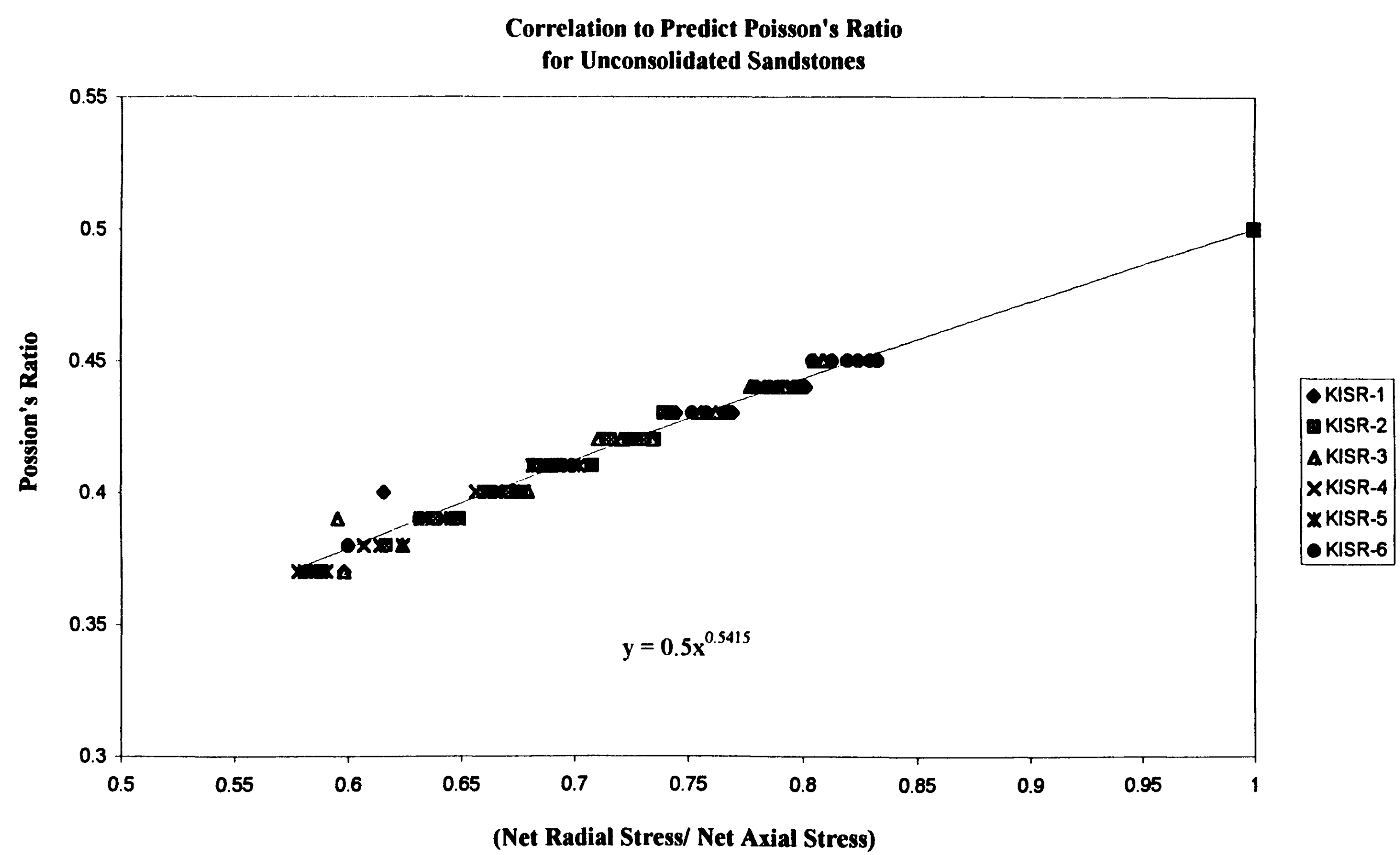

Figure. 7-2a Correlation to predict Poisson's ratio from stress conditions - Study No. 4

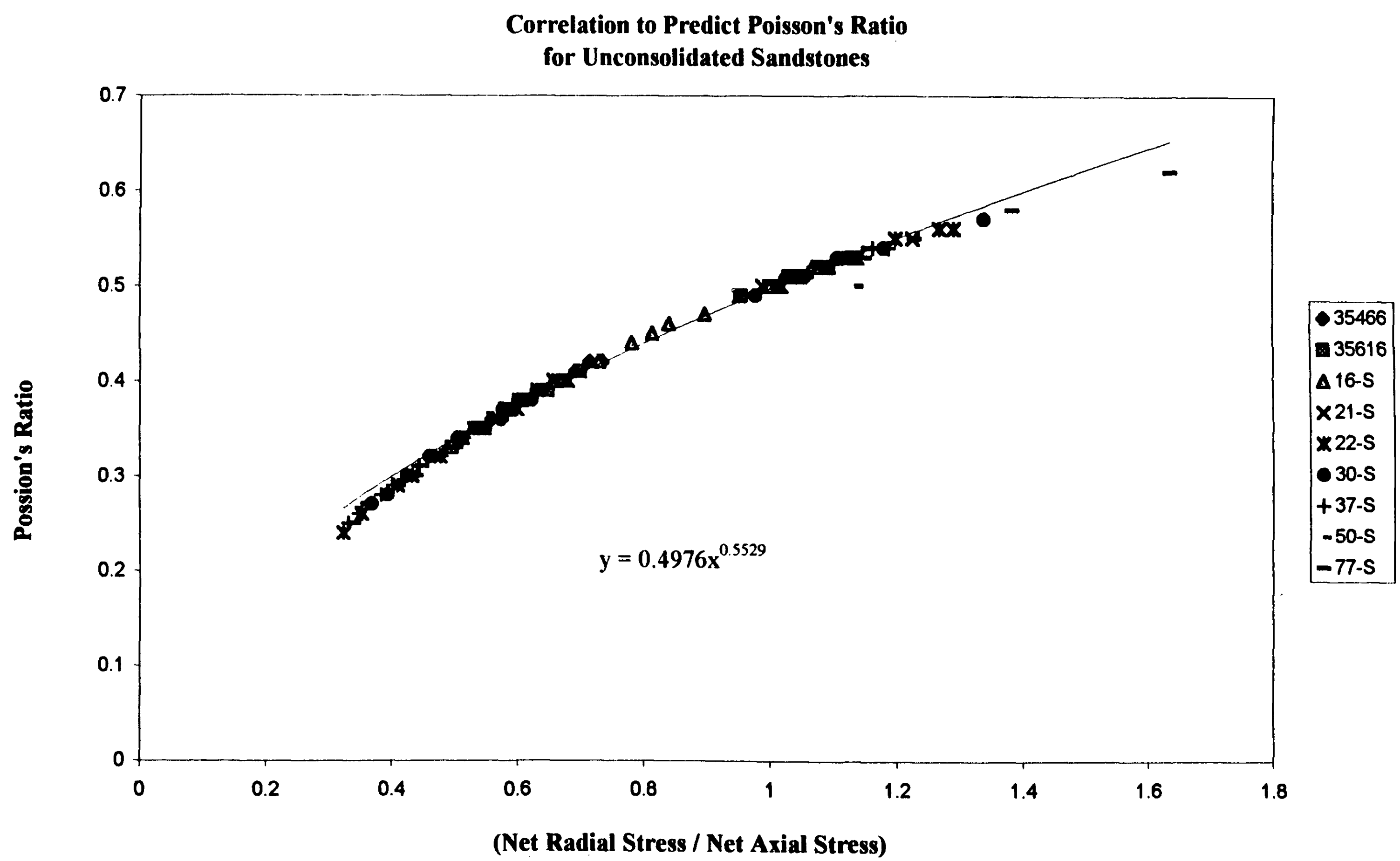

Figure. 7-2b: Correlation to predict Poisson's ratio from stress conditions - unconsolidated sand.

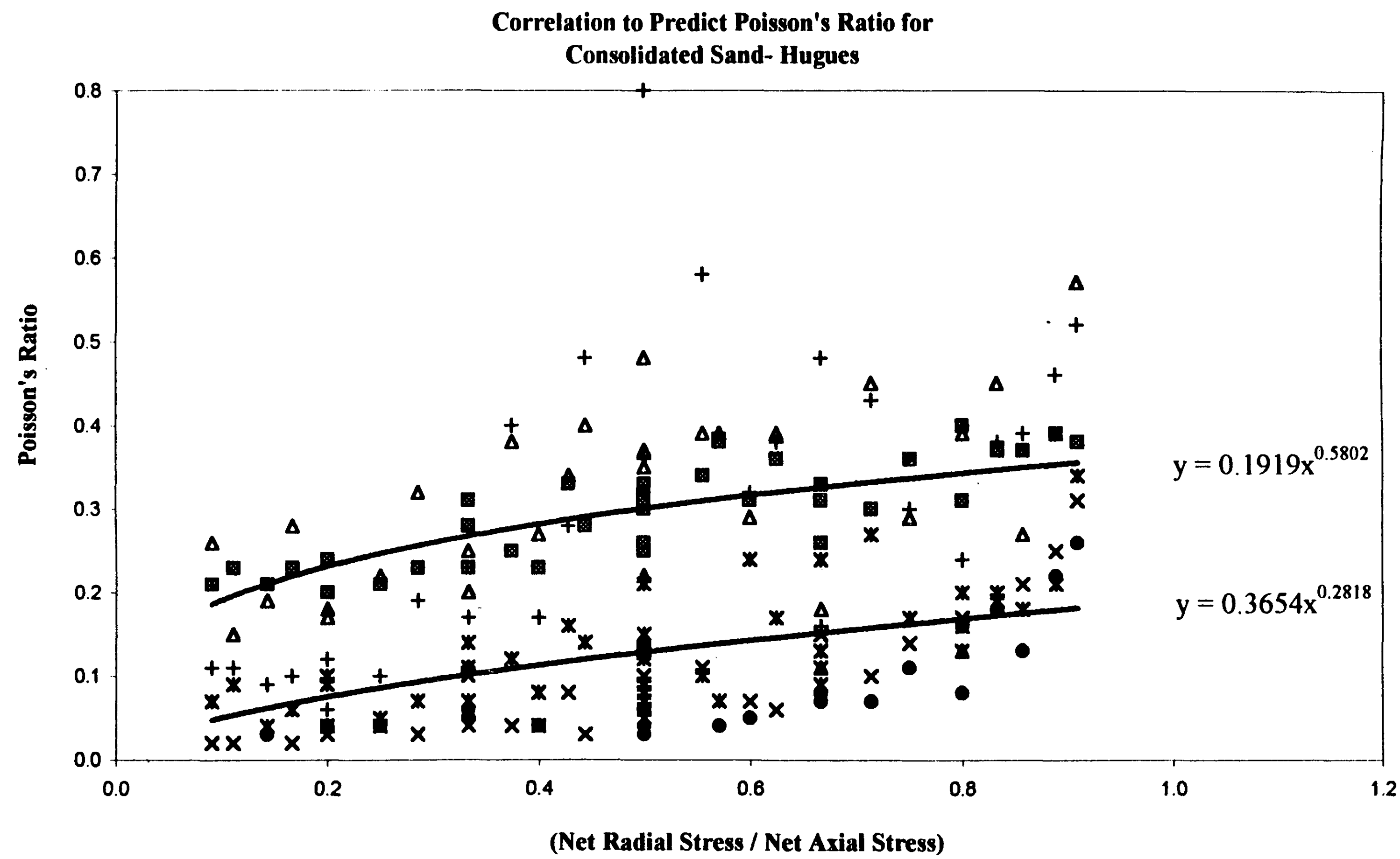

Figure. 7-3: Correlation to predicting Poisson's ratio from static test measurements by Hugues.

sand; pore pressure was increased initially until it reached reservoir conditions, then decreased with the start of the compressibility test. In the consolidated sand test, pore pressure was set to zero and only axial and confining stress were applied. Applying pore pressure to the sample while changing confining stress kept the sample's grains more compacted. Having a zero pore pressure and applying confining stress up to 6000 psi could cause more compaction. Another reason for the poor fit could be due to the test procedure Hugues used for the measurements and analysis.

In Hugues' study, lateral stress was constant while axial stress was increased and decreased; then lateral stress was increased and kept constant while axial stress was increased and decreased again. Samples could have reached the plastic conditions where some of the deformed volume could not retain its original conditions. For unconsolidated sand, pore pressure, confining stress, and ram stress were varied simultaneously. Sometimes one pressure or stress was kept constant, but if samples reached the plastic condition, the sample was not retested for compressibility. There could be other reasons why no correlation was established for the consolidated sand that will only be known if more sample data becomes available.

7.3 Using Porosity from Well Logs to Calculate Compressibility

Since Method 2 proved to give good compressibility predictions by using porosity and stress, it was also desirable to test the validity of the method with porosity values measured from well logs . Using porosity from well logs to predict compressibility will eliminate laboratory measurements. It is recommended to measure porosity at two or three stresses to generate a power law equation or polynomial as discussed earlier in

ARTHUR LAKES LIBRARY
COLORADO SCHOOL OF MINES
GOLDEN, CO 80401

Chapter 4. Data from sonic, acoustic, and other logging tools are commonly used in oil fields and can be valuable information in calculating porosity values.
Porosity measured from density logs is defined as:

$$\phi = \frac{\rho_m - \rho_b}{\rho_m - \rho_f}$$

where ρ_b = bulk density

ρ_m = matrix density

ρ_f = fluid density

Another way to measure porosity is by using acoustic log as follows:

$$\phi = \frac{\Delta t - \Delta tm}{\Delta tf - \Delta tm} * \frac{1}{Cp}$$

$$Cp = \frac{\Delta t_{sh} * c_{sh}}{100}$$

where Δt = acoustic travel from the borehole acoustic log

Δtm = acoustic travel time for the rock matrix

Δtf = acoustic travel time for interstitial fluids

C_{sh} = shale compaction coefficient

In conclusion, if data from a reservoir (porosity, permeability, flow-rate, and stress) can be used to predict compressibility, it will eliminate laboratory measurements. If the correlation to predict Poisson's ratio proved to be valid for both consolidated and unconsolidated sand, the correlation will be useful to convert laboratory data to reservoir conditions. Minimizing or eliminating the amount of laboratory data has a great potential to save money and consume less time.

CHAPTER 8.
NOMENCLATURE

All attempts were made to maintain consistency in nomenclature

English Symbols:

A	Cross section area
a,b	Point of best fit
a_k	Point of best fit
av	(-slope) of the straight line transformation by Jones
C	Decay constant arbitrarily set to 3E-6
Cm	Uniaxial compaction coefficient
cf	Pore compressibility
c_b	Bulk compressibility
c_e	Effective compressibility of the reservoir
c_o	Oil compressibility
c_g	Gas compressibility
c_w	Water compressibility
c_t	Total compressibility
c_b	Bulk compressibility
cc_f	Cumulative compressibility

c_{sh} Shale compaction coefficient

dp Pressure change (from integral)

i Initial conditions

Jm Function relates the normalized permeability to normalized porosity

k Permeability

k_i Initial permeability

k_n Normalized permeability

L Length

m Slope of the straight line equation

N Initial oil-in-place

N_p Oil production during the pressure decline

P_p Pore pressure

Q Flow rate

Qi Initial flow rate

STRS Net Stress = σ

Vi Initial volume

V_p Pore volume

V_b Bulk volume

V_g Grain volume

Greek Symbols:

ϕ (phi) Porosity

ϕ_n Normalized porosity

β The ratio of the rock matrix to rock bulk compressibility

ΔP Pressure difference

μ	Viscosity of fluids
σ	Net stress
$\sigma *$	Empirical value = 3000 psi (Jones)
σ_H	Horizontal stress
σ_Z	Axial stress
ρ_m	Matrix density
ρ_b	Bulk density
ρ_f	Fluid density
Δt	Acoustic travel time for the borehole
Δt_m	Acoustic travel time for the matrix
Δt_f	Acoustic travel time for the fluids
Δt_{sh}	Acoustic travel time for shale
v	Poisson's ratio

REFERENCES

Adams, S. H. & Williamson, E. D. (1923). The Compressibility of Minerals and Rocks at High Pressure. *Carnegie Institute of Geophysics Laboratory*(April), Vol. 195, No. 484, 475-529.

Anderson, M. A. (1985). *Predicting Reservoir Conditions Pore-Volume Compressibility from Hydrostatic-Stress Laboratory Data.* Paper presented at the 60th Annual Technical Conference and Exhibition of the Society of Petroleum Engineers (Sep. 22-25). Paper No. 14213, Las Vegas, NV.

Bell, F. G. (1983). *Fundamentals of Engineering Geology*. London, England: Butterworth & Co.

Bishop, A. W. & Henkel, D. J. (1962). *The Measurement of Soil Properties in the Triaxial Test*, 2nd ed., London, England: E. J. Arnold & Son, Ltd.

Botset, H. G. & Reed, D. W. (1935). Experiment of Compressibility of Sand(July), *American Association of Petroleum Geology*, Vol. 19, No. 7, 1053-1060.

Charles, B. Carpenter & Ceorge B Spencer, (1940). *Measurements of Compressibility of Consolidated Oil-Bearing Sandstones*. United States Department of the Interior, R. I. 3540.

Chierici, G. L., Ciucci, G. M., Eva, F. & Long, G. (1967). *Effect of Overburden Pressure on Some Petrophysical Parameters of Reservoir Rocks*. Proc. 7th World Petroleum Conference, Mexico City, 309-330.

Dobrynin, V. M. (1962). Effect of Overburden Pressure on Some Properties of Sandstone(December). *Society of Petroleum Engineering Journal*. 360-366.

Djebbar T. and Erle C. (1996). Petrophysics: Theory and Practice of Measuring Reservoir Rock and Fluid Transport Properties. Gulf Publishing Company, Houston, Texas.

Farmer, I. (1983). *Engineering Behavior of Rocks*, 2nd Ed. London, England: Chapman and Hall Ltd.

Fatt, I. (1958). Pore Volume Compressibilities of Sandstone Reservoir Rocks(March). *Journal of Petroleum Technology*, 64-66.

Geerstma, J. (1953). The Effect of Fluid Decline on Volumetric Changes of Porous Rocks: *Trans. AIME*, Vol. 210, 331-340.

Gnirk, P. E. (1972). The Mechanical Behavior of Uncased Wellbores Situated in Elastic/ Plastic Media Under Hydrostatic Stress. *Trans. AIME*, Vol. 253, 49-59.

Hall, H. N. (1953). Compressibility of Reservoir Rocks. *Trans. AIME*, Vol.198, 309-311.

Hawkins, M. F., Jr. (1955). Material Balance in Expansion Type Reservoirs Above Bubble Point, *Trans. AIME,* Vol. 204, 267-273.

Hobson, G. D. & Mrosovsky, I: (1956). Material Balance Above the Bubble Point, *Trans. AIME*, Vol. 207, 347-352.

Hundall, J. S., (1934). Unpublished paper read before theAmerican Association of Petroleum Geology Annual Meeting(March), Dallas, Texas.

Jones, S. C. (1988). Two Point Determination of Permeability and PV vs. Net Confining Stress (March), *Society of Petroleum Engineering, Formation Evaluation*, 235-241.

Keelan, Dare K. (1977). Core Analysis manual of Core Laboratories, Inc.

Nelson, R. A. (1980). A Discussion of The Approximation of Subsurface (Burial) Stress Conditions in Laboratory Experiments, *American Association of Petroleum Geology*, 311-321.

Newman, G. H. (1973). Pore Volume Compressibility of Consolidated, Friable, and Unconsolidated Reservoir Rocks Under Hydrostatic Loading (February), *Journal of Petroleum Technology*, 129-134.

Ruddy, I. Et al. (1989). Rock Compressibility, Compaction, and Subsidence in High Porosity Chalk Reservoirs-A case Study of Valhall Field (July), *Journal of Petroleum Technology*, 741-746.

Sampath, K. (1982). A New Method to Measure Pore Volume Compressibility of Sandstones (June), *Journal of Petroleum Technology*, 1360-1362.

Stiler Jr. J. H. (1988). The Use of Routine and Special Core Analysis in Characterizing Brent Group Reservoirs (Oct. 16-19), *Society of Petroleum Engineering* 18386, Paper Presented at The European Petroleum Conference, North Sea, UK.

Teeuw, D. (1971). Prediction of Formation Compressibility For Laboratory Compressibility Data, *Trans. AIME.* Vol. 251, 263-271.

Van der Knaap, W. (1960). Effect of Changing The Porous Volume in Oil-Bearing Rock on The Estimate of Oil Reservoirs, *Erdoel kohle* 13, No. 5, 305-312.

Van der Knaap, W. (1959). Nonlinear Behavior of Elastic Porous Media, *Trans. AIME*, Vol. 213, 362-364.

Van Tuyl, F. M. & Beckstrom, R. C. The Effect of Pressure on the Migration and Accumulation of Petroleum (October), *American Association of Petroleum Geology*, Vol. 10, No. 10, 917-930.

Zimmerman, R. W., Somerton, W. H., & King, M. S. (1986). Compressibility of Porous Rocks, *Journal of Geophysics Research*, No. B12-91, 765-777.

APPENDICES

APPENDIX A-1

Porosity - Stress relationship for unconsolidated sand - Study No. 2

APPENDIX A-1

Porosity-Stress relationship for unconsolidated sand

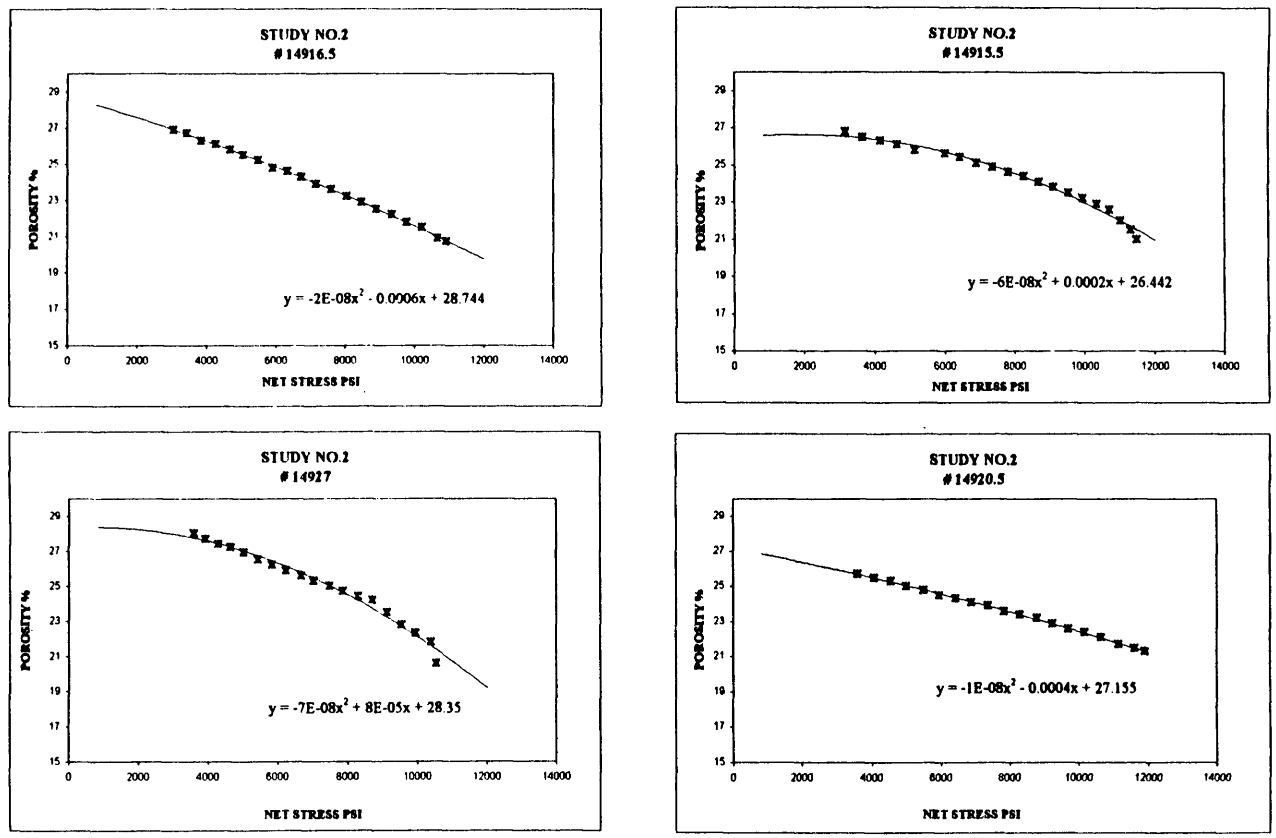

APPENDIX A-1

Porosity-Stress relationship for unconsolidated sand

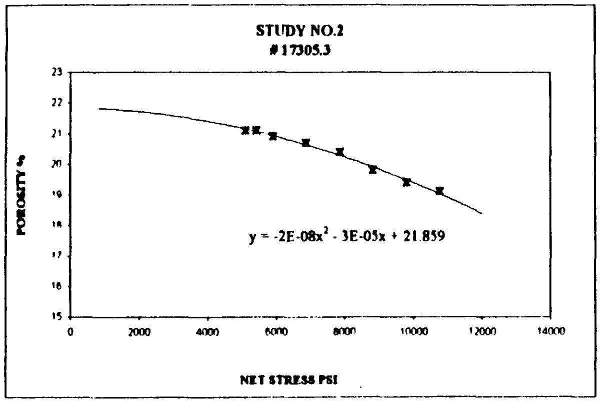

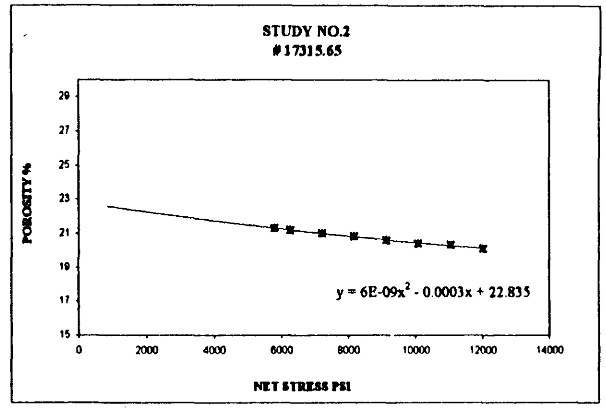

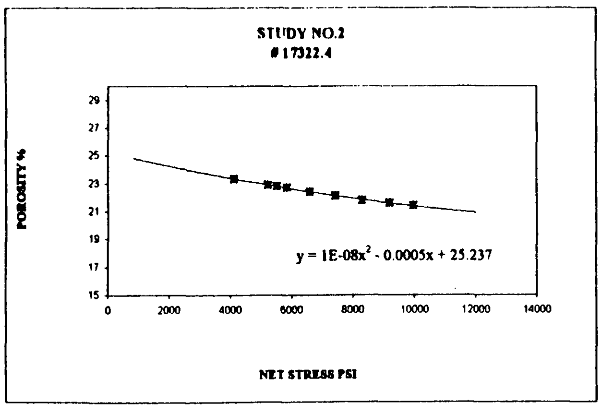

APPENDIX A-2

Porosity - Stress relationship for unconsolidated sand - Study No. 4

APPENDIX A-2
Porosity-Stress relationship for unconsolidated sand

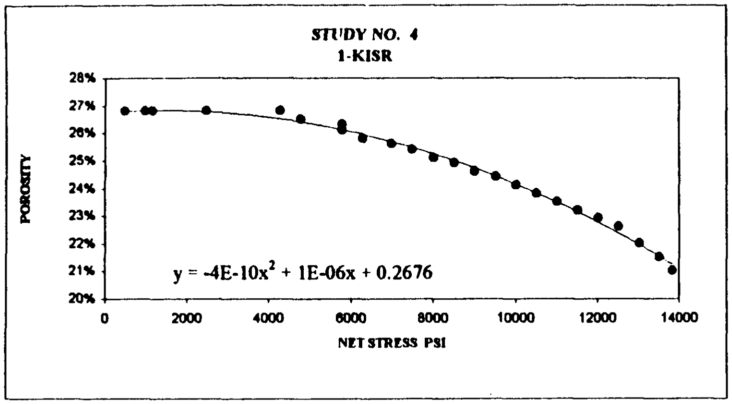

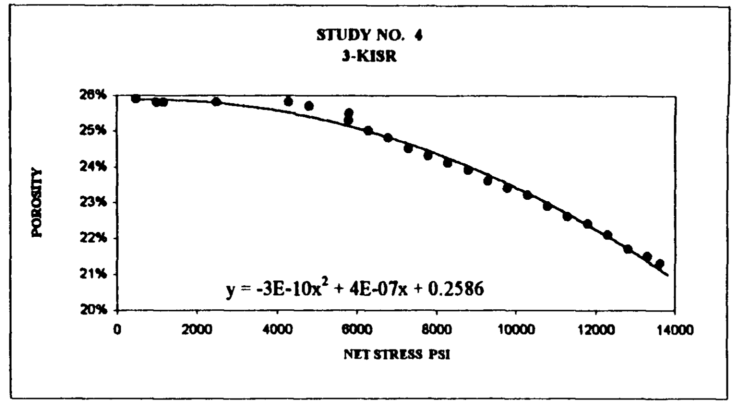

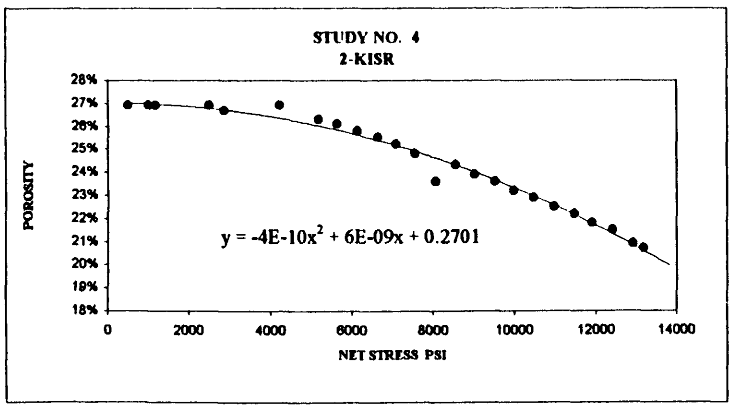

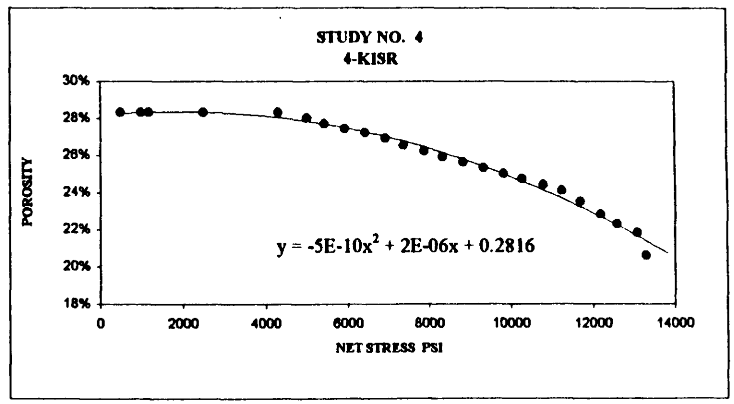

APPENDIX A-2

Porosity-Stress relationship for unconsolidated sand

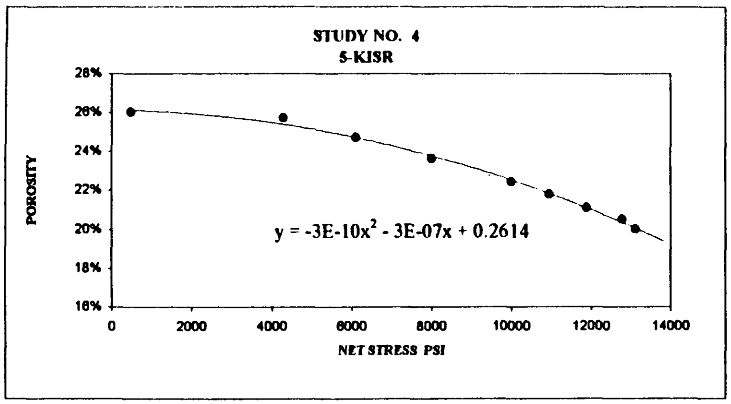

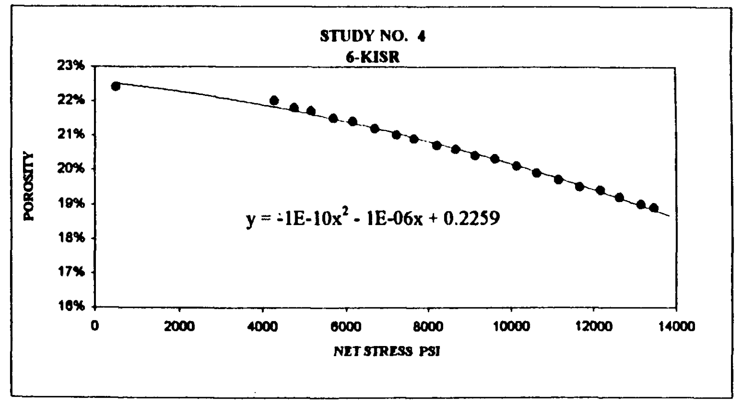

APPENDIX B-1

Correlations to predict and smooth pore compressibility - Study No. 1

APPENDIX B-1

Correlations to predict and smooth pore compressibility - Study No. 1

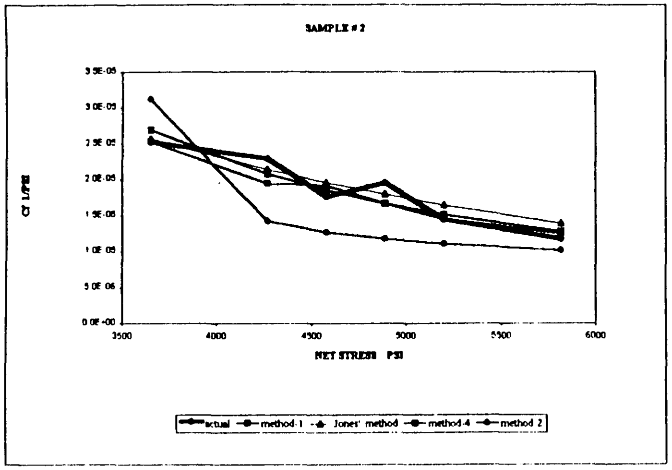

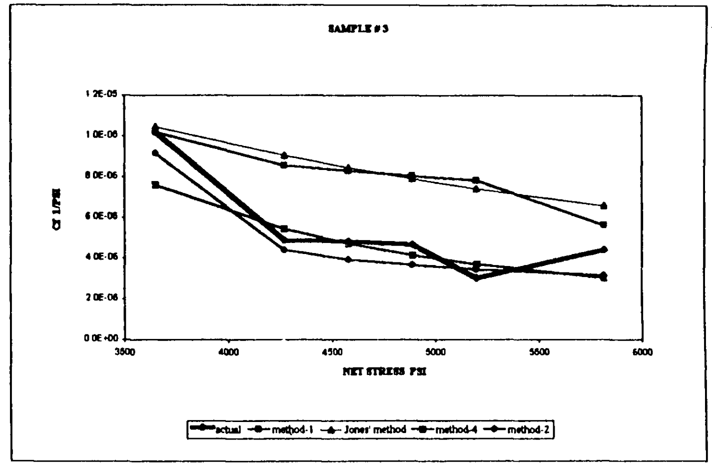

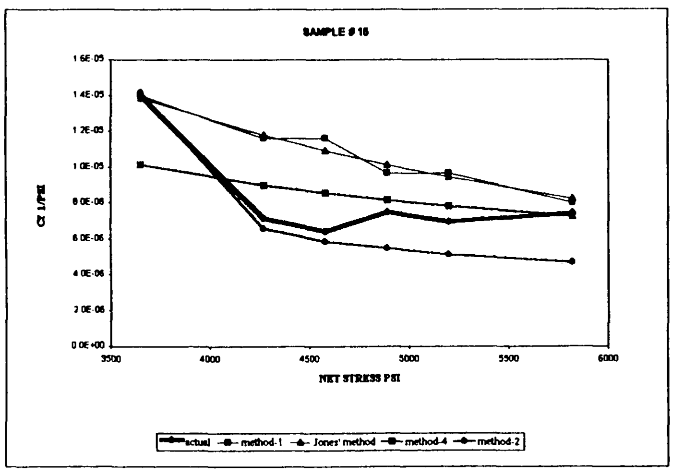

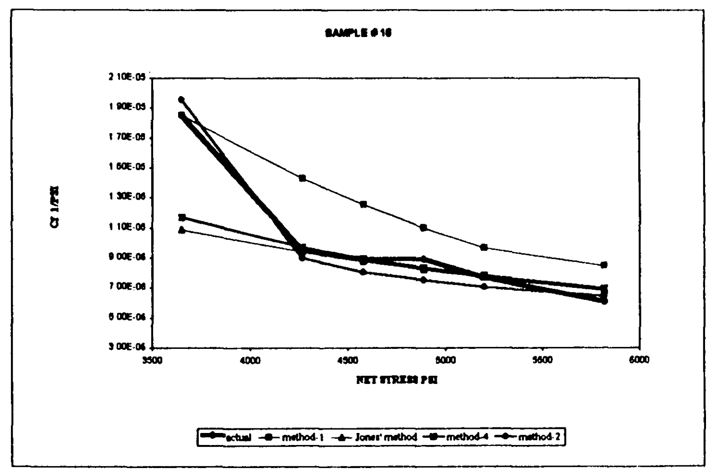

ARTHUR LAKES LIBRARY
COLORADO SCHOOL OF MINES
GOLDEN, CO 80401

APPENDIX B-2

Correlations to predict and smooth pore compressibility - Study No. 2

APPENDIX B-2
Correlations to predict and smooth pore compressibility - Study No. 2

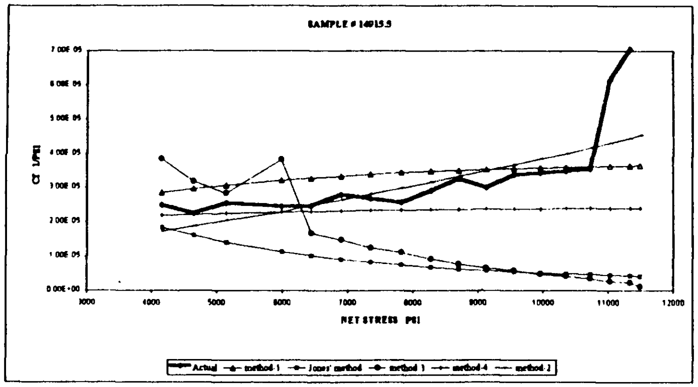

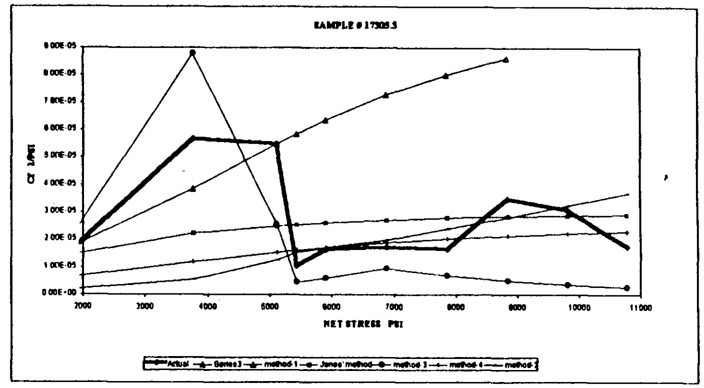

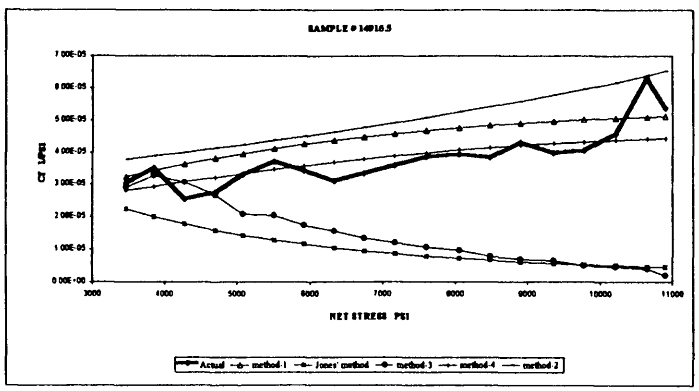

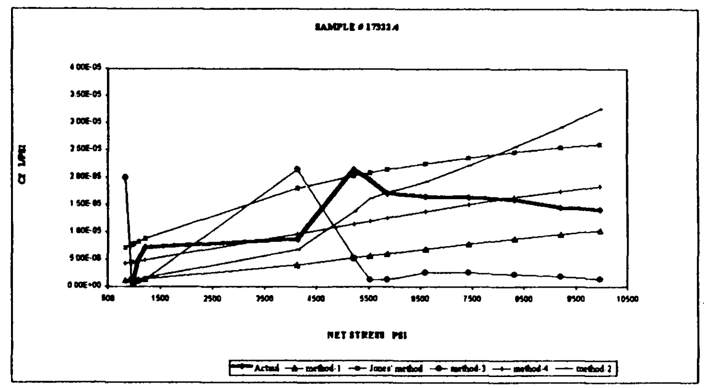

APPENDIX B-2

Correlations to predict and smooth pore compressibility - Study No. 2

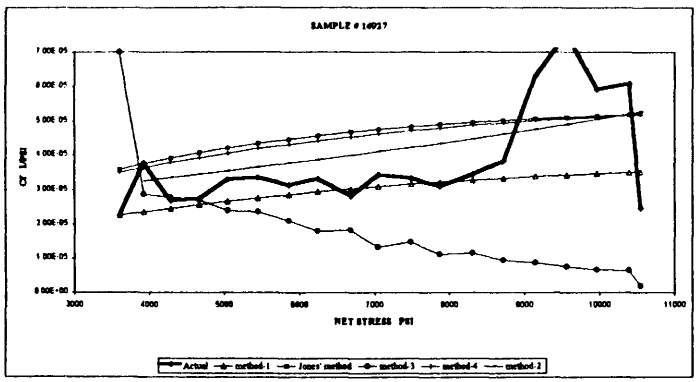

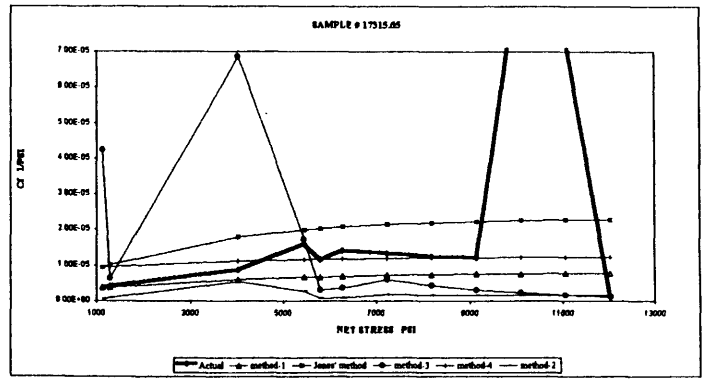

APPENDIX B-3

Correlations to predict and smooth pore compressibility - Study No. 3

APPENDIX B-3

Correlations to predict and smooth pore compressibility - Study No. 3

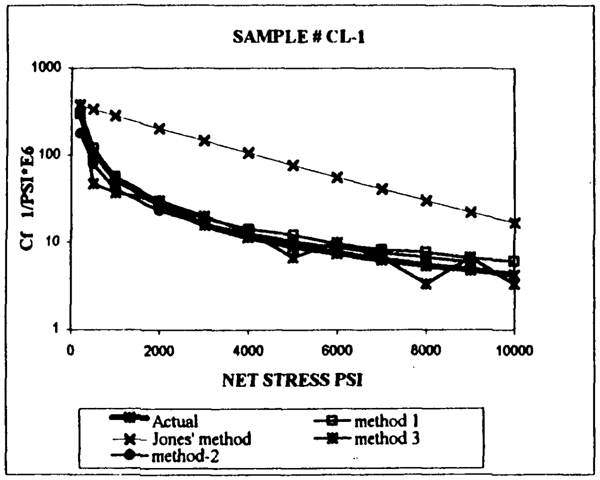

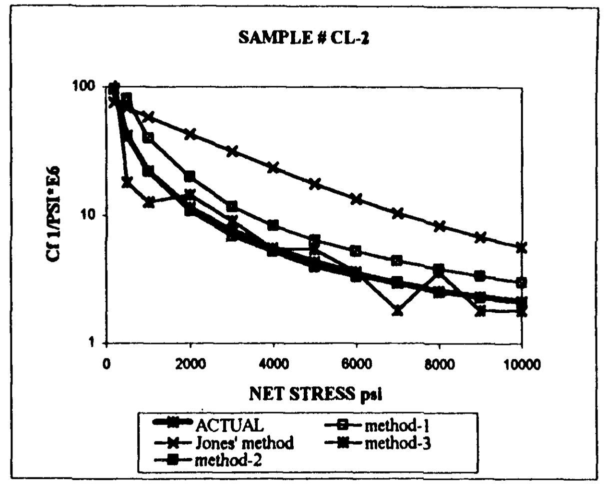

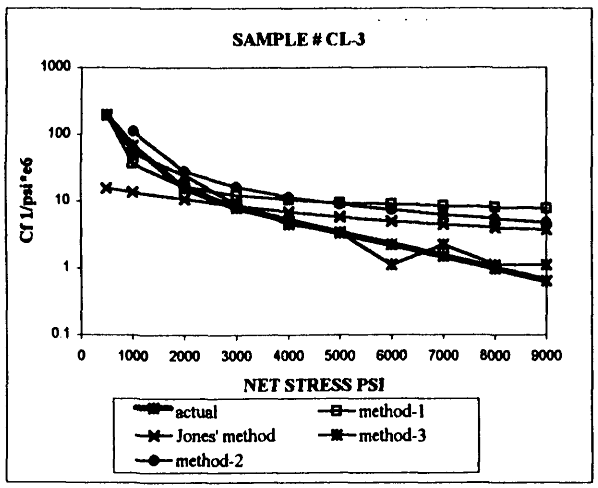

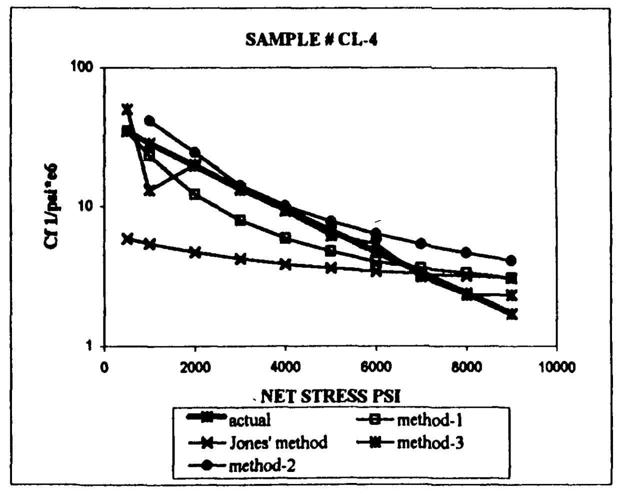

APPENDIX B-3

Correlations to predict and smooth pore compressibility - Study No. 3

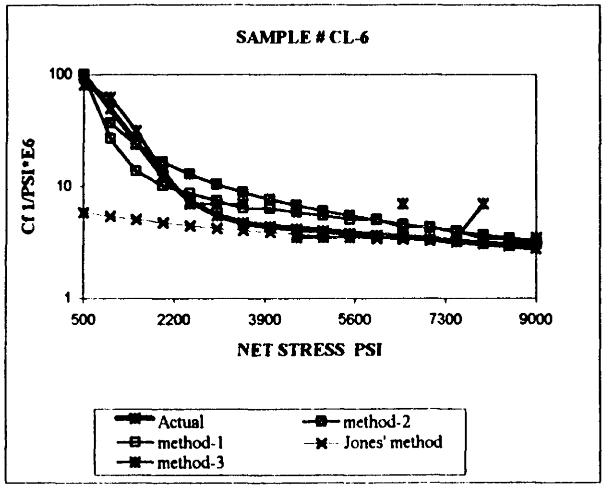

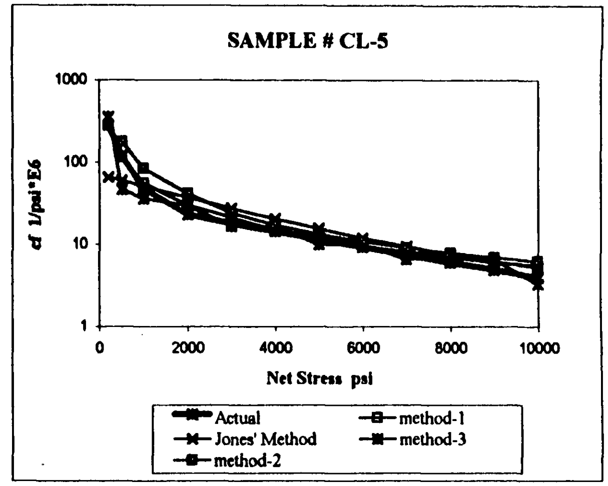

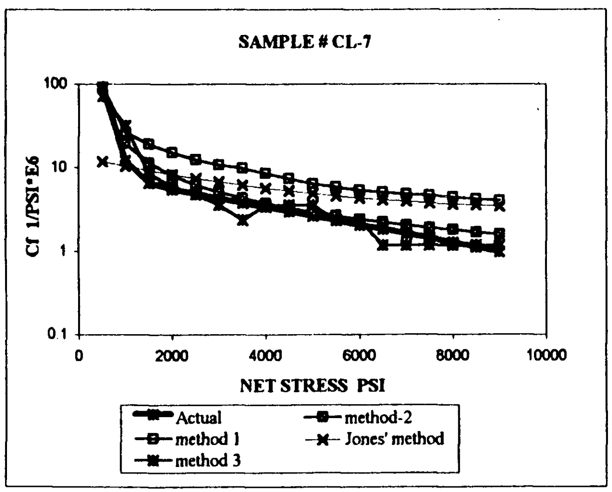

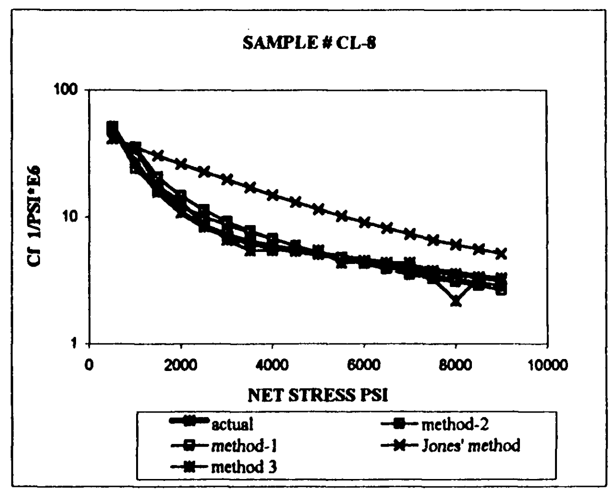

APPENDIX B-3

Correlations to predict and smooth pore compressibility - Study No. 3

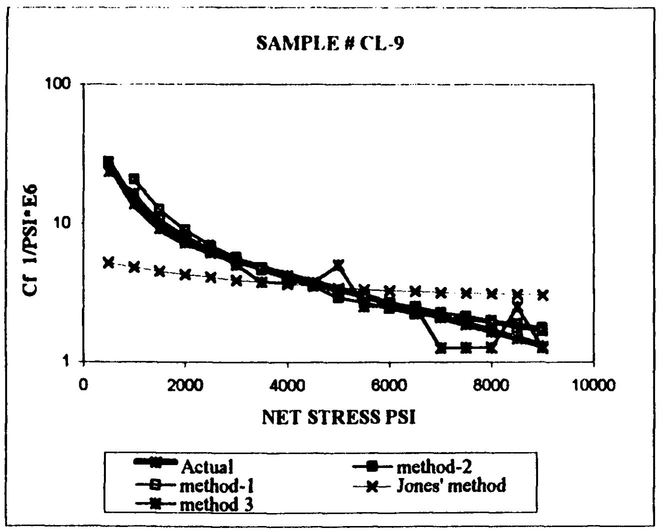

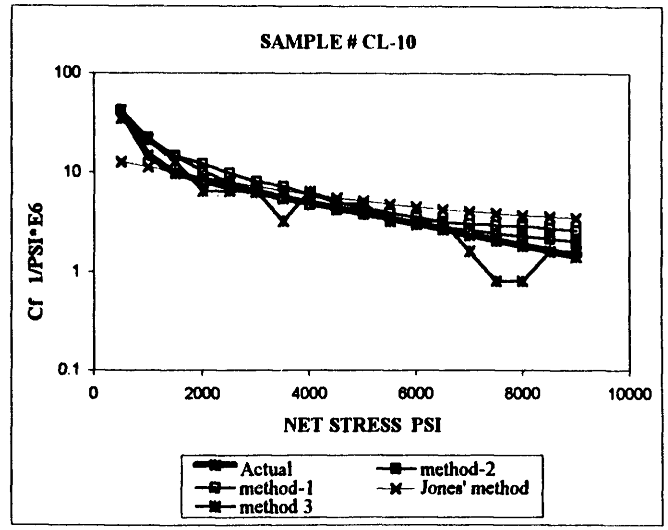

APPENDIX B-4

Correlations to predict and smooth pore compressibility - Study No. 4

APPENDIX B-4
Correlations to predict and smooth pore compressibility - Study No. 4

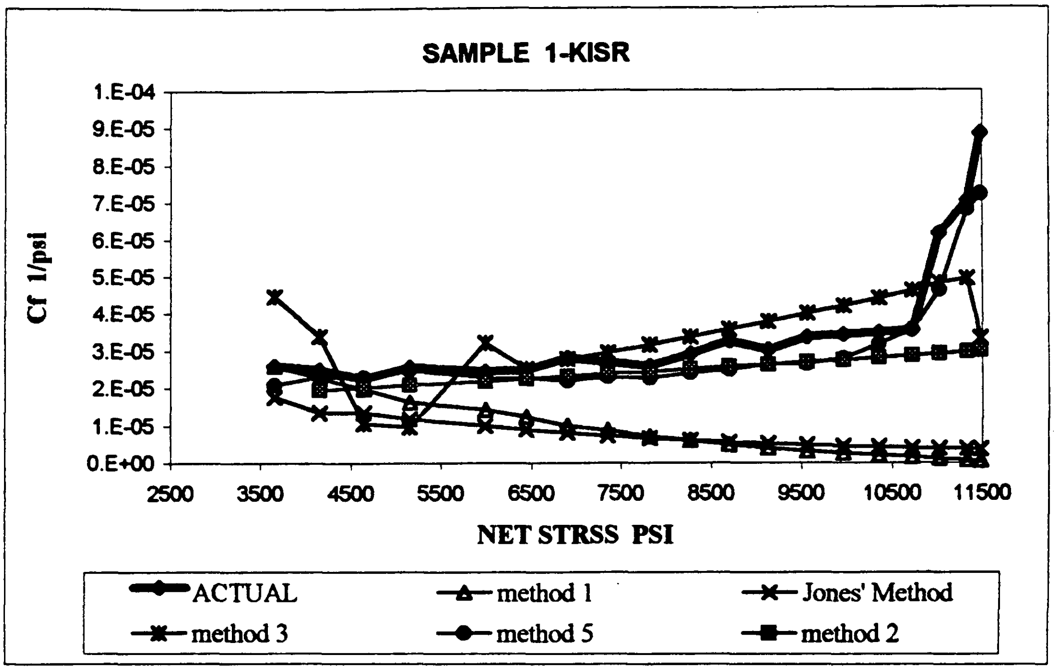

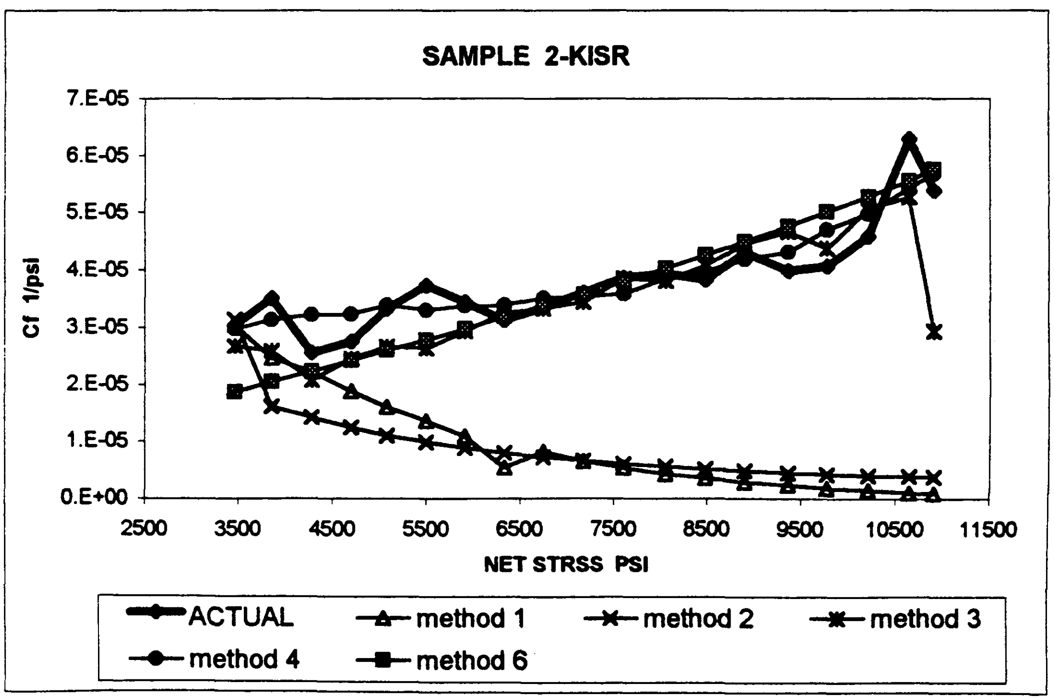

APPENDIX B-4

Correlations to predict and smooth pore compressibility - Study No. 4

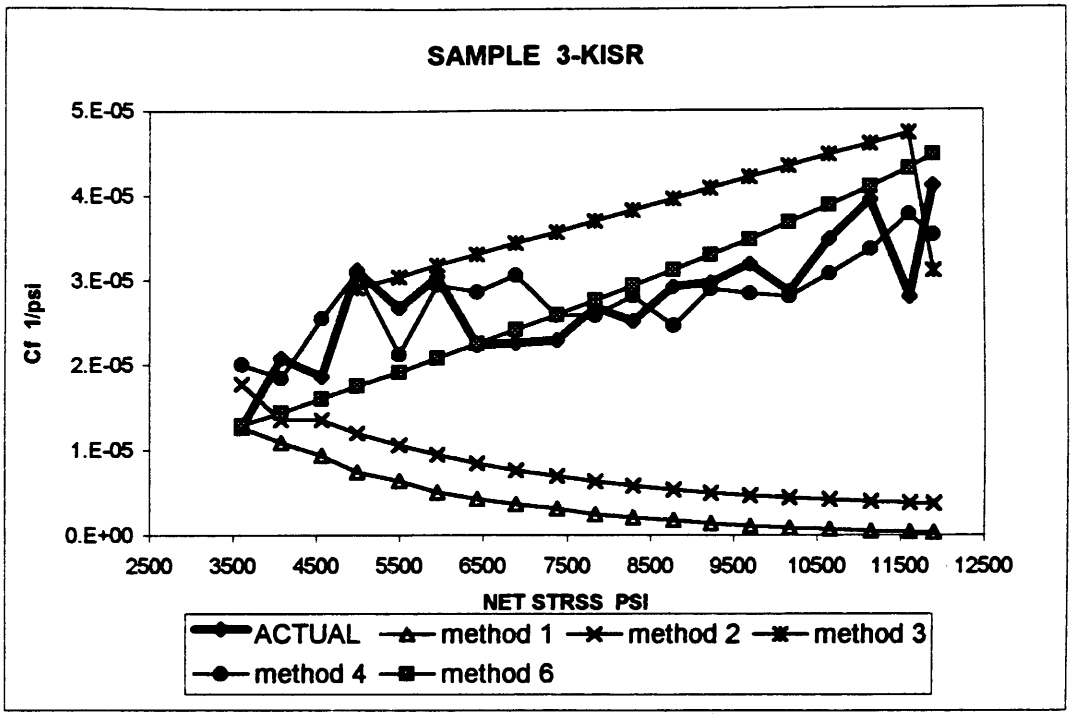

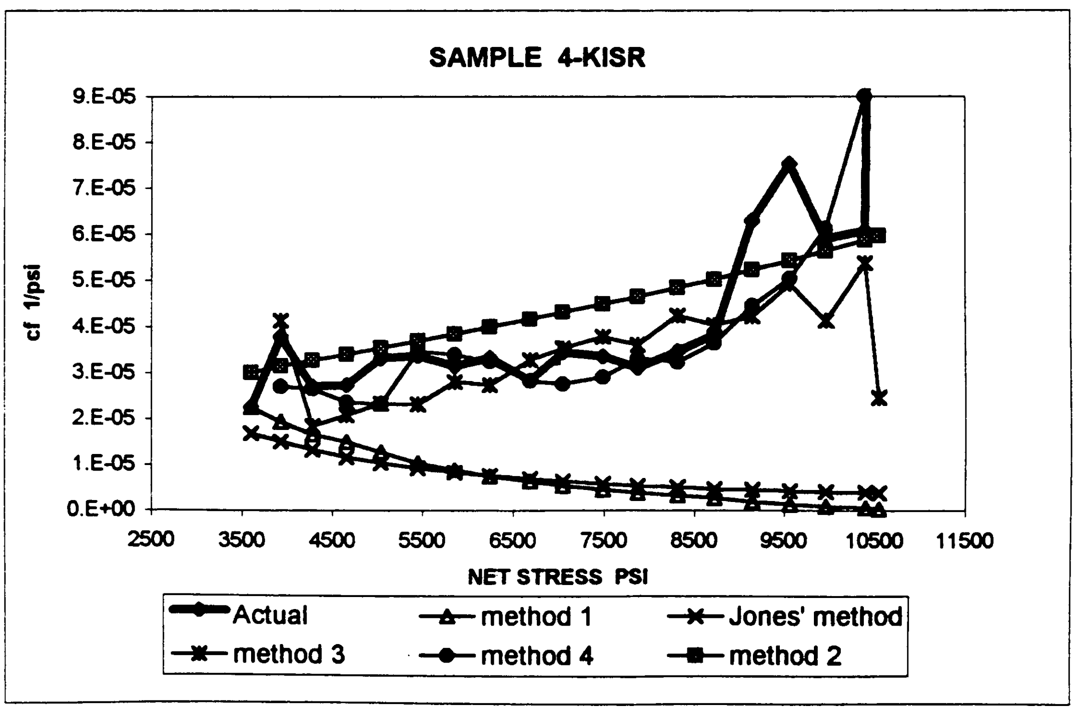

APPENDIX B-4

Correlations to predict and smooth pore compressibility - Study No. 4

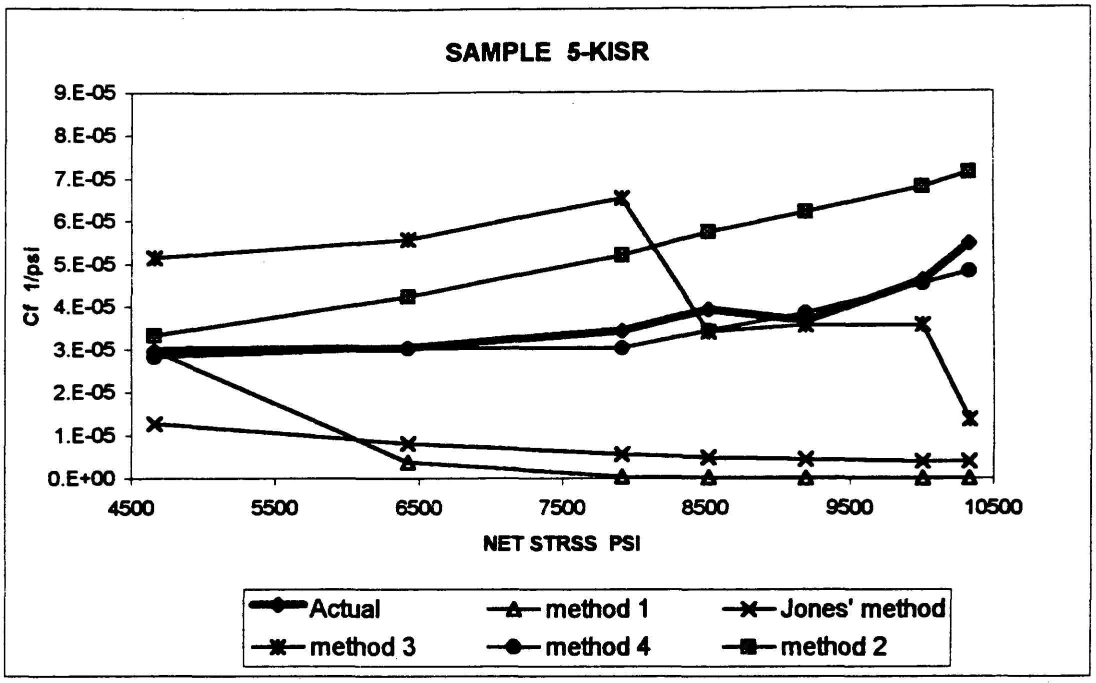

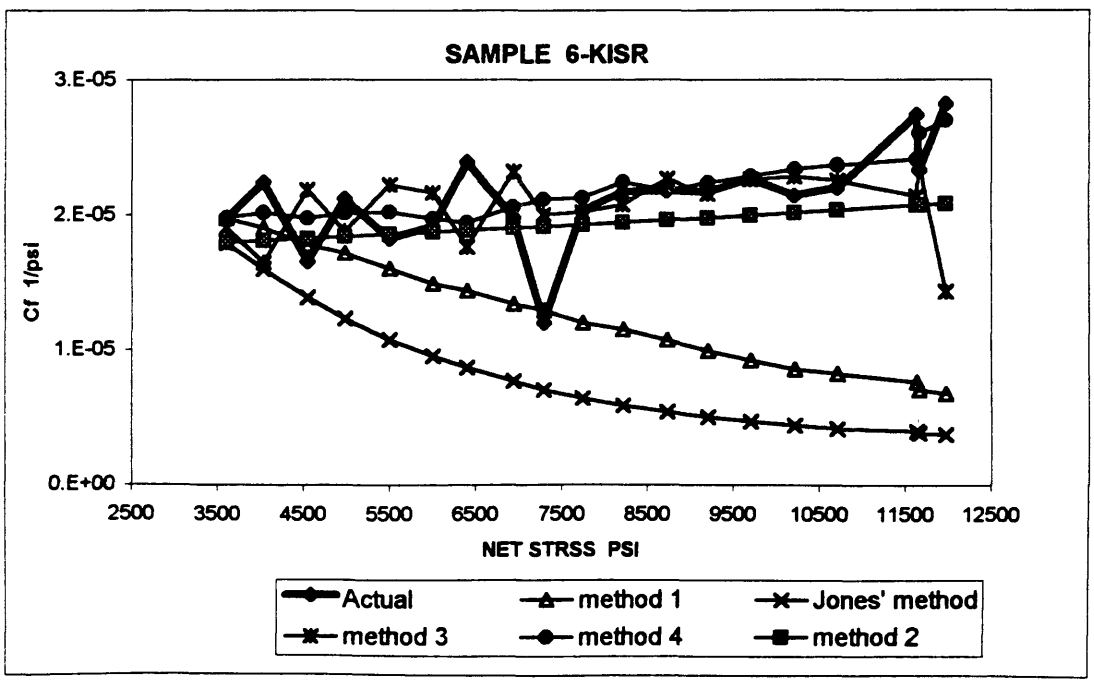

APPENDIX C-1

Pore Compressibility vs. Jm for consolidated sand - Study No. 1

ARTHUR LAKES LIBRARY
COLORADO SCHOOL OF MINES
GOLDEN, CO 80401

APPENDIX C-1

Pore Compressibility vs. Jm for Consolidated Sand - Study No. 1

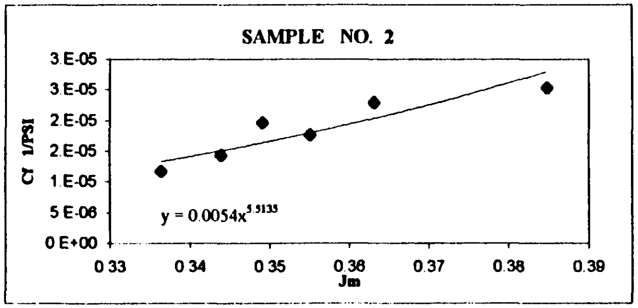

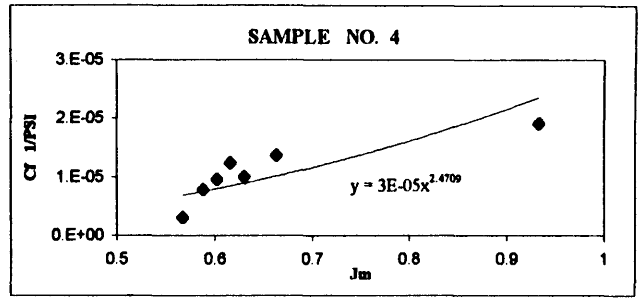

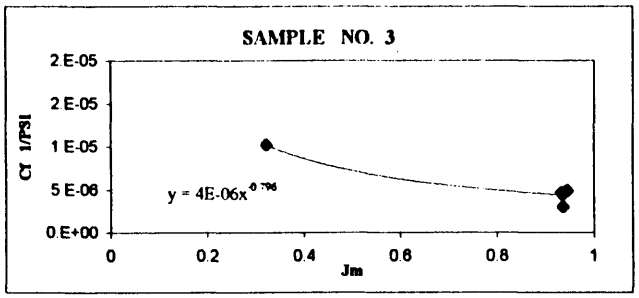

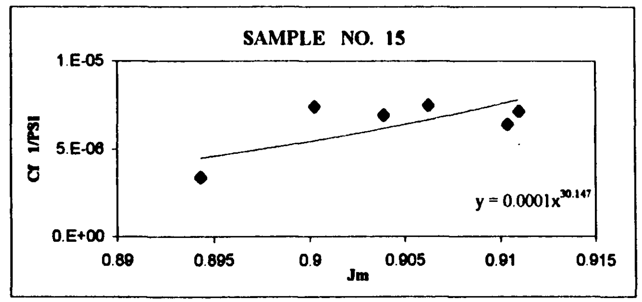

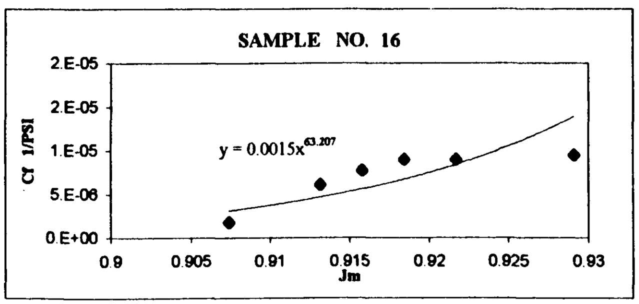

APPENDIX C-2

Pore Compressibility vs. Jm for unconsolidated sand - Study No. 2

APPENDIX C-2
Pore Compressibility vs. Jm for Unconsolidated Sand - Study No. 2

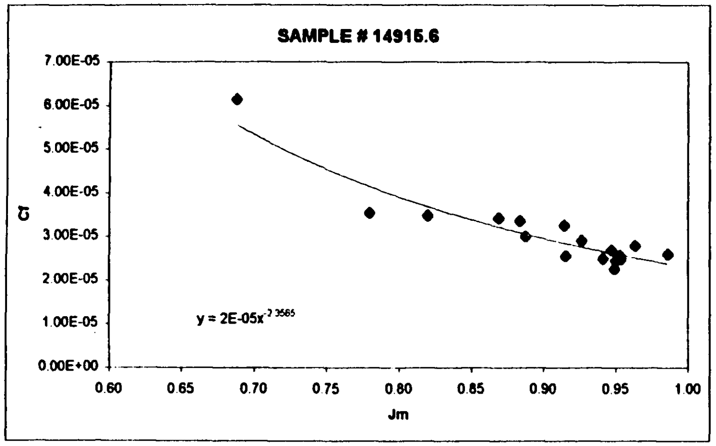

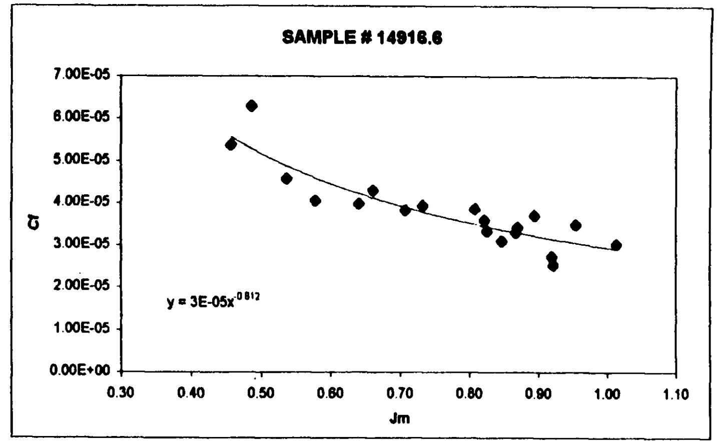

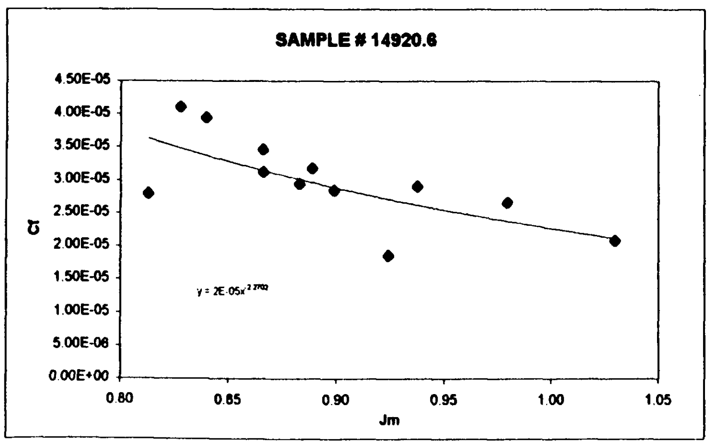

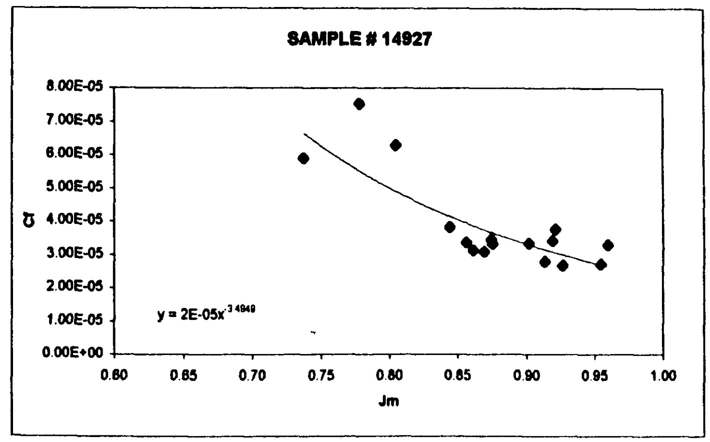

APPENDIX C-2
Pore Compressibility vs. Jm for Unconsolidated Sand - Study No. 2

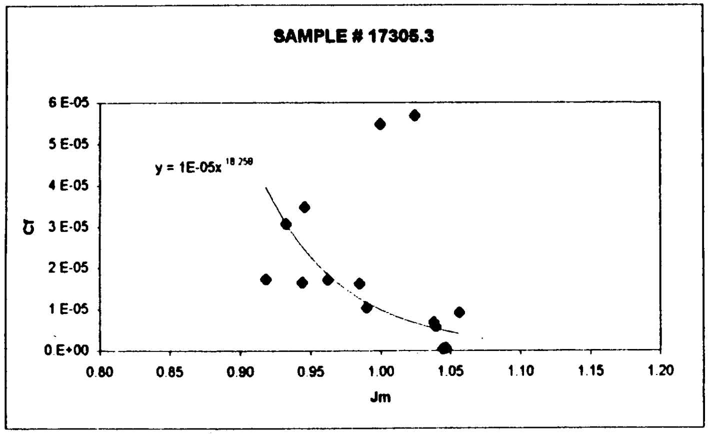

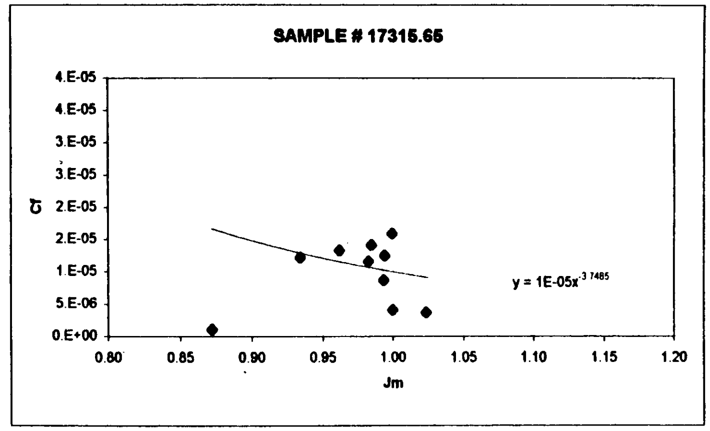

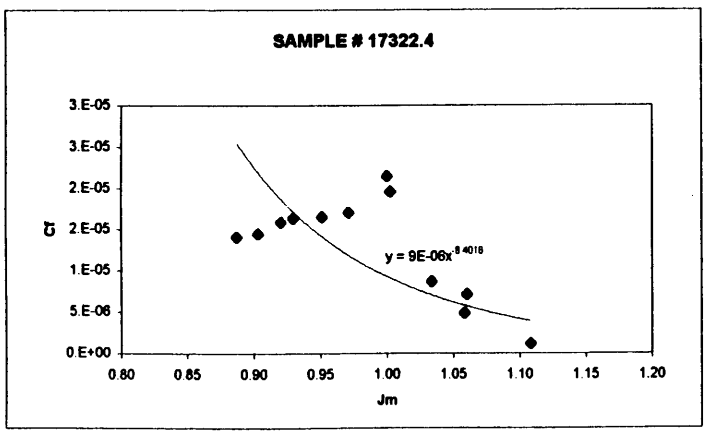

APPENDIX C-3

Pore Compressibility vs. Jm for unconsolidated sand - Study No. 4

APPENDIX C-3
Pore Compressibility vs. Jm for Unconsolidated Sand - Study No. 4

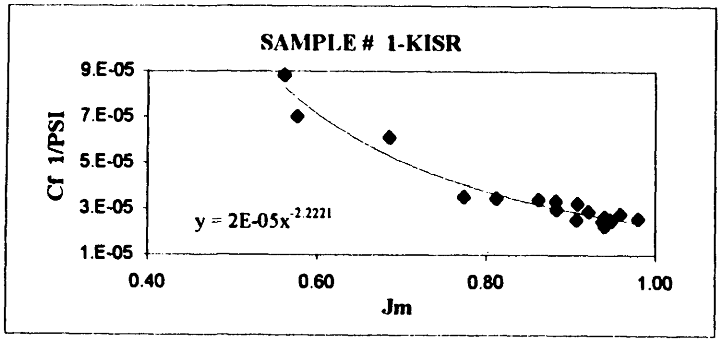

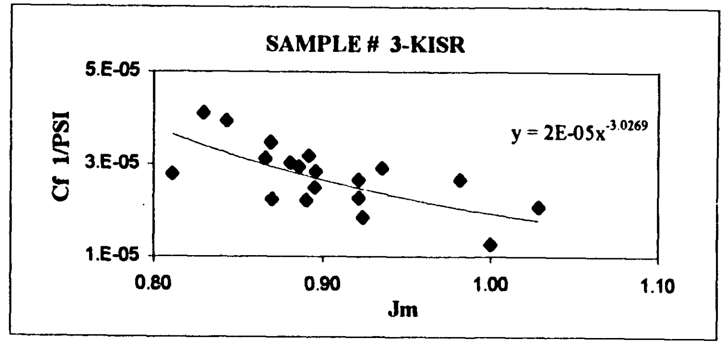

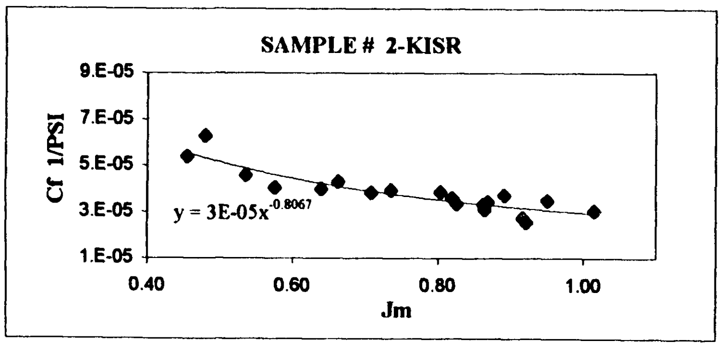

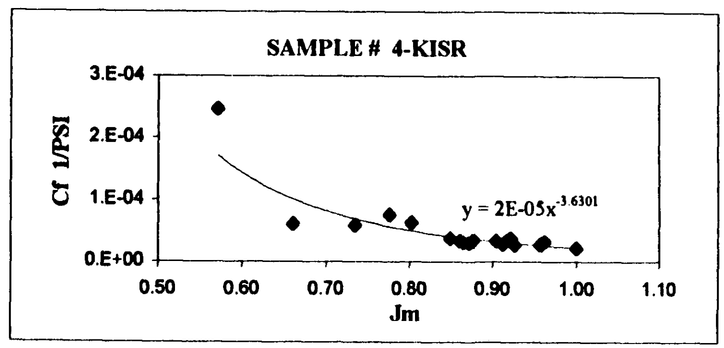

APPENDIX C-3
Pore Compressibility vs. Jm for Unconsolidated Sand - Study No. 4

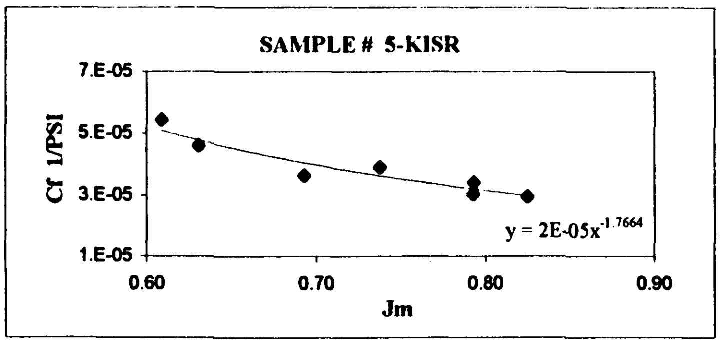

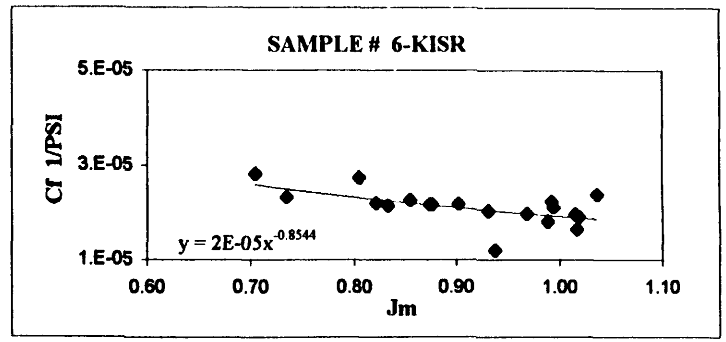

APPENDIX D-1

Basic Rock Properties and Pore Volume Compressibility Measurements for Consolidated Sandstone - Study No. 1

APPENDIX D-1

STUDY NO.1

BASIC ROCK PROPERTIES AND PORE COMPRESSIBILITY MEASURMENTS

SAMPLE ID #	STRESS PSI	POROSITY %	Vp CC	Kair md	Cf 1/psi measured	Km	φm	Jm	1-exp (-STRS/3000)	CUM Cf 1/PSI	Cf METHOD-1	Cf METHOD-2	CUM Cf METHOD-3	Cf METHOD-3	Cf METHOD-4	Cf JONES'
2	800	16.2	3.08	14.90	0	1.00	1.00	1.00	0.23	0.00E+00						
	3652	15.2	2.89	2.07	2.53E-05	0.14	0.94	0.38	0.70	2.53E-05	2.53E-05	3.12E-05	-2.10E-05	-2.10E-05	2.69E-05	2.56E-05
	4271	15.0	2.85	1.82	2.29E-05	0.12	0.93	0.36	0.76	4.82E-05	1.94E-05	1.41E-05	1.30E-05	3.40E-05	2.07E-05	2.14E-05
	4581	15.0	2.85	1.74	1.76E-05	0.12	0.93	0.36	0.78	6.58E-05	1.91E-05	1.26E-05	1.48E-05	1.79E-06	1.85E-05	1.96E-05
	4890	14.9	2.83	1.67	1.96E-05	0.11	0.92	0.35	0.80	8.54E-05	1.66E-05	1.18E-05	3.27E-05	1.79E-05	1.66E-05	1.79E-05
	5200	14.8	2.81	1.61	1.44E-05	0.11	0.91	0.34	0.82	9.98E-05	1.44E-05	1.10E-05	5.06E-05	1.79E-05	1.51E-05	1.65E-05
	5819	14.7	2.79	1.53	1.17E-05	0.10	0.91	0.34	0.86	1.12E-04	1.25E-05	1.01E-05	6.85E-05	1.79E-05	1.27E-05	1.39E-05
	5200	14.6	2.77	1.40	-1.80E-05	0.09	0.90	0.32	0.82							
3	800	26.1	4.96	330	0	1.00	1.00	1.00	0.23	0.00E+00						
	3652	25.6	4.86	290	1.02E-05	0.88	0.98	0.95	0.70	1.02E-05	1.02E-05	9.14E-06	1.56E-05	1.56E-05	7.58E-06	1.04E-05
	4271	25.5	4.85	286	4.88E-06	0.87	0.98	0.94	0.76	1.51E-05	8.54E-06	4.39E-06	2.22E-05	6.67E-06	5.43E-06	9.04E-06
	4581	25.5	4.85	285	4.81E-06	0.86	0.98	0.94	0.78	1.99E-05	8.29E-06	3.92E-06	2.33E-05	1.11E-06	4.70E-06	8.44E-06
	4890	25.5	4.85	283	4.68E-06	0.86	0.98	0.94	0.80	2.46E-05	8.05E-06	3.66E-06	2.44E-05	1.11E-06	4.13E-06	7.90E-06
	5200	25.5	4.85	282	3.01E-06	0.85	0.98	0.93	0.82	2.76E-05	7.81E-06	3.43E-06	2.56E-05	1.11E-06	3.68E-06	7.41E-06
	5819	25.4	4.83	279	4.42E-06	0.85	0.97	0.93	0.86	3.20E-05	5.63E-06	3.15E-06	3.78E-05	1.22E-05	3.01E-06	6.58E-06
	5200	25.5	4.85	281	4.67E-06	0.85	0.98	0.93	0.82							
4	800	20.2	3.84	24.9	0	1	1	1	0.23	0.00E+00						
	3652	19.1	3.63	10.4	1.92E-05	0.42	0.95	0.66	0.70	1.92E-05	1.92E-05	2.65E-05	4.70E-05	4.70E-05	2.20E-05	1.88E-05
	4271	19.0	3.61	9.3	1.37E-05	0.37	0.94	0.63	0.76	3.29E-05	1.66E-05	1.21E-05	6.04E-05	1.34E-05	1.65E-05	1.58E-05
	4581	18.9	3.59	8.9	1.01E-05	0.35	0.94	0.62	0.78	4.30E-05	1.44E-05	1.08E-05	7.38E-05	1.34E-05	1.44E-05	1.45E-05
	4890	18.8	3.57	8.4	1.24E-05	0.34	0.93	0.60	0.80	5.54E-05	1.25E-05	1.01E-05	8.71E-05	1.34E-05	1.28E-05	1.34E-05
	5200	18.8	3.57	8.0	9.60E-06	0.32	0.93	0.59	0.82	6.50E-05	1.25E-05	9.44E-06	8.71E-05	0.00E+00	1.15E-05	1.24E-05
	5819	18.7	3.55	7.4	7.82E-06	0.30	0.93	0.57	0.86	7.28E-05	1.08E-05	8.66E-06	1.00E-04	1.34E-05	9.44E-06	1.06E-05
	5200	18.7	3.55	7.5	3.06E-06	0.30	0.93	0.57	0.82							
15	800	30.2	5.74	2041	0	1	1	1.00	0.23	0.00E+00						
	3652	29.4	5.59	1649	1.40E-05	0.81	0.97	0.91	0.70	1.40E-05	1.40E-05	1.42E-05	1.80E-05	1.80E-05	1.01E-05	1.38E-05
	4271	29.3	5.57	1641	7.15E-06	0.80	0.97	0.91	0.76	2.12E-05	1.16E-05	6.56E-06	3.03E-05	1.23E-05	8.98E-06	1.18E-05
	4581	29.3	5.57	1626	6.41E-06	0.80	0.97	0.91	0.78	2.76E-05	1.16E-05	5.85E-06	3.03E-05	0.00E+00	8.53E-06	1.09E-05
	4890	29.2	5.55	1612	7.48E-06	0.79	0.97	0.90	0.80	3.50E-05	9.64E-06	5.47E-06	4.25E-05	1.23E-05	8.14E-06	1.01E-05
	5200	29.2	5.55	1599	6.94E-06	0.78	0.97	0.90	0.82	4.20E-05	9.64E-06	5.13E-06	4.25E-05	0.00E+00	7.81E-06	9.43E-06
	5819	29.1	5.53	1573	7.43E-06	0.77	0.96	0.89	0.86	4.94E-05	7.99E-06	4.70E-06	5.48E-05	1.23E-05	7.26E-06	8.22E-06
	5200	29.1	5.53	1583	3.41E-06	0.78			0.82							
16	800	33.1	6.29	5950	0	1	1	1	0.23	0.00E+00						
	3652	32.1	6.10	4981	1.85E-05	0.837	0.970	0.929	0.70	1.85E-05	1.85E-05	1.95E-05	1.25E-05	1.25E-05	1.17E-05	1.09E-05
	4271	31.9	6.06	4871	9.49E-06	0.819	0.964	0.922	0.76	2.80E-05	1.43E-05	8.98E-06	2.70E-05	1.45E-05	9.68E-06	9.38E-06
	4581	31.8	6.04	4822	8.93E-06	0.810	0.961	0.918	0.78	3.69E-05	1.25E-05	8.00E-06	3.43E-05	7.25E-06	8.93E-06	8.75E-06
	4890	31.7	6.02	4779	8.93E-06	0.803	0.958	0.916	0.80	4.59E-05	1.10E-05	7.47E-06	4.15E-05	7.25E-06	8.30E-06	8.18E-06
	5200	31.6	6.00	4736	7.68E-06	0.796	0.955	0.913	0.82	5.35E-05	9.64E-06	7.01E-06	4.88E-05	7.25E-06	7.77E-06	7.67E-06
	5819	31.5	5.99	4662	6.06E-06	0.784	0.952	0.907	0.86	5.96E-05	8.45E-06	6.42E-06	5.60E-05	7.25E-06	6.94E-06	6.78E-06

APPENDIX D-2

Basic Rock Properties and Pore Volume Compressibility Measurements for Unconsolidated Sandstone - Study No. 2

APPENDIX D-2
STUDY NO. 2
BASIC ROCK PROPERTIES AND PORE COMPRESSIBILITY MEASURMENTS

SAMPLE	STRESS	POROSITY	K air	Km	Vp	Vp-ratio	Vp(1+strsC)	1-EXP	Jm	Cf 1/PSI	cum H-Cf	NORM phi	Cf	Cf	Cf	CUM Cf	Cf	Cf
ID #	PSI	%	md		CC			(-STRS/3000)		MEASURED		%	METHOD1	METHOD-2	JONES'	METHOD-3	METHOD-3	METHOD-4
14915.5	3158	26.8	1389	1.00	22.48	1.00	22.69	0.63	1.00			1.000						2.11E-05
	3658	26.5	1335	0.96	22.19	0.99	22.44	0.69	0.99	2.60E-05	2.60E-05	0.989	2.74E-05	1.56E-05	3.77E-05	3.79E-05	3.79E-05	2.15E-05
	4158	26.3	1208	0.87	21.92	0.98	22.19	0.73	0.94	2.50E-05	5.10E-05	0.981	2.86E-05	1.72E-05	4.00E-05	7.62E-05	3.83E-05	2.19E-05
	4644	26.1	1218	0.88	21.67	0.96	21.97	0.77	0.95	2.26E-05	7.36E-05	0.974	2.97E-05	1.88E-05	4.19E-05	1.08E-04	3.19E-05	2.22E-05
	5151	25.8	1120	0.81	21.40	0.95	21.73	0.80	0.92	2.56E-05	9.92E-05	0.963	3.07E-05	2.05E-05	4.36E-05	1.36E-04	2.84E-05	2.25E-05
	5993	25.6	1197	0.86	21.14	0.94	21.52	0.85	0.95	2.45E-05	1.24E-04	0.955	3.21E-05	2.28E-05	4.59E-05	1.75E-04	3.82E-05	2.29E-05
	6443	25.4	1197	0.86	20.88	0.93	21.28	0.87	0.98	2.48E-05	1.49E-04	0.948	3.28E-05	2.49E-05	4.69E-05	1.91E-04	1.66E-05	2.31E-05
	6903	25.1	1208	0.87	20.59	0.92	21.02	0.89	0.96	2.80E-05	1.77E-04	0.937	3.34E-05	2.66E-05	4.78E-05	2.06E-04	1.47E-05	2.33E-05
	7357	24.9	1157	0.83	20.32	0.90	20.77	0.90	0.95	2.69E-05	2.03E-04	0.929	3.39E-05	2.82E-05	4.86E-05	2.18E-04	1.28E-05	2.34E-05
	7823	24.6	1157	0.83	20.06	0.89	20.53	0.92	0.95	2.58E-05	2.29E-04	0.918	3.44E-05	2.99E-05	4.93E-05	2.30E-04	1.11E-05	2.35E-05
	8270	24.4	1085	0.78	19.77	0.88	20.26	0.93	0.93	2.91E-05	2.58E-04	0.910	3.47E-05	3.16E-05	4.98E-05	2.39E-04	9.24E-06	2.36E-05
	8703	24.1	1044	0.75	19.46	0.87	19.96	0.94	0.91	3.26E-05	2.91E-04	0.899	3.51E-05	3.32E-05	5.03E-05	2.47E-04	7.78E-06	2.37E-05
	9130	23.8	971	0.70	19.17	0.85	19.69	0.94	0.89	3.01E-05	3.21E-04	0.888	3.54E-05	3.49E-05	5.07E-05	2.53E-04	6.70E-06	2.38E-05
	9563	23.5	951	0.68	18.85	0.84	19.39	0.95	0.88	3.36E-05	3.55E-04	0.877	3.56E-05	3.67E-05	5.10E-05	2.59E-04	5.93E-06	2.38E-05
	9963	23.2	908	0.65	18.55	0.82	19.09	0.96	0.87	3.42E-05	3.89E-04	0.866	3.59E-05	3.83E-05	5.13E-05	2.64E-04	4.80E-06	2.39E-05
	10357	22.9	798	0.57	18.22	0.81	18.78	0.96	0.82	3.48E-05	4.24E-04	0.854	3.60E-05	4.00E-05	5.16E-05	2.68E-04	4.17E-06	2.39E-05
	10723	22.6	712	0.51	17.90	0.80	18.48	0.97	0.78	3.54E-05	4.59E-04	0.843	3.62E-05	4.16E-05	5.18E-05	2.72E-04	3.43E-06	2.40E-05
	11030	22	540	0.39	17.37	0.77	17.94	0.97	0.69	6.14E-05	5.20E-04	0.821	3.63E-05	4.31E-05	5.19E-05	2.74E-04	2.59E-06	2.40E-05
	11333	21.5	376	0.27	16.78	0.75	17.35	0.97	0.58	7.03E-05	5.91E-04	0.802	3.64E-05	4.44E-05	5.21E-05	2.76E-04	2.32E-06	2.40E-05
	11487	21	353	0.25	16.32	0.73	16.88	0.97	0.57	8.83E-05	6.79E-04	0.784	3.65E-05	4.53E-05	5.21E-05	2.78E-04	1.10E-06	2.41E-05
14916.5	3060	26.9	878.38	1	17.70	1	17.86	0.63	1.00			1.000			3.93E-05			
	3463	26.7	896.30	1.0204	17.46	0.9864	17.64	0.68	1.01	3.03E-05	3.03E-05	0.993	3.24E-05	3.77E-05	4.19E-05	2.91E-05	2.91E-05	2.80E-05
	3857	26.3	784.31	0.8929	17.16	0.9828	17.36	0.72	0.96	3.50E-05	6.53E-05	0.978	3.43E-05	3.88E-05	4.42E-05	6.17E-05	3.27E-05	2.94E-05
	4280	26.1	725.89	0.8264	16.94	0.9702	17.16	0.75	0.92	2.54E-05	9.07E-05	0.970	3.63E-05	4.00E-05	4.63E-05	9.24E-05	3.07E-05	3.08E-05
	4703	25.8	714.12	0.813	16.72	0.9576	16.96	0.78	0.92	2.74E-05	1.18E-04	0.959	3.81E-05	4.12E-05	4.81E-05	1.19E-04	2.67E-05	3.22E-05
	5080	25.5	627.43	0.7143	16.44	0.9416	16.69	0.81	0.87	3.31E-05	1.51E-04	0.948	3.95E-05	4.24E-05	4.95E-05	1.40E-04	2.09E-05	3.34E-05
	5500	25.2	660.45	0.7519	16.14	0.9244	16.41	0.83	0.90	3.71E-05	1.88E-04	0.937	4.11E-05	4.37E-05	5.09E-05	1.60E-04	2.04E-05	3.46E-05
	5913	24.8	614.25	0.6993	15.87	0.9089	16.15	0.86	0.87	3.43E-05	2.23E-04	0.922	4.24E-05	4.50E-05	5.21E-05	1.78E-04	1.75E-05	3.58E-05
	6333	24.6	577.89	0.6579	15.63	0.8952	15.93	0.87	0.85	3.11E-05	2.54E-04	0.914	4.37E-05	4.64E-05	5.32E-05	1.94E-04	1.56E-05	3.69E-05
	6747	24.3	542.22	0.6173	15.37	0.8803	15.68	0.89	0.83	3.34E-05	2.87E-04	0.903	4.48E-05	4.78E-05	5.41E-05	2.07E-04	1.34E-05	3.79E-05
	7170	23.9	529.14	0.6024	15.1	0.8648	15.42	0.90	0.82	3.60E-05	3.23E-04	0.888	4.58E-05	4.92E-05	5.49E-05	2.19E-04	1.19E-05	3.89E-05
	7603	23.6	504.80	0.5747	14.81	0.8482	15.15	0.92	0.81	3.86E-05	3.62E-04	0.877	4.68E-05	5.08E-05	5.57E-05	2.30E-04	1.06E-05	3.98E-05
	8053	23.2	408.53	0.4651	14.53	0.8322	14.88	0.93	0.73	3.94E-05	4.01E-04	0.862	4.76E-05	5.25E-05	5.63E-05	2.39E-04	9.56E-06	4.06E-05
	8477	22.9	377.00	0.4292	14.26	0.8167	14.62	0.94	0.71	3.83E-05	4.39E-04	0.851	4.83E-05	5.41E-05	5.68E-05	2.47E-04	7.81E-06	4.14E-05
	8900	22.5	321.75	0.3663	13.96	0.7995	14.33	0.95	0.66	4.30E-05	4.82E-04	0.836	4.90E-05	5.58E-05	5.73E-05	2.54E-04	6.78E-06	4.20E-05
	9360	22.2	298.74	0.3401	13.68	0.7835	14.06	0.95	0.64	3.98E-05	5.22E-04	0.825	4.96E-05	5.78E-05	5.77E-05	2.60E-04	6.38E-06	4.27E-05
	9775	21.8	238.66	0.2717	13.41	0.768	13.80	0.96	0.58	4.06E-05	5.63E-04	0.810	5.00E-05	5.96E-05	5.81E-05	2.65E-04	4.99E-06	4.32E-05
	10213	21.5	202.38	0.2304	13.11	0.7509	13.51	0.96	0.54	4.58E-05	6.09E-04	0.799	5.05E-05	6.16E-05	5.84E-05	2.70E-04	4.58E-06	4.37E-05
	10650	20.9	161.80	0.1842	12.71	0.728	13.12	0.97	0.49	6.29E-05	6.72E-04	0.777	5.09E-05	6.37E-05	5.87E-05	2.74E-04	3.96E-06	4.41E-05
	10907	20.7	141.42	0.161	12.5	0.7159	12.91	0.97	0.46	5.38E-05	7.25E-04	0.770	5.11E-05	6.51E-05	5.88E-05	2.76E-04	2.08E-06	4.43E-05
14920.5	3606	0.257	961.10	1	18.076	1	18.27	0.63	1.00	1.26E-05	1.26E-05	1.000	1.26E-05		3.38E-05	1.00E-05	1.00E-05	1.91E-05
	4078	0.255	1011.65	1.0526	17.89	0.9897	18.11	0.68	1.03	2.09E-05	3.35E-05	0.992	1.34E-05	2.11E-05	3.60E-05	4.71E-05	3.71E-05	2.04E-05
	4571	0.253	807.61	0.8403	17.725	0.9806	17.97	0.72	0.92	1.86E-05	5.21E-05	0.984	1.41E-05	2.12E-05	3.80E-05	8.10E-05	3.39E-05	2.17E-05
	4998	0.25	701.51	0.7299	17.453	0.9655	17.71	0.75	0.87	3.12E-05	8.33E-05	0.973	1.47E-05	2.13E-05	3.96E-05	1.07E-04	2.58E-05	2.28E-05
	5498	0.248	889.88	0.9259	17.224	0.9529	17.51	0.78	0.98	2.66E-05	1.10E-04	0.965	1.54E-05	2.14E-05	4.11E-05	1.33E-04	2.66E-05	2.40E-05
	5951	0.245	711.89	0.7407	16.967	0.9386	17.27	0.81	0.88	3.03E-05	1.40E-04	0.953	1.60E-05	2.15E-05	4.24E-05	1.55E-04	2.11E-05	2.50E-05
	6431	0.243	717.27	0.7463	16.781	0.9284	17.10	0.83	0.89	2.22E-05	1.62E-04	0.946	1.65E-05	2.16E-05	4.35E-05	1.74E-04	1.97E-05	2.60E-05
	6891	0.241	686.51	0.7143	16.595	0.9181	16.94	0.85	0.87	2.24E-05	1.85E-04	0.938	1.70E-05	2.17E-05	4.45E-05	1.91E-04	1.65E-05	2.69E-05
	7378	0.239	762.83	0.7937	16.409	0.9078	16.77	0.87	0.92	2.27E-05	2.07E-04	0.930	1.74E-05	2.19E-05	4.54E-05	2.06E-04	1.54E-05	2.78E-05
	7838	0.236	591.27	0.6152	16.194	0.8959	16.57	0.89	0.82	2.66E-05	2.34E-04	0.918	1.78E-05	2.20E-05	4.62E-05	2.19E-04	1.27E-05	2.86E-05
	8291	0.234	701.51	0.7299	15.994	0.8848	16.39	0.90	0.90	2.50E-05	2.59E-04	0.911	1.81E-05	2.21E-05	4.68E-05	2.30E-04	1.10E-05	2.92E-05
	8784	0.232	762.83	0.7937	15.765	0.8722	16.18	0.91	0.94	2.91E-05	2.88E-04	0.903	1.85E-05	2.22E-05	4.75E-05	2.40E-04	1.05E-05	2.99E-05
	9231	0.229	667.39	0.6944	15.536	0.8595	15.97	0.92	0.88	2.95E-05	3.18E-04	0.891	1.87E-05	2.23E-05	4.80E-05	2.49E-04	8.38E-06	3.05E-05
	9704	0.226	667.39	0.6944	15.293	0.846	15.74	0.93	0.89	3.18E-05	3.49E-04	0.879	1.90E-05	2.25E-05	4.84E-05	2.57E-04	7.81E-06	3.10E-05
	10178	0.224	676.81	0.7042	15.078	0.8341	15.54	0.94	0.90	2.85E-05	3.78E-04	0.872	1.92E-05	2.26E-05	4.88E-05	2.63E-04	6.86E-06	3.15E-05
	10658	0.221	620.10	0.6452	14.821	0.8199	15.29	0.95	0.87	3.47E-05	4.13E-04	0.860	1.94E-05	2.27E-05	4.92E-05	2.70E-04	6.09E-06	3.19E-05
	11151	0.217	572.05	0.5952	14.535	0.8041	15.02	0.95	0.84	3.94E-05	4.52E-04	0.844	1.96E-05	2.29E-05	4.95E-05	2.75E-04	5.47E-06	3.23E-05
	11618	0.215	531.01	0.5525	14.335	0.793	14.83	0.96	0.81	2.79E-05	4.80E-04	0.837	1.98E-05	2.30E-05	4.98E-05	2.80E-04	4.53E-06	3.27E-05

APPENDIX D-2
STUDY NO. 2
BASIC ROCK PROPERTIES AND PORE COMPRESSIBILITY MEASURMENTS

SAMPLE ID #	STRESS PSI	POROSITY %	K air md	Km	Vp CC	Vp-ratio	Vp(1+strsC)	XP(-STRS/3	Jm	Cf 1/PSI MEASURED	cum H-Cf	NORM phi %	Cf METHOD1	Cf METHOD-2	Cf JONES'	CUM Cf METHOD-3	Cf METHOD-3	Cf METHOD-4
	11964	0.213	546.10	0.5682	14.149	0.7828	14.65	0.96	0.83	4.11E-05	3.21E-04	0.829	1.99E-05	2.31E-05	4.99E-05	2.82E-04	2.50E-06	3.29E-05
14927	3600	0.28	3624.18	1	23.02	1	23.27	0.63	1.00	2.25E-05	2.25E-05	1.000	2.25E-05		3.58E-05	7.00E-05	7.00E-05	3.50E-05
	3930	0.277	3045.40	0.8403	22.66	0.9844	22.93	0.66	0.92	3.76E-05	6.01E-05	0.989	2.35E-05	3.26E-05	3.75E-05	9.85E-05	2.85E-05	3.64E-05
	4283	0.274	3045.40	0.8403	22.36	0.9713	22.65	0.70	0.93	2.68E-05	8.69E-05	0.979	2.45E-05	3.35E-05	3.91E-05	1.26E-04	2.78E-05	3.78E-05
	4663	0.272	3207.40	0.885	22.06	0.9583	22.37	0.73	0.95	2.72E-05	1.14E-04	0.971	2.56E-05	3.44E-05	4.07E-05	1.53E-04	2.70E-05	3.92E-05
	5037	0.269	3207.40	0.885	21.7	0.9427	22.03	0.75	0.96	3.30E-05	1.47E-04	0.961	2.65E-05	3.54E-05	4.21E-05	1.77E-04	2.39E-05	4.05E-05
	5447	0.265	2516.63	0.6944	21.35	0.9275	21.70	0.78	0.86	3.35E-05	1.81E-04	0.946	2.76E-05	3.65E-05	4.35E-05	2.01E-04	2.35E-05	4.19E-05
	5853	0.262	2516.63	0.6944	21.02	0.9131	21.39	0.80	0.86	3.13E-05	2.12E-04	0.936	2.85E-05	3.76E-05	4.47E-05	2.22E-04	2.08E-05	4.31E-05
	6243	0.259	2570.27	0.7092	20.67	0.8979	21.06	0.82	0.88	3.32E-05	2.45E-04	0.925	2.93E-05	3.87E-05	4.57E-05	2.39E-04	1.79E-05	4.42E-05
	6683	0.256	2766.70	0.7634	20.39	0.8858	20.80	0.84	0.91	2.80E-05	2.73E-04	0.914	3.02E-05	3.99E-05	4.68E-05	2.57E-04	1.80E-05	4.54E-05
	7043	0.253	2766.70	0.7634	20.04	0.8705	20.46	0.86	0.92	3.42E-05	3.07E-04	0.904	3.08E-05	4.10E-05	4.75E-05	2.71E-04	1.32E-05	4.63E-05
	7490	0.25	2632.60	0.7264	19.72	0.8566	20.16	0.88	0.90	3.34E-05	3.41E-04	0.893	3.16E-05	4.23E-05	4.84E-05	2.85E-04	1.46E-05	4.73E-05
	7873	0.247	2416.24	0.6667	19.42	0.8436	19.88	0.89	0.87	3.09E-05	3.72E-04	0.882	3.22E-05	4.35E-05	4.90E-05	2.96E-04	1.12E-05	4.80E-05
	8313	0.244	2416.24	0.6667	19.09	0.8293	19.57	0.90	0.87	3.45E-05	4.06E-04	0.871	3.28E-05	4.49E-05	4.97E-05	3.08E-04	1.14E-05	4.88E-05
	8723	0.241	2223.43	0.6135	18.73	0.8136	19.22	0.91	0.84	3.82E-05	4.44E-04	0.861	3.33E-05	4.62E-05	5.03E-05	3.17E-04	9.47E-06	4.95E-05
	9147	0.235	1969.74	0.5435	18.16	0.7889	18.66	0.92	0.80	6.30E-05	5.07E-04	0.839	3.38E-05	4.76E-05	5.08E-05	3.26E-04	8.72E-06	5.02E-05
	9560	0.228	1785.27	0.4926	17.5	0.7602	18.00	0.93	0.78	7.53E-05	5.83E-04	0.814	3.43E-05	4.91E-05	5.12E-05	3.33E-04	7.56E-06	5.07E-05
	9960	0.223	1568.91	0.4329	17	0.7385	17.51	0.94	0.74	5.90E-05	6.42E-04	0.796	3.46E-05	5.05E-05	5.16E-05	3.40E-04	6.54E-06	5.12E-05
	10400	0.218	1245.27	0.3436	16.5	0.7168	17.01	0.94	0.66	6.07E-05	7.02E-04	0.779	3.50E-05	5.21E-05	5.20E-05	3.46E-04	6.40E-06	5.17E-05
	10547	0.206	865.09	0.2387	15.29	0.6642	15.77	0.95	0.57	2.46E-05	7.27E-04	0.736	3.51E-05	5.29E-05	5.21E-05	3.48E-04	1.97E-06	5.19E-05
17305.3	980	22	130.58	1.1628	10.31	1.053	10.34	0.28	1.06	9.23E-06	9.23E-06	1.043	9.23E-06		1.05E-05	7.00E-05	7.00E-05	4.14E-06
	1009	21.4	126.18	1.1236	9.95	1.016	9.98	0.29	1.04	6.83E-06	1.61E-05	1.043	9.44E-06	-1.95E-08	1.06E-05	7.17E-05	1.71E-06	4.21E-06
	1195	21.5	124.78	1.1111	9.96	1.017	10.00	0.33	1.05	6.82E-07	1.67E-05	1.014	1.08E-05	3.61E-07	1.18E-05	8.23E-05	1.06E-05	4.65E-06
	1249	21.7	124.78	1.1111	10.02	1.022	10.06	0.34	1.04	5.44E-07	1.73E-05	1.019	1.12E-05	7.86E-07	1.21E-05	8.52E-05	2.95E-06	4.79E-06
	1327	21.4	124.78	1.1111	10.13	1.034	10.17	0.36	1.04	5.75E-06	2.30E-05	1.028	1.19E-05	1.02E-06	1.26E-05	8.94E-05	4.16E-06	4.98E-06
	3764	21.6	120.76	1.0753	10.08	1.029	10.19	0.71	1.02	5.68E-05	7.98E-05	1.024	3.85E-05	5.53E-06	2.21E-05	1.77E-04	8.79E-05	1.18E-05
	5114	21.1	112.30	1	9.8	1	9.95	0.82	1.00	5.48E-05	1.35E-04	1.000	5.49E-05	1.24E-05	2.49E-05	2.03E-04	2.54E-05	1.54E-05
	5432	21.1	110.10	0.9804	9.76	0.996	9.92	0.84	0.99	1.05E-05	1.45E-04	1.000	5.84E-05	1.55E-05	2.54E-05	2.07E-04	4.50E-06	1.61E-05
	5907	20.9	107.98	0.9615	9.68	0.988	9.85	0.86	0.99	1.63E-05	1.61E-04	0.991	6.35E-05	1.70E-05	2.60E-05	2.13E-04	5.89E-06	1.71E-05
	6879	20.7	102.09	0.9091	9.52	0.971	9.72	0.90	0.96	1.73E-05	1.79E-04	0.981	7.27E-05	1.99E-05	2.70E-05	2.23E-04	9.51E-06	1.89E-05
	7858	20.4	96.81	0.8621	9.36	0.956	9.58	0.93	0.94	1.66E-05	1.95E-04	0.967	8.02E-05	2.38E-05	2.78E-05	2.30E-04	6.92E-06	2.03E-05
	8839	19.8	94.37	0.8403	9.05	0.923	9.29	0.95	0.95	3.48E-05	2.30E-04	0.938	8.61E-05	2.79E-05	2.83E-05	2.35E-04	5.00E-06	2.14E-05
	9815	19.4	89.84	0.8	8.78	0.896	9.04	0.96	0.93	3.07E-05	2.61E-04	0.919	9.07E-05	3.23E-05	2.87E-05	2.38E-04	3.59E-06	2.22E-05
	10788	19.1	85.73	0.7634	8.85	0.881	9.14	0.97	0.92	1.74E-05	2.78E-04	0.905	9.41E-05	3.69E-05	2.90E-05	2.41E-04	2.59E-06	2.28E-05
17315.65	1062	22.2	420.88	1.0753	7.5	1.048	7.52	0.30	1.02		0.00E+00	1.037						9.34E-06
	979	22.1	420.88	1.0753	7.46	1.041	7.48	0.28	1.02		0.00E+00	1.033		-5.49E-07				9.27E-06
	1026	22.1	425.46	1.087	7.45	1.041	7.47	0.29	1.03		0.00E+00	1.033		2.94E-07				9.31E-06
	1121	22.2	425.46	1.087	7.51	1.049	7.54	0.31	1.02	3.66E-06	3.66E-06	1.037	3.71E-06	5.47E-07	9.33E-06	4.24E-05	4.24E-05	9.39E-06
	1281	22.3	407.73	1.0417	7.57	1.057	7.60	0.35	1.00	4.14E-06	7.80E-06	1.042	3.86E-06	8.17E-07	1.01E-05	4.87E-05	6.27E-06	9.52E-06
	4028	21.9	395.36	1.0101	7.39	1.032	7.48	0.74	0.99	8.75E-06	1.66E-05	1.023	5.94E-06	5.48E-06	1.80E-05	1.17E-04	6.86E-05	1.11E-05
	5445	21.4	391.41	1	7.16	1	7.28	0.84	1.00	1.59E-05	3.25E-05	1.000	6.63E-06	2.75E-06	2.00E-05	1.35E-04	1.72E-05	1.16E-05
	5793	21.3	376.34	0.9615	7.13	0.996	7.25	0.85	0.98	1.16E-05	4.41E-05	0.995	6.76E-06	6.98E-07	2.03E-05	1.38E-04	3.13E-06	1.17E-05
	6265	21.2	376.34	0.9615	7.08	0.989	7.21	0.88	0.99	1.41E-05	5.82E-05	0.991	6.93E-06	9.14E-07	2.08E-05	1.41E-04	3.70E-06	1.18E-05
	7225	21	355.83	0.9091	6.99	0.976	7.14	0.91	0.96	1.33E-05	7.15E-05	0.981	7.19E-06	1.74E-06	2.14E-05	1.47E-04	5.95E-06	1.20E-05
	8184	20.8	376.34	0.9615	6.9	0.964	7.07	0.93	0.99	1.25E-05	8.40E-05	0.972	7.40E-06	1.68E-06	2.19E-05	1.52E-04	4.32E-06	1.21E-05
	9141	20.6	328.90	0.8403	6.82	0.952	7.01	0.95	0.93	1.22E-05	9.62E-05	0.963	7.55E-06	1.64E-06	2.23E-05	1.55E-04	3.13E-06	1.22E-05
	10094	20.4	318.22	0.813	6.75	0.943	6.95	0.97	0.92	9.47E-05	1.91E-04	0.953	7.66E-06	1.60E-06	2.25E-05	1.57E-04	2.27E-06	1.22E-05
	11063	20.3	294.30	0.7519	6.7	0.936	6.92	0.97	0.89	7.46E-05	2.65E-04	0.949	7.74E-06	1.61E-06	2.27E-05	1.59E-04	1.67E-06	1.23E-05
	12031	20.1	279.58	0.7143	6.63	0.926	6.87	0.98	0.87	1.15E-06	2.67E-04	0.939	7.80E-06	1.59E-06	2.29E-05	1.60E-04	1.21E-06	1.23E-05
17322.4	826	23.4	293.69	1.1765	9.65	1.026	9.67	0.15	1.07			1.022	1.19E-06		7.07E-06	2.00E-05	2.00E-05	4.30E-06
	955	23.3	300.75	1.2048	9.58	1.019	9.61	0.17	1.09			1.017	1.27E-06	7.48E-07	7.65E-06	2.13E-05	1.34E-06	4.48E-06
	994	23.3	312.04	1.25	9.59	1.02	9.62	0.18	1.11	1.19E-06	1.19E-06	1.017	1.29E-06	1.03E-06	7.82E-06	2.17E-05	3.98E-07	4.53E-06
	1087	23.5	286.92	1.1494	9.69	1.03	9.72	0.20	1.06	4.85E-06	6.04E-06	1.026	1.35E-06	1.25E-06	8.23E-06	2.27E-05	9.37E-07	4.66E-06
	1214	23.7	290.27	1.1628	9.82	1.044	9.86	0.22	1.06	7.10E-06	1.31E-05	1.035	1.44E-06	1.62E-06	8.77E-06	2.39E-05	1.25E-06	4.85E-06
	4132	23.3	271.35	1.087	9.57	1.018	9.69	0.56	1.03	8.72E-06	2.19E-05	1.017	4.09E-06	6.81E-06	1.80E-05	4.54E-05	2.15E-05	9.63E-06
	5229	22.9	249.63	1	9.4	1	9.55	0.65	1.00	2.15E-05	4.34E-05	1.000	5.32E-06	1.37E-05	2.03E-05	5.08E-05	5.35E-06	1.15E-05
	5527	22.8	249.63	1	9.34	0.993	9.49	0.67	1.00	1.96E-05	6.30E-05	0.996	5.66E-06	1.61E-05	2.09E-05	5.20E-05	1.26E-06	1.20E-05
	5859	22.7	233.30	0.9346	9.26	0.985	9.42	0.69	0.97	1.71E-05	8.01E-05	0.991	6.04E-06	1.72E-05	2.14E-05	5.34E-05	1.32E-06	1.26E-05
	6594	22.4	220.92	0.885	9.11	0.969	9.29	0.73	0.95	1.65E-05	9.66E-05	0.978	6.87E-06	1.93E-05	2.26E-05	5.60E-05	2.63E-06	1.38E-05
	7431	22.1	208.02	0.8333	8.96	0.953	9.16	0.77	0.93	1.64E-05	1.13E-04	0.965	7.80E-06	2.22E-05	2.37E-05	5.85E-05	2.56E-06	1.51E-05
	8321	21.8	201.33	0.8065	8.82	0.938	9.04	0.81	0.92	1.59E-05	1.29E-04	0.952	8.73E-06	2.56E-05	2.47E-05	6.08E-05	2.29E-06	1.63E-05
	9208	21.6	192.02	0.7692	8.7	0.925	8.94	0.84	0.90	1.45E-05	1.43E-04	0.943	9.59E-06	2.92E-05	2.55E-05	6.27E-05	1.91E-06	1.75E-05
	9969	21.4	183.55	0.7353	8.58	0.912	8.84	0.86	0.89	1.41E-05	1.57E-04	0.934	1.03E-05	3.26E-05	2.61E-05	6.41E-05	1.39E-06	1.84E-05

APPENDIX D-3

Basic Rock Properties and Pore Volume Compressibility Measurements for Consolidated Sandstone - Study No. 3

APPENDIX D-3
STUDY NO. 3
BASIC ROCK PROPERTY AND PORE COMPRESSIBILITY MEASUREMENTS

SAMPLE ID NO.	Hydrostatic NETS PSI	Vp cc	NORM PORE-VOL Vp/Vpi	phi STRESSED POROSITY %	phi/phi* NORM. POROSITY	MEASURED Hydrostatic Cf 1/PSI*e6	MEASURED Unaxial Cf * Tr 1/PSI*e6	MEASURED CUM. Cf 1/PSI*E6	Cf 1/PSI*E6 METHOD-1	Cf METHOD-2	Cf 1/PSI*E6 METHOD-3	1-EXP (-STRS/3000)	Cf 1/PSI*E6 JONES'
CL-1	200	6.2	1	2.83	1.000	303.02	187.87	303	303.02		375.60	0.064	369.72
	500	5.89	0.95	2.69	0.951	111.59	69.19	415	121.09	178.63	46.93	0.154	334.82
	1000	5.63	0.907	2.58	0.912	52.41	32.5	467	56.92	80.46	36.87	0.283	283.87
	2000	5.43	0.875	2.49	0.880	27.56	17.09	495	29.95	40.19	30.17	0.487	204.24
	3000	5.3	0.855	2.43	0.859	15.62	9.81	510	19.27	23.30	20.11	0.632	147.18
	4000	5.21	0.84	2.39	0.845	11.56	7.17	522	14.28	16.47	13.41	0.736	106.29
	5000	5.16	0.833	2.37	0.837	9.07	5.62	531	12.26	12.74	6.70	0.811	76.99
	6000	5.11	0.824	2.34	0.827	7.43	4.61	538	9.74	10.40	10.06	0.865	56.00
	7000	5.07	0.817	2.32	0.820	6.28	3.9	545	8.34	8.78	6.70	0.903	40.95
	8000	5.03	0.81	2.31	0.816	5.43	3.37	550	7.71	7.60	3.35	0.931	30.17
	9000	4.99	0.805	2.29	0.809	4.78	2.96	555	6.59	6.70	6.70	0.950	22.44
	10000	4.96	0.8	2.28	0.806	4.26	2.64	559	6.09	5.99	3.35	0.964	16.90
	200	5.75	0.927	2.63	0.929								
CL-2	200	2.79	1	5.32	1.000	96.91	60.08	96.91	96.91		125.50	0.064	75.66
	500	2.74	0.981	5.22	0.981	42.06	26.07	138.97	40.75	80.81	18.07	0.154	68.74
	1000	2.69	0.966	5.15	0.968	22.06	13.67	161.03	22.00	40.15	12.65	0.283	58.64
	2000	2.65	0.951	5.07	0.953	11.37	7.05	172.4	10.76	20.06	14.45	0.487	42.86
	3000	2.63	0.942	5.02	0.944	7.53	4.67	179.93	6.85	46.31	9.03	0.632	31.55
	4000	2.61	0.935	4.99	0.938	5.52	3.43	185.45	5.21	47.86	5.42	0.736	23.44
	5000	2.59	0.93	4.96	0.932	4.31	2.67	189.76	3.95	49.41	5.42	0.811	17.63
	6000	2.58	0.926	4.94	0.929	3.5	2.17	193.26	3.29	50.96	3.61	0.865	13.46
	7000	2.57	0.923	4.93	0.927	2.95	1.83	196.21	3.00	52.52	1.81	0.903	10.47
	8000	2.57	0.92	4.91	0.923	2.57	1.59	198.78	2.49	54.07	3.61	0.931	8.33
	9000	2.56	0.918	4.9	0.921	2.3	1.43	201.08	2.27	55.62	1.81	0.950	6.79
	10000	2.55	0.916	4.89	0.919	2.12	1.31	203.2	2.07	57.18	1.81	0.964	5.68
CL-3	500	0.457	1	8.02	1.000	193.53	119.99	193.53	193.53		198.50	0.154	15.58
	1000	0.43	0.941	7.54	0.940	67.42	41.8	260.95	36.34	111.16	53.31	0.283	13.64
	2000	0.416	0.909	7.32	0.913	15.59	9.67	276.54	16.29	28.05	24.43	0.487	10.61
	3000	0.41	0.897	7.24	0.903	7.87	4.88	284.41	12.09	16.29	8.88	0.632	8.44
	4000	0.407	0.891	7.2	0.898	5.01	3.11	289.42	10.41	11.52	4.44	0.736	6.88
	5000	0.406	0.887	7.17	0.894	3.31	2.05	292.73	9.29	8.91	3.33	0.811	5.76
	6000	0.405	0.885	7.16	0.893	2.2	1.36	294.93	8.95	7.27	1.11	0.865	4.96
	7000	0.404	0.883	7.14	0.890	1.46	0.9	296.39	8.30	6.14	2.22	0.903	4.38
	8000	0.403	0.881	7.13	0.889	0.97	0.6	297.36	7.99	5.32	1.11	0.931	3.96
	9000	0.403	0.88	7.12	0.888	0.64	0.4	298	7.69	4.69	1.11	0.950	3.66
CL-4	500	0.705	1	12	1.000	35.03	21.72	35.03	35.03		50.40	0.154	5.90
	1000	0.694	0.985	11.83	0.986	28.7	17.79	63.73	23.22	41.64	13.18	0.283	5.45
	2000	0.677	0.96	11.57	0.964	19.56	12.13	83.29	12.24	24.54	20.17	0.487	4.74
	3000	0.665	0.944	11.4	0.950	13.54	8.39	96.83	7.99	14.25	13.18	0.632	4.24
	4000	0.658	0.933	11.28	0.940	9.47	5.87	106.3	5.86	10.08	9.31	0.736	3.87
	5000	0.652	0.925	11.2	0.933	6.67	4.13	112.97	4.80	7.80	6.20	0.811	3.60
	6000	0.648	0.919	11.13	0.928	4.72	2.93	117.69	4.00	6.36	5.43	0.865	3.41
	7000	0.645	0.915	11.09	0.924	3.36	2.08	121.05	3.61	5.37	3.10	0.903	3.27
	8000	0.643	0.912	11.06	0.922	2.39	1.48	123.44	3.34	4.65	2.33	0.931	3.17
	9000	0.642	0.91	11.03	0.919	1.71	1.06	125.15	3.09	4.10	2.33	0.950	3.09

APPENDIX D-3
STUDY NO. 3
BASIC ROCK PROPERTY AND PORE COMPRESSIBILITY MEASUREMENTS

SAMPLE ID NO.	Hydrostatic NETS PSI	Vp cc	NORM PORE-VOL Vp/Vpi	phi STRESSED POROSITY %	phi/phi* NORM. POROSITY	MEASURED Hydrostatic Cf 1/PSI*e6	MEASURED Unaxial Cf * Tr 1/PSI*e6	CUM. Cf 1/PSI*E6	Cf 1/PSI*E6 METHOD-1	Cf METHOD-2	Cf 1/PSI*E6 METHOD-3	1-EXP (-STRS/3000)	Cf 1/PSI*E6 JONE'S
												0.000	
CL-5	200	1.14	1	2.81	1.000	279.34	173.19	279.34	279.34		359.00	0.064	65.80
	500	1.07	0.946	2.67	0.950	120.63	74.79	399.97	115.74	178.89	46.37	0.154	59.82
	1000	1.03	0.907	2.56	0.911	48.77	30.23	448.74	56.04	84.29	36.43	0.283	51.09
	2000	0.99	0.876	2.47	0.879	23.01	14.26	471.75	30.24	42.10	29.81	0.487	37.45
	3000	0.97	0.856	2.42	0.861	17.75	11	489.50	21.25	24.40	16.56	0.632	27.67
	4000	0.95	0.84	2.37	0.843	14.29	8.86	503.79	14.83	17.24	16.56	0.736	20.66
	5000	0.94	0.827	2.34	0.833	11.54	7.15	515.33	11.90	13.34	9.94	0.811	15.64
	6000	0.93	0.817	2.31	0.822	9.32	5.78	524.65	9.53	10.89	9.94	0.865	12.03
	7000	0.92	0.808	2.29	0.815	7.52	4.66	532.17	8.20	9.19	6.62	0.903	9.45
	8000	0.91	0.802	2.27	0.808	6.07	3.77	538.24	7.05	7.96	6.62	0.931	7.59
	9000	0.9	0.796	2.25	0.801	4.91	3.04	543.15	6.05	7.01	6.62	0.950	6.26
	10000	0.9	0.792	2.24	0.797	3.96	2.46	547.11	5.61	6.27	3.31	0.964	5.31
												0.000	
CL-6	500	0.708	1	5.26	1.000	100.14	61.98	100.14	100.14		80.94	0.154	5.90
	1000	0.683	0.965	5.08	0.966	49.35	30.55	149.49	26.89	36.83	63.05	0.283	5.45
	1500	0.67	0.947	4.99	0.949	25	15.47	174.49	13.69	23.39	31.52	0.393	5.07
	2000	0.664	0.938	4.95	0.941	12.59	7.79	187.08	10.10	16.56	14.01	0.487	4.74
	2500	0.661	0.933	4.93	0.937	7.41	4.59	194.49	8.67	12.83	7.01	0.565	4.47
	3000	0.658	0.929	4.91	0.933	5.46	3.38	199.95	7.44	10.47	7.01	0.632	4.24
	3500	0.656	0.927	4.89	0.930	4.71	2.91	204.66	6.38	8.85	7.01	0.689	4.04
	4000	0.655	0.926	4.89	0.930	4.36	2.7	209.02	6.38	7.66		0.736	3.87
	4500	0.654	0.923	4.88	0.928	4.15	2.57	213.17	5.90	6.75	3.50	0.777	3.73
	5000	0.653	0.922	4.87	0.926	3.97	2.46	217.14	5.46	6.04	3.50	0.811	3.60
	5500	0.652	0.92	4.86	0.924	3.8	2.36	220.94	5.05	5.46	3.50	0.840	3.50
	6000	0.651	0.919	4.86	0.924	3.64	2.26	224.58	5.05	4.99		0.865	3.41
	6500	0.649	0.917	4.84	0.920	3.49	2.16	228.07	4.32	4.58	7.01	0.885	3.34
	7000	0.648	0.916	4.84	0.920	3.34	2.06	231.41	4.32	4.24		0.903	3.27
	7500	0.647	0.913	4.83	0.918	3.19	1.98	234.6	4.00	3.95	3.50	0.918	3.22
	8000	0.645	0.91	4.81	0.914	3.05	1.89	237.65	3.42	3.69	7.01	0.931	3.17
	8500	0.644	0.909	4.81	0.914	2.92	1.81	240.57	3.42	3.47		0.941	3.13
	9000	0.643	0.908	4.8	0.913	2.8	1.74	243.37	3.16	3.27	3.50	0.950	3.09
CL-7	500	15.92	1	19.22	1.000	92.25	54.7	92.25	92.25		71.14	0.154	11.69
	1000	15.64	0.982	18.95	0.986	12.1	7.17	104.35	26.38	19.45	31.98	0.283	10.35
	1500	15.57	0.978	18.88	0.982	6.47	3.84	110.82	19.01	11.34	8.29	0.393	9.21
	2000	15.52	0.975	18.83	0.980	5.47	3.24	116.29	15.04	8.03	5.92	0.487	8.25
	2500	15.48	0.972	18.79	0.978	4.83	2.86	121.12	12.46	6.22	4.74	0.565	7.44
	3000	15.45	0.97	18.76	0.976	4.27	2.53	125.39	10.81	5.08	3.55	0.632	6.75
	3500	15.43	0.969	18.74	0.975	3.78	2.24	129.17	9.84	4.29	2.37	0.689	6.17
	4000	15.39	0.967	18.71	0.973	3.35	1.98	132.52	8.54	3.72	3.55	0.736	5.67
	4500	15.36	0.965	18.68	0.972	2.96	1.76	135.48	7.41	3.28	3.55	0.777	5.25
	5000	15.34	0.963	18.65	0.970	2.62	1.55	138.1	6.43	2.93	3.55	0.811	4.89
	5500	15.31	0.962	18.63	0.969	2.32	1.37	140.42	5.84	2.65	2.37	0.840	4.59
	6000	15.3	0.961	18.61	0.968	2.05	1.22	142.47	5.31	2.42	2.37	0.865	4.34
	6500	15.28	0.96	18.6	0.968	1.82	1.08	144.29	5.07	2.22	1.18	0.885	4.12
	7000	15.27	0.959	18.59	0.967	1.61	0.95	145.9	4.83	2.06	1.18	0.903	3.93
	7500	15.27	0.959	18.58	0.967	1.42	0.84	147.32	4.61	1.92	1.18	0.918	3.78
	8000	15.26	0.958	18.57	0.966	1.26	0.75	148.58	4.39	1.79	1.18	0.931	3.64
	8500	15.25	0.957	18.56	0.966	1.11	0.66	149.69	4.19	1.68	1.18	0.941	3.53
	9000	15.24	0.957	18.55	0.965	0.99	0.58	150.68	3.99	1.59	1.18	0.950	3.43

ARTHUR LAKES LIBRARY
COLORADO SCHOOL OF MINES
GOLDEN, CO 80401

APPENDIX D-3
STUDY NO. 3
BASIC ROCK PROPERTY AND PORE COMPRESSIBILITY MEASUREMENTS

SAMPLE ID NO.	Hydrostatic NETS PSI	Vp cc	NORM PORE-VOL Vp/Vpi	phi STRESSED POROSITY %	phi/phi* NORM. POROSITY	MEASURED Hydrostatic Cf 1/PSI*E6	MEASURED Uniaxial Cf * Tr 1/PSI*E6	CUM. Cf 1/PSI*E6	Cf 1/PSI*E6 METHOD-1	Cf METHOD-2	Cf 1/PSI*E6 METHOD-3	1-EXP (-STRS/3000)	Cf 1/PSI*E6 JONE'S
CL-8	500	14.96	1	20.59	1.000	51.23	30.38	51.23	51.23		41.22	0.15	41.46
	1000	14.87	0.981	20.28	0.985	26.86	15.93	78.09	24.26	35.69	34.17	0.28	35.55
	1500	14.52	0.971	20.12	0.98	15.89	9.43	93.98	16.43	20.74	17.64	0.39	30.56
	2000	14.41	0.964	20	0.971	10.84	6.43	104.82	12.23	14.67	13.23	0.49	26.31
	2500	14.34	0.959	19.92	0.967	8.4	4.98	113.22	10.04	11.35	8.82	0.57	22.73
	3000	14.29	0.956	19.86	0.965	7.12	4.22	120.34	8.66	9.26	6.61	0.63	19.69
	3500	14.24	0.953	19.81	0.962	6.36	3.77	126.7	7.64	7.82	5.51	0.69	17.12
	4000	14.2	0.95	19.76	0.960	5.85	3.47	132.55	6.75	6.77	5.51	0.74	14.94
	4500	14.16	0.947	19.71	0.957	5.45	3.23	138	5.96	5.97	5.51	0.78	13.10
	5000	14.11	0.944	19.66	0.955	5.11	3.03	143.11	5.26	5.33	5.51	0.81	11.64
	5500	14.07	0.941	19.62	0.953	4.81	2.85	147.92	4.76	4.82	4.41	0.84	10.22
	6000	14.04	0.939	19.58	0.951	4.53	2.69	152.45	4.30	4.40	4.41	0.86	9.10
	6500	14	0.937	19.54	0.949	4.28	2.54	156.73	3.89	4.04	4.41	0.89	8.15
	7000	13.97	0.935	19.5	0.947	4.03	2.33	160.76	3.51	3.74	4.41	0.90	7.34
	7500	13.94	0.933	19.47	0.946	3.81	2.26	164.57	3.26	3.48	3.31	0.92	6.66
	8000	13.92	0.931	19.45	0.945	3.59	2.13	168.16	3.10	3.26	2.20	0.93	6.09
	8500	13.89	0.93	19.42	0.943	3.39	2.01	171.55	2.87	3.06	3.31	0.94	5.60
	9000	13.87	0.928	19.39	0.942	3.2	1.9	174.75	2.66	2.88	3.31	0.95	5.18
CL-9	500	13.58	1	17.2	1.000	27.58	16.35	27.58	27.58		23.60	0.15	5.20
	1000	13.46	0.991	17.07	0.992	13.66	8.1	41.24	15.32	20.61	16.40	0.28	4.86
	1500	13.37	0.985	16.99	0.988	9.08	5.38	50.32	10.64	12.64	10.09	0.39	4.56
	2000	13.32	0.981	16.93	0.984	7.21	4.27	57.53	8.09	8.96	7.57	0.49	4.32
	2500	13.27	0.977	16.88	0.981	6.16	3.65	63.69	6.43	6.94	6.31	0.57	4.11
	3000	13.24	0.975	16.84	0.979	5.4	3.2	69.09	5.35	5.66	6.04	0.63	3.93
	3500	13.21	0.973	16.81	0.977	4.78	2.84	73.87	4.66	4.79	3.78	0.69	3.78
	4000	13.18	0.97	16.78	0.976	4.24	2.52	78.11	4.06	4.14	3.78	0.74	3.65
	4500	13.16	0.968	16.75	0.974	3.77	2.24	81.88	3.53	3.65	3.78	0.78	3.54
	5000	13.11	0.966	16.71	0.972	3.35	1.99	85.23	2.93	3.27	5.04	0.81	3.45
	5500	13.09	0.964	16.69	0.970	2.98	1.76	88.21	2.67	2.95	2.52	0.84	3.37
	6000	13.07	0.963	16.67	0.969	2.64	1.57	90.85	2.44	2.70	2.52	0.86	3.30
	6500	13.06	0.961	16.65	0.968	2.35	1.39	93.2	2.22	2.48	2.52	0.89	3.24
	7000	13.04	0.961	16.64	0.967	2.09	1.24	95.29	2.12	2.29	1.26	0.90	3.19
	7500	13.04	0.96	16.63	0.967	1.86	1.1	97.15	2.02	2.14	1.26	0.92	3.15
	8000	13.03	0.959	16.62	0.966	1.65	0.98	98.8	1.93	2.00	1.26	0.93	3.11
	8500	13.01	0.958	16.6	0.965	1.47	0.87	100.27	1.76	1.88	2.52	0.94	3.08
	9000	13	0.957	16.59	0.965	1.3	0.77	101.57	1.68	1.77	1.26	0.95	3.06
CL-10	500	10.93	1	12.99	1.000	42.53	25.22	42.53	42.53		34.93	0.15	12.76
	1000	10.8	0.988	12.86	0.990	14.8	8.78	57.33	22.23	22.64	21.09	0.28	11.26
	1500	10.73	0.981	12.78	0.984	9.68	5.74	67.01	14.86	14.47	12.97	0.39	9.98
	2000	10.68	0.977	12.74	0.981	8.06	4.78	75.07	12.14	10.26	6.49	0.49	8.90
	2500	10.64	0.974	12.7	0.978	7.05	4.18	82.12	9.91	7.94	6.49	0.57	7.99
	3000	10.61	0.971	12.66	0.975	6.23	3.69	88.35	8.08	6.48	6.49	0.63	7.22
	3500	10.59	0.968	12.64	0.973	5.51	3.27	93.86	7.30	5.48	3.24	0.69	6.56
	4000	10.56	0.965	12.6	0.970	4.87	2.89	98.73	5.95	4.74	6.49	0.74	6.00
	4500	10.52	0.963	12.57	0.968	4.31	2.56	103.04	5.10	4.18	4.87	0.78	5.53
	5000	10.49	0.96	12.54	0.965	3.81	2.26	106.85	4.37	3.74	4.87	0.81	5.13
	5500	10.47	0.958	12.52	0.964	3.37	2	110.22	3.95	3.38	3.24	0.84	4.80
	6000	10.46	0.957	12.5	0.962	2.99	1.77	113.21	3.56	3.09	3.24	0.86	4.51
	6500	10.44	0.955	12.48	0.961	2.64	1.57	115.85	3.21	2.84	3.24	0.89	4.26
	7000	10.43	0.954	12.47	0.960	2.34	1.39	118.19	3.06	2.63	1.62	0.90	4.06
	7500	10.42	0.954	12.465	0.960	2.07	1.23	120.26	2.97	2.45	0.81	0.92	3.88
	8000	10.42	0.953	12.46	0.959	1.83	1.08	122.09	2.89	2.29	0.81	0.93	3.73
	8500	10.4	0.952	12.45	0.958	1.62	0.96	123.71	2.75	2.16	1.62	0.94	3.60
	9000	10.39	0.951	12.44	0.958	1.43	0.85	125.14	2.81	2.02	1.62	0.96	3.50

APPENDIX D-4

Basic Rock Properties and Pore Volume Compressibility Measurements for Unconsolidated Sandstone - Study No. 4

APPENDIX D-4
STUDY NO. 4
BASIC ROCK PROPERTIES AND PORE COMPRESSIBILITY MEASUREMENTS

Sample ID	RAM PRESSURE	SLEEVE PRESSURE	PORE PRESSURE	Del (PORE - VOLUME)	NET STRESS	NET SLEEVE	POISSONS' RATIO	C(por-vol) 1/PSI	AVG NET STRESS	Vp ss	POROSITY %	CUM Cf 1/PSI	φ (MEAN)	NORMAL K (md)	K (md)	Jm	METHOD 1	Cf METHOD 2	CUM Cf. METHOD 3	Cf METHOD 3	Cf METHD 4	METHOD JONES'
1-KISR	3000	3000	2000	0.000	1000	1000	0.5		1000	22.48	0.27		1.01	1.24	1722	1.11						
	14133	12400	9320	0.288	4813	3080	0.39	2.60E-05	3658	22.19	0.27	2.60E-06	1.00	0.96	1333	0.98	2.6E-06		4.47E-05	4.47E-05	2.09E-05	1.8E-05
	14133	12400	8820	0.274	5813	3580	0.4	2.50E-05	4158	21.92	0.26	5.10E-06	0.99	0.87	1208	0.94	2.6E-06	1.96E-05	7.87E-05	3.40E-05	2.32E-05	1.4E-05
	14133	12380	8320	0.245	5813	4060	0.41	2.26E-05	4644	21.67	0.26	7.36E-06	0.98	0.87	1208	0.94	2.6E-06	2.02E-05	8.92E-05	1.05E-05	2.30E-05	1.4E-05
	14133	12390	7820	0.274	6313	4570	0.42	2.56E-05	5151	21.40	0.26	9.92E-05	0.97	0.80	1111	0.91	2.6E-06	2.08E-05	9.88E-05	9.58E-06	2.49E-05	1.2E-05
	14340	12800	7320	0.259	7020	5480	0.44	2.45E-05	5993	21.14	0.26	1.24E-04	0.97	0.86	1194	0.94	2.6E-06	2.18E-05	1.31E-04	3.20E-05	2.28E-05	1.0E-05
	14340	12725	6820	0.259	7520	5905	0.44	2.48E-05	6443	20.88	0.25	1.49E-04	0.96	0.86	1194	0.95	2.6E-06	2.25E-05	1.56E-04	2.52E-05	2.26E-05	8.9E-06
	14350	12660	6320	0.288	8030	6340	0.44	2.80E-05	6903	20.59	0.25	1.77E-04	0.96	0.87	1208	0.96	2.6E-06	2.31E-05	1.84E-04	2.78E-05	2.20E-05	8.0E-06
	14350	12590	5820	0.273	8530	6770	0.44	2.69E-05	7357	20.32	0.25	2.03E-04	0.94	0.83	1153	0.94	2.6E-06	2.37E-05	2.13E-04	2.94E-05	2.30E-05	7.2E-06
	14350	12540	5320	0.259	9030	7220	0.44	2.58E-05	7823	20.06	0.25	2.29E-04	0.93	0.83	1153	0.95	2.6E-06	2.44E-05	2.45E-04	3.15E-05	2.26E-05	6.5E-06
	14350	12460	4820	0.288	9530	7640	0.44	2.91E-05	8270	19.77	0.24	2.58E-04	0.92	0.78	1083	0.92	2.6E-06	2.50E-05	2.78E-04	3.36E-05	2.40E-05	6.0E-06
	14350	12360	4320	0.317	10030	8040	0.44	3.26E-05	8703	19.46	0.24	2.91E-04	0.91	0.75	1042	0.91	2.6E-06	2.56E-05	3.14E-04	3.66E-05	2.48E-05	5.5E-06
	14350	12250	3820	0.288	10530	8430	0.44	3.01E-05	9130	19.17	0.24	3.21E-04	0.90	0.70	972	0.88	2.6E-06	2.62E-05	3.52E-04	3.77E-05	2.64E-05	5.1E-06
	14350	12150	3320	0.317	11030	8830	0.44	3.36E-05	9563	18.85	0.24	3.55E-04	0.89	0.69	968	0.88	2.6E-06	2.69E-05	3.91E-04	3.98E-05	2.64E-05	4.8E-06
	14350	12000	2820	0.317	11530	9180	0.44	3.42E-05	9963	18.53	0.23	3.89E-04	0.88	0.65	903	0.86	2.6E-06	2.75E-05	4.33E-04	4.19E-05	2.78E-05	4.5E-06
	14350	11840	2320	0.317	12030	9520	0.44	3.48E-05	10357	18.22	0.23	4.24E-04	0.86	0.67	792	0.81	2.6E-06	2.81E-05	4.77E-04	4.40E-05	3.18E-05	4.2E-06
	14350	11640	1820	0.317	12530	9820	0.44	3.54E-05	10723	17.90	0.23	4.59E-04	0.85	0.61	708	0.77	2.6E-06	2.86E-05	5.23E-04	4.81E-05	3.54E-05	4.0E-06
	14350	11350	1320	0.533	13030	10030	0.43	6.14E-05	11030	17.37	0.22	5.20E-04	0.83	0.39	542	0.69	2.6E-06	2.92E-05	5.72E-04	4.82E-05	4.83E-05	3.8E-06
	14340	11060	820	0.590	13520	10240	0.43	7.03E-05	11333	16.78	0.22	5.91E-04	0.81	0.27	375	0.58	2.6E-06	2.96E-05	6.21E-04	4.92E-05	6.79E-05	3.7E-06
	14340	10810	500	0.461	13840	10310	0.43	8.83E-05	11487	16.32	0.21	6.79E-04	0.79	0.25	347	0.56	2.6E-06	2.99E-05	6.54E-04	3.32E-05	7.21E-05	3.6E-06
2-KISR	1000	1000	500	0.000	500	500	0.5		500	17.70	0.27											
	14000	12175	9320	0.243	2855	0.38	0.37	3.03E-05	3463	17.46	0.27	3.03E-06	1.00	1.03	905	1.01	3.0E-06	1.66E-05	2.66E-05	2.66E-05	2.96E-05	3.1E-05
	14000	12015	8820	0.300	5180	3195	0.38	3.50E-05	3857	17.16	0.26	3.50E-05	0.99	0.89	782	0.95	3.0E-06	1.86E-05	1.04E-04	2.58E-05	3.13E-05	1.6E-05
	13960	11920	8320	0.215	5640	3600	0.39	2.54E-05	4280	16.94	0.26	6.04E-05	0.98	0.83	729	0.92	3.0E-06	2.04E-05	1.25E-04	2.06E-05	3.20E-05	1.4E-05
	13960	11905	7820	0.229	6140	3985	0.39	2.74E-05	4703	16.72	0.26	8.78E-05	0.97	0.81	711	0.92	3.0E-06	2.22E-05	1.49E-04	2.44E-05	3.22E-05	1.2E-05
	13900	11620	7320	0.272	6640	4300	0.39	3.31E-05	5080	16.44	0.26	1.21E-04	0.96	0.71	624	0.86	3.0E-06	2.40E-05	1.76E-04	2.65E-05	3.38E-05	1.1E-05
	13920	11520	6820	0.300	7100	4700	0.4	3.72E-05	5500	16.14	0.25	1.58E-04	0.94	0.75	659	0.89	3.0E-06	2.58E-05	2.02E-04	2.62E-05	3.29E-05	9.8E-06
	13900	11400	6320	0.272	7580	5080	0.4	3.43E-05	5913	15.87	0.25	1.92E-04	0.93	0.70	615	0.87	3.0E-06	2.77E-05	2.31E-04	2.92E-05	3.36E-05	8.8E-06
	13900	11280	5820	0.243	8080	5460	0.4	3.11E-05	6333	15.63	0.24	2.24E-04	0.88	0.66	580	0.86	3.0E-06	2.96E-05	2.63E-04	3.26E-05	3.38E-05	7.9E-06
	13880	11160	5320	0.257	8560	5840	0.41	3.34E-05	6747	15.37	0.24	2.57E-04	0.91	0.62	545	0.83	3.0E-06	3.16E-05	2.97E-04	3.31E-05	3.60E-05	7.2E-06
	13850	11060	4820	0.272	9030	6240	0.41	3.60E-05	7170	15.10	0.24	2.93E-04	0.90	0.60	527	0.82	3.0E-06	3.36E-05	3.31E-04	3.43E-05	3.53E-05	6.5E-06
	13850	10960	4320	0.286	9530	6610	0.41	3.86E-05	7603	14.81	0.24	3.32E-04	0.88	0.57	501	0.80	3.0E-06	3.57E-05	3.69E-04	3.85E-05	3.58E-05	6.0E-06
	13820	10900	3820	0.286	10000	7080	0.41	3.94E-05	8053	14.53	0.23	3.71E-04	0.87	0.47	413	0.74	3.0E-06	3.79E-05	4.07E-04	3.81E-05	3.84E-05	5.5E-06
	13800	10795	3320	0.272	10480	7475	0.42	3.82E-05	8477	14.26	0.23	4.09E-04	0.86	0.43	378	0.71	3.0E-06	4.02E-05	4.48E-04	4.08E-05	3.96E-05	5.1E-06
	13800	10680	2820	0.300	10980	7860	0.42	4.30E-05	8900	13.96	0.23	4.52E-04	0.84	0.37	325	0.66	3.0E-06	4.26E-05	4.93E-04	4.45E-05	4.18E-05	4.8E-06
	13800	10620	2320	0.272	11480	8300	0.42	3.98E-05	9360	13.68	0.22	4.92E-04	0.83	0.34	299	0.64	3.0E-06	4.49E-05	5.39E-04	4.66E-05	4.30E-05	4.5E-06
	13750	10518	1820	0.272	11930	8698	0.42	4.06E-05	9775	13.41	0.22	5.33E-04	0.82	0.27	237	0.58	3.0E-06	4.75E-05	5.83E-04	4.37E-05	4.69E-05	4.3E-06
	13750	10425	1320	0.300	12430	9105	0.42	4.58E-05	10213	13.11	0.22	5.78E-04	0.81	0.23	202	0.53	3.0E-06	5.00E-05	6.33E-04	5.05E-05	4.97E-05	4.1E-06
	13750	10330	820	0.400	12930	9510	0.42	6.29E-05	10650	12.71	0.21	6.41E-04	0.78	0.18	168	0.48	3.0E-06	5.27E-05	6.86E-04	5.26E-05	5.43E-05	3.9E-06
	13700	10260	500	0.215	13200	9760	0.43	5.38E-05	10907	12.50	0.21	6.95E-04	0.78	0.16	141	0.45	3.0E-06	5.55E-05	7.15E-04	2.93E-05	5.67E-05	3.8E-06

APPENDIX D-4
STUDY NO. 4
BASIC ROCK PROPERTIES AND PORE COMPRESSIBILITY MEASUREMENTS

Sample ID	RAM PRESSURE	SLEEVE PRESSURE	PORE PRESSURE	Del (PORE - VOLUME)	NET STRESS	NET SLEEVE	POISSONS' RATIO	C(por-vol) 1/PSI	AVG NET STRESS	Vp **	POROSITY %	CUM Cf 1/PSI	Φ (MEAN)	NORMAL K (md)	K (md)	Jm	METHOD 1	Cf METHOD 2	CUM Cf. METHOD 3	Cf METHOD 3	Cf METHD 4	METHOD JONES'
3-KI5R	1000	1000	500	0.000	500		0.5		500	18.19	0.26			0.96	913							
	14133	12400	9820	0.000	4313	2580	0.37		3158	18.19	0.26	1.26E-05	1.00	1.00	961		1.3E-05	1.11E-05	1.67E-04		2.00E-05	1.8E-05
	11133	12323	9320	0.114	4813	3003	0.38	1.26E-05	3606	18.08	0.26	3.34E-05	0.99	1.06	1009	1.03	1.3E-05	1.28E-05	2.21E-04		1.84E-05	1.4E-05
	14133	12280	8820	0.186	5813	3460	0.39	2.08E-05	4078	17.89	0.26	5.20E-05	0.98	0.84	807	0.92	1.3E-05	1.43E-05	2.21E-04		2.54E-05	1.4E-05
	14133	12270	8320	0.165	5813	3990	0.4	1.86E-05	4571	17.73	0.25	8.32E-05	0.97	0.73	702	0.87	1.3E-05	1.59E-05	2.50E-04	2.90E-05	3.09E-05	1.2E-05
	14133	12160	7820	0.272	6313	4340	0.41	3.12E-05	4998	17.45	0.25	1.10E-04	0.96	0.93	894	0.98	1.3E-05	1.75E-05	2.80E-04	3.03E-05	2.11E-05	1.1E-05
	14133	12160	7320	0.229	6813	4840	0.42	2.66E-05	5498	17.22	0.25	1.40E-04	0.95	0.74	711	0.88	1.3E-05	1.91E-05	3.12E-04	3.16E-05	2.93E-05	9.3E-06
	14133	12090	6820	0.257	7313	5270	0.42	3.03E-05	5951	16.97	0.25	1.62E-04	0.95	0.75	721	0.89	1.3E-05	2.07E-05	3.45E-04	3.29E-05	2.84E-05	8.4E-06
	14133	12060	6320	0.186	7813	5740	0.42	2.22E-05	6431	16.78	0.24	1.85E-04	0.94	0.71	682	0.87	1.3E-05	2.23E-05	3.79E-04	3.42E-05	3.05E-05	7.5E-06
	14133	12000	5820	0.186	8313	6180	0.43	2.24E-05	6891	16.60	0.24	2.07E-04	0.93	0.79	759	0.92	1.3E-05	2.40E-05	4.16E-04	3.55E-05	2.56E-05	6.8E-06
	14133	11980	5320	0.186	8813	6660	0.43	2.27E-05	7378	16.41	0.24	2.34E-04	0.92	0.78	750	0.92	1.3E-05	2.57E-05	4.52E-04	3.69E-05	2.56E-05	6.2E-06
	14133	11920	4820	0.215	9313	7100	0.43	2.66E-05	7838	16.19	0.24	2.59E-04	0.91	0.73	702	0.90	1.3E-05	2.75E-05	4.90E-04	3.82E-05	2.79E-05	5.7E-06
	14133	11850	4320	0.200	9813	7530	0.43	2.50E-05	8291	15.99	0.23	2.88E-04	0.90	0.79	759	0.94	1.3E-05	2.92E-05	5.29E-04	3.95E-05	2.45E-05	5.3E-06
	14133	11840	3820	0.229	10313	8020	0.44	2.91E-05	8784	15.77	0.23	3.18E-04	0.89	0.70	673	0.89	1.3E-05	3.10E-05	5.70E-04	4.08E-05	2.88E-05	4.9E-06
	14133	11760	3320	0.229	10813	8440	0.44	2.95E-05	9231	15.54	0.23	3.49E-04	0.88	0.70	673	0.89	1.3E-05	3.29E-05	6.12E-04	4.21E-05	2.82E-05	4.6E-06
	14133	11720	2820	0.243	11313	8900	0.44	3.18E-05	9704	15.29	0.23	3.76E-04	0.87	0.70	673	0.90	1.3E-05	3.47E-05	6.56E-04	4.34E-05	2.79E-05	4.3E-06
	14133	11680	2320	0.210	11813	9340	0.44	2.85E-05	10178	15.08	0.22	4.13E-04	0.86	0.65	626	0.87	1.3E-05	3.67E-05	7.00E-04	4.47E-05	3.05E-05	4.1E-06
	14133	11650	1820	0.257	12313	9830	0.44	3.47E-05	10658	14.82	0.22	4.52E-04	0.84	0.60	577	0.84	1.2E-05	3.88E-05	7.46E-04	4.60E-05	3.35E-05	3.9E-06
	14133	11640	1320	0.286	12813	10320	0.45	3.94E-05	11151	14.54	0.22	4.80E-04	0.84	0.55	529	0.81	1.2E-05	4.09E-05	7.94E-04	4.73E-05	3.77E-05	3.8E-06
	14133	11590	820	0.200	13313	10770	0.45	2.79E-05	11618	14.34	0.22	5.21E-04	0.83	0.57	548	0.83	1.2E-05	4.31E-05	8.26E-04	3.10E-05	3.62E-05	3.7E-06
	14133	11540	500	0.186	13633	11040	0.45	4.11E-05	11904	14.15	0.21											
4-KI5R	1000	1000	500	0.000	500	500	0.5		500	23.32	0.28			1.00	3624							
	14250	12135	9240	0.300	5010	2895	0.37	2.25E-05	3600	23.02	0.28	6.02E-05	0.99	0.84	3044	0.92	2.2E-05	3.00E-05	4.12E-05	4.12E-05	2.69E-05	1.5E-05
	14250	12000	8820	0.358	5430	3180	0.37	3.77E-05	3930	22.66	0.28	8.71E-05	0.98	0.84	3044	0.93	2.2E-05	3.13E-05	5.94E-05	1.82E-05	2.64E-05	1.3E-05
	14250	11780	8320	0.300	5930	3460	0.37	2.69E-05	4283	22.36	0.27	1.14E-04	0.97	0.89	3226	0.96	2.2E-05	3.26E-05	8.01E-05	2.07E-05	2.34E-05	1.2E-05
	14250	11600	7820	0.300	6430	3780	0.37	2.72E-05	4663	22.06	0.27	1.47E-04	0.96	0.89	3226	0.96	2.2E-05	3.39E-05	1.03E-04	2.32E-05	2.30E-05	1.0E-05
	14250	11410	7320	0.358	6930	4090	0.37	3.30E-05	5037	21.70	0.27	1.81E-04	0.95	0.70	2537	0.86	2.2E-05	3.52E-05	1.26E-04	2.30E-05	3.46E-05	9.2E-06
	14200	11300	6820	0.358	7380	4480	0.38	3.35E-05	5447	21.35	0.27	2.12E-04	0.94	0.70	2537	0.86	2.2E-05	3.67E-05	1.54E-04	2.79E-05	3.39E-05	8.2E-06
	14200	11160	6320	0.329	7880	4840	0.38	3.12E-05	5853	21.02	0.26	2.45E-04	0.93	0.71	2573	0.88	2.2E-05	3.82E-05	1.81E-04	2.72E-05	3.23E-05	7.5E-06
	14150	11020	5820	0.343	8330	5200	0.38	3.32E-05	6243	20.67	0.26	2.73E-04	0.91	0.76	2754	0.91	2.2E-05	3.97E-05	2.14E-04	3.26E-05	2.80E-05	6.8E-06
	14150	10930	5320	0.286	8830	5610	0.39	2.81E-05	6683	20.39	0.26	3.08E-04	0.90	0.76	2754	0.92	2.2E-05	4.14E-05	2.49E-04	3.51E-05	2.74E-05	6.2E-06
	14150	10720	4820	0.343	9330	5900	0.39	3.42E-05	7043	20.04	0.25	3.41E-04	0.89	0.73	2646	0.90	2.2E-05	4.30E-05	2.87E-04	3.76E-05	2.88E-05	5.7E-06
	14150	10640	4320	0.329	9830	6320	0.39	3.34E-05	7490	19.72	0.25	3.72E-04	0.88	0.67	2428	0.87	2.2E-05	4.47E-05	3.23E-04	3.59E-05	3.30E-05	5.3E-06
	14100	10490	3820	0.300	10280	6670	0.39	3.09E-05	7873	19.42	0.25	4.06E-04	0.87	0.67	2428	0.88	2.2E-05	4.65E-05	3.65E-04	4.23E-05	3.22E-05	4.9E-06
	14100	10400	3320	0.329	10780	7080	0.4	3.45E-05	8313	19.09	0.24	4.45E-04	0.86	0.62	2247	0.85	2.2E-05	4.83E-05	4.05E-04	4.02E-05	3.63E-05	4.6E-06
	14050	10290	2820	0.358	11230	7470	0.4	3.82E-05	8723	18.73	0.24	5.08E-04	0.84	0.64	1957	0.80	2.2E-05	5.02E-05	4.47E-04	4.22E-05	4.45E-05	4.4E-06
	14000	10200	2320	0.572	11680	7880	0.4	6.30E-05	9147	18.16	0.24	5.83E-04	0.81	0.49	1776	0.78	2.2E-05	5.22E-05	4.96E-04	4.92E-05	5.03E-05	4.2E-06
	14000	10070	1820	0.659	12180	8250	0.4	7.53E-05	9560	17.50	0.23	6.42E-04	0.80	0.43	1558	0.73	2.2E-05	5.43E-05	5.38E-04	4.12E-05	6.12E-05	4.0E-06
	13900	9970	1320	0.501	12580	8650	0.41	5.90E-05	9960	17.00	0.22	7.03E-04	0.78	0.34	1232	0.66	2.2E-05	5.63E-05	5.91E-04	5.37E-05	9.00E-05	3.8E-06
	13900	9880	820	0.501	13080	9060	0.41	6.07E-05	10400	16.50	0.22	9.49E-04	0.74	0.24	870	0.57	2.2E-05	5.86E-05	6.16E-04	2.44E-05	1.63E-04	3.6E-06
	13800	9670	500	1.202	13300	9170	0.41	2.46E-04	10547	15.29	0.21							5.97E-05				

APPENDIX D-4
STUDY NO. 4
BASIC ROCK PROPERTIES AND PORE COMPRESSIBILITY MEASUREMENTS

Sample ID	RAM PRESSURE	SLEEVE PRESSURE	PORE PRESSURE	Del (PORE - VOLUME)	NET STRESS	NET SLEEVE	POISSONS' RATIO	C(por-vol) 1/PSI	AVG NET STRESS	Vp ee	POROSITY %	CUM Cf 1/PSI	Φ (MEAN)	NORMAL K (md)	K (md)	Jm	METHOD 1	Cf METHOD 2	CUM Cf. METHOD 3	Cf METHOD 3	Cf METHD 4	METHOD JONES'
5-KISR	14110	123320	9810	0.000	4300	2510	0.37	0.00E+00	3107	21.31	0.26	6.99E-05	0.96	0.60	769		3.0E-06	3.33E-05	1.07E-04	6.56E-06	3.02E-05	8.0E-06
	14100	11940	8000	1.087	6100	3940	0.39	2.96E-05	4660	20.22	0.25	9.40E-05	0.91	0.67	731	0.79	3.0E-06	4.23E-05	1.72E-04	6.50E-05	3.01E-06	6.5E-06
ka =	14020	11630	6000	1.158	8020	5630	0.41	3.03E-05	6427	19.06	0.24	1.33E-04	0.88	0.48	615	0.74	3.0E-06	5.17E-05	2.06E-04	3.40E-05	3.42E-05	4.6E-06
1282.23	14000	10880	4000	1.216	10000	6880	0.41	3.41E-05	7920	17.85	0.22	1.70E-04	0.86	0.41	526	0.69	2.9E-06	5.72E-05	2.41E-04	3.64E-05	3.82E-05	4.3E-06
	13950	10310	3000	0.673	10950	7310	0.4	3.92E-05	8523	17.17	0.22	2.16E-04	0.83	0.33	423	0.63	2.9E-05	6.16E-05	2.77E-04	3.55E-05	4.52E-05	3.9E-06
	13800	9760	1910	0.656	11890	7850	0.4	3.64E-05	9197	16.52	0.21	2.70E-04	0.81	0.30	385	0.61	2.9E-05	6.77E-05	2.90E-04	1.34E-05	4.81E-06	3.8E-06
	13800	9630	1010	0.657	12790	8620	0.4	4.60E-05	10010	15.86	0.21					#DIV/0!		7.11E-05				
	13620	9440	500	0.429	13120	8940	0.41	5.45E-05	10333	15.43	0.20			1.12	1178	#DIV/0!			-6.00E-06			
														1.05	1105				1.39E-04	1.39E-04		
6-KISR	1000	1000	500	0.000	500	500	0.5		500	19.83	0.22	1.97E-06	1.00	1.03	1084		2.0E-06		1.58E-04	1.91E-05	1.97E-06	1.8E-05
	14100	12380	9800	0.000	4300	2580	0.38		3153	19.83	0.22	4.21E-05	1.00	0.98	1031		2.0E-06	1.79E-05	1.75E-04	1.64E-05	2.01E-05	1.6E-05
ka =	14100	12340	9320	0.166	4780	3020	0.39	1.97E-05	3607	19.64	0.22	6.06E-05	0.99	1.02	1073	1.02	2.0E-06	1.81E-05	1.96E-04	2.18E-06	1.97E-06	1.4E-06
1052	14050	12310	8860	0.200	5190	3450	0.4	2.24E-05	4030	19.44	0.22	7.98E-05	0.98	0.97	1020	0.99	2.0E-06	1.82E-05	2.15E-04	1.88E-05	2.01E-05	1.2E-06
	14050	12270	8320	0.172	5730	3950	0.41	1.65E-05	4543	19.27	0.22	9.80E-05	0.97	0.96	999	0.99	2.0E-05	1.84E-05	2.37E-04	2.22E-05	2.02E-06	1.1E-06
	14050	12240	7860	0.186	6190	4380	0.41	2.12E-05	4983	19.08	0.21	1.17E-04	0.96	1.00	1052	1.02	2.0E-06	1.85E-05	2.59E-04	2.16E-05	1.97E-06	9.5E-06
	14050	12205	7320	0.186	6730	4885	0.42	1.82E-05	5500	18.90	0.21	1.41E-04	0.96	1.03	1084	1.04	2.0E-06	1.87E-05	2.77E-04	1.76E-05	1.94E-06	8.6E-06
	14050	12180	6800	0.186	7250	5380	0.43	1.91E-05	6003	18.71	0.21	1.61E-04	0.95	0.89	936	0.97	2.0E-05	1.88E-05	3.00E-04	2.32E-05	2.06E-05	7.7E-06
	14050	12150	6380	0.186	7670	5770	0.43	2.39E-05	6403	18.53	0.21	1.73E-04	0.94	0.83	873	0.94	2.0E-06	1.90E-05	3.20E-04	2.00E-05	2.11E-06	7.0E-06
	14050	12130	5830	0.200	8220	6300	0.43	1.98E-05	6940	18.33	0.21	1.93E-04	0.94	0.81	862	0.93	2.0E-06	1.91E-05	3.40E-04	2.02E-05	2.13E-06	6.4E-06
	14000	11900	5310	0.114	8690	6590	0.43	1.20E-05	7290	18.21	0.21	2.16E-04	0.93	0.71	747	0.87	2.0E-06	1.93E-05	3.61E-04	2.06E-05	2.25E-06	6.9E-06
	14000	11880	4840	0.172	9160	7040	0.43	2.03E-05	7747	18.04	0.20	2.37E-04	0.92	0.75	789	0.90	1.9E-06	1.94E-05	3.83E-04	2.27E-05	2.18E-06	6.4E-06
	14000	11870	4360	0.186	9640	7510	0.44	2.17E-05	8220	17.85	0.20	2.58E-04	0.91	0.70	736	0.88	1.9E-06	1.96E-06	4.05E-04	2.16E-05	2.24E-06	5.0E-06
	14000	11860	3840	0.200	10160	8020	0.44	2.18E-05	8733	17.65	0.20	2.81E-04	0.90	0.66	694	0.85	1.9E-06	1.98E-05	4.28E-04	2.26E-05	2.29E-05	4.7E-06
	14000	11840	3350	0.186	10650	8490	0.44	2.17E-05	9210	17.47	0.20	3.02E-04	0.89	0.62	662	0.83	1.9E-06	2.00E-05	4.50E-04	2.28E-05	2.34E-06	4.4E-06
	14000	11820	2840	0.200	11160	8980	0.45	2.27E-05	9707	17.27	0.20	3.24E-04	0.89	0.60	631	0.82	1.9E-06	2.01E-05	4.73E-04	2.26E-05	2.37E-05	4.2E-06
	14000	11820	2330	0.186	11670	9490	0.45	2.14E-05	10217	17.08	0.20	3.52E-04	0.98	0.67	600	0.80	1.9E-06	2.03E-05	4.94E-04	2.14E-05	2.41E-05	4.0E-06
	14000	11810	1830	0.186	12170	9980	0.45	2.20E-05	10710	16.90	0.19	3.75E-04	0.87	0.47	494	0.73	1.9E-06	2.07E-05	5.18E-04	2.38E-05	2.60E-05	3.6E-06
	14000	11785	1360	0.215	12640	10425	0.45	2.74E-05	11633	16.68	0.19	4.03E-04	0.87	0.43	462	0.70	1.9E-06	2.07E-05	5.32E-04	1.43E-06	2.70E-05	3.7E-06

APPENDIX E-1

Sample Calculations - Method No. 1

APPENDIX. E-1

SAMPLE CALCULATIONS

METHOD NO. 1

STUDY NO. 1 SAMPLE 2 IS USED FOR SAMPLE CALCULATION.

NET-STRESS PSI	POROSITY %	NORMALIZED POROSITY	Cf 1/PSI MEASURED	Cf 1/PSI PREDICTED	% DIFFERENCE
800	16.2	***	***	***	
3652	15.2	1.00	2.53E-05	2.53E-05	0%
4271	15.0	0.99	2.29E-05	1.94E-05	15%
4581	15.0	0.99	1.76E-05	1.91E-05	-9%
4890	14.9	0.98	1.96E-05	1.66E-05	15%
5200	14.8	0.97	1.44E-05	1.44E-05	0%
5819	14.7	0.97	1.17E-05	1.25E-05	-8%

Net Stress = Net Radial - Net Axial
= (Axial stress - confining pressure) - (Axial stress - pore pressure)

Calculation Procedure:

1) Plot normalized porosity vs. net stress.

2) Best fit the data with a power law equation

Y = aX^b

Y = 22.25 (X) ^ -0.0472

where b is the power exponent, Y = porosity, and X = Net Stress.

b = -0.0472

-1/b = 21.19

3) Calculate pore volume compressibility, @ 4890 psi

cf 1/psi (predicted) = cfi * (porosity)^ (-1/b)

cf (4890) = 2.53E-6*(0.98)^21. 1.65E-06 1/psi

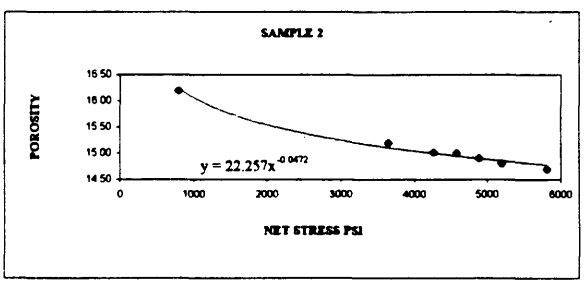

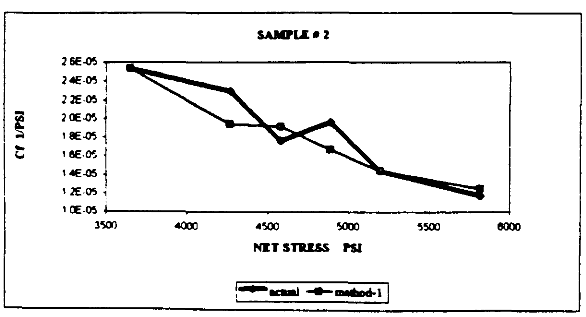

APPENDIX E-2

Sample Calculations - Method No. 2

APPENDIX E-2

SAMPLE CALCULATIONS

METHOD NO. 2

STUDY NO. 2, SAMPLE 14915.5 IS USED FOR SAMPLE CALCULATION.

NET STRESS PSI	POROSITY %	cf 1/psi MEASURED	cf 1/psi PREDICTED	% DIFFERENCE
3158	26.8	2.60E-05	1.56E-05	40%
3658	26.5	2.50E-05	1.72E-05	31%
4158	26.3	2.26E-05	1.88E-05	17%
7357	24.9	2.58E-05	2.99E-05	-16%
7823	24.6	2.91E-05	3.16E-05	-9%
8270	24.4	3.26E-05	3.32E-05	-2%
8703	24.1	3.01E-05	3.49E-05	-16%
9130	23.8	3.36E-05	3.67E-05	-9%
9563	23.5	3.42E-05	3.83E-05	-12%
9963	23.2	3.48E-05	4.00E-05	-15%
10357	22.9	3.54E-05	4.16E-05	-18%
10723	22.6	6.14E-05	4.31E-05	30%
11030	22.0	7.03E-05	4.44E-05	37%

Calculation Procedure:

1) Plot porosity vs. net stress
2) For consolidated sand, a power law equation best fit the data, and for unconsoliadted sand, a polynomial equation is more representitive.
   Usually three or four porosity points are enough to establish the polynomial equation.

$$Y = aX^2 + bX + c$$

$$Y = -4E\text{-}8X^2 + 2E\text{-}5X + 27.022$$

where Y = porosity, and X = net stress.

3) Calculate pore compressibility.

Predicted cf = -(f-1)/f * d(-f/(f-1))/dp

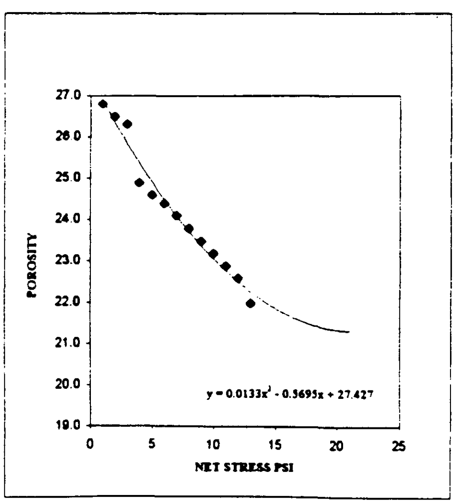

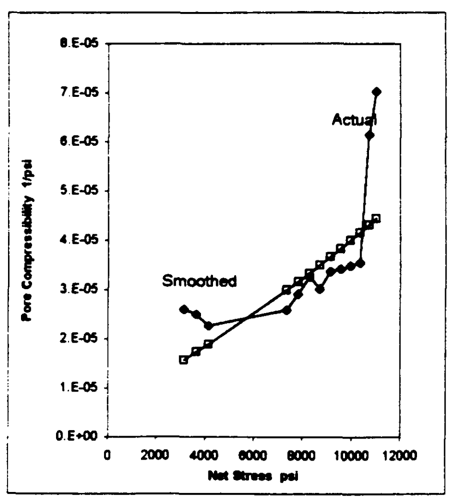

APPENDIX E-3

Sample Calculations - Method No. 3

APPENDIX E-3

SAMPLE CALCULATIONS

METHOD NO. 3

STUDY NO. 4, SAMPLE 2-KISR IS USED FOR SAMPLE CALCULATION.

Net Stress psi	POROSITY (F) %	(Fi-F)/Fi	cf 1/psi MEASURED	ccf 1/psi MEASURED	ccf 1/psi PREDICTED	cf 1/psi PREDICTED	% cf DIFFERENCE	% ccf DIFFERENCE
2855	0.267	0.00	3.03E-05	3.03E-05	3.00E-05	3.00E-05	1%	1%
5180	0.263	0.01	3.50E-05	6.53E-05	6.15E-05	3.15E-05	10%	6%
5640	0.261	0.02	2.54E-05	9.07E-05	9.37E-05	3.22E-05	-27%	-3%
6140	0.258	0.03	2.74E-05	1.18E-04	1.27E-04	3.34E-05	-22%	-8%
6640	0.255	0.04	3.31E-05	1.51E-04	1.62E-04	3.45E-05	-4%	-7%
7100	0.252	0.06	3.72E-05	1.88E-04	1.97E-04	3.56E-05	4%	-5%
7580	0.248	0.07	3.43E-05	2.23E-04	2.34E-04	3.71E-05	-8%	-5%
8080	0.236	0.12	3.11E-05	2.54E-04	2.76E-04	4.16E-05	-34%	-9%
8560	0.243	0.09	3.34E-05	2.87E-04	3.15E-04	3.90E-05	-17%	-10%
9030	0.239	0.10	3.60E-05	3.23E-04	3.55E-04	4.05E-05	-12%	-10%
9530	0.236	0.12	3.86E-05	3.62E-04	3.97E-04	4.16E-05	-8%	-10%
10000	0.232	0.13	3.94E-05	4.01E-04	4.40E-04	4.31E-05	-9%	-10%
10480	0.229	0.14	3.82E-05	4.39E-04	4.84E-04	4.42E-05	-16%	-10%
10980	0.225	0.16	4.30E-05	4.82E-04	5.30E-04	4.57E-05	-6%	-10%
11480	0.222	0.17	3.98E-05	5.22E-04	5.77E-04	4.69E-05	-18%	-10%
11930	0.218	0.18	4.06E-05	5.63E-04	6.25E-04	4.84E-05	-19%	-11%
12430	0.215	0.19	4.58E-05	6.09E-04	6.75E-04	4.95E-05	-8%	-11%
12930	0.209	0.22	6.29E-05	6.72E-04	7.27E-04	5.17E-05	18%	-8%
13200	0.207	0.22	5.38E-05	7.25E-04	7.79E-04	5.25E-05	2%	-7%

Calculation Procedure:

1) Calculate the void ratio from porosity

void ratio = (fi - f) / fi

2) Plot void ratio vs three or more points of the cumulative compressibility
3) Fit the data with straight line equation Y = mX + b
Equation of line Y = 0.0001X + 3E-5 where Y= ccf and X = void ratio

4) Calculate cumulative pore volume compressibility (ccf) for values at higher stress
porosity at higher stress can be obtained from power law equation
as discussed earlier.

ccf = 0.0001(void ratio) + 3E-5 @ 5640 psi
ccf =0.0001*0.02+3E-5 = 3.22E-05

5) Calculate cf from ccf.

ccf (2885) = 3.00E-05 1/psi
ccf (5180) = 6.15E-05 1/psi
ccf (5640) = 9.37E-05 1/psi

cf (2885) = 3.00E-05 1/psi
cf (5180) =ccf(5180)-ccf(2885)= 3.15E-05 1/psi
cf(5640) = ccf(5640) - ccf(5180) - ccf(2885) = 3.22E-05 1/psi

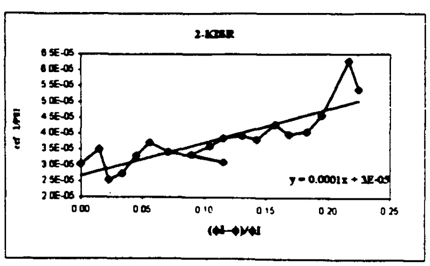

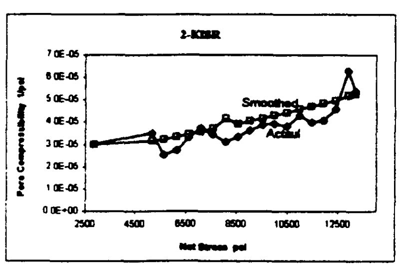

APPENDIX E-4

Sample Calculations - Method No. 4

APPENDIX E-4

SAMPLE CALCULATIONS

METHOD NO. 4

STUDY NO. 2, SAMPLE 14916.5 IS USED FOR SAMPLE CALCULATION.

Net Stress psi	Jm	cf 1/psi MEASURED	cf 1/psi PREDICTED	% DIFFERENCE
3463	1.01	3.03E-05	2.97E-05	2%
3857	0.96	3.50E-05	3.11E-05	12%
4280	0.92	2.54E-05	3.20E-05	-21%
4703	0.92	2.74E-05	3.21E-05	-15%
5080	0.87	3.31E-05	3.37E-05	-2%
5500	0.90	3.71E-05	3.28E-05	13%
5913	0.87	3.43E-05	3.36E-05	2%
6333	0.85	3.11E-05	3.43E-05	-9%
6747	0.83	3.34E-05	3.50E-05	-5%
7170	0.82	3.60E-05	3.51E-05	2%
7603	0.81	3.86E-05	3.56E-05	8%
8053	0.73	3.94E-05	3.85E-05	2%
8477	0.71	3.83E-05	3.96E-05	-3%
8900	0.66	4.30E-05	4.19E-05	3%
9360	0.64	3.98E-05	4.30E-05	-7%
9775	0.58	4.06E-05	4.68E-05	-13%
10213	0.54	4.58E-05	4.97E-05	-8%
10650	0.49	6.29E-05	5.38E-05	17%
10907	0.46	5.38E-05	5.66E-05	-5%

Predict cf 1/psi from Jm vs. cf power law equation to smooth data

Calculation Procedure

1) Calculate Jm

$$Jm = (Km/\phi m)^{0.5}$$

2) Plot Jm vs. Stress to estimate values at higher stress.

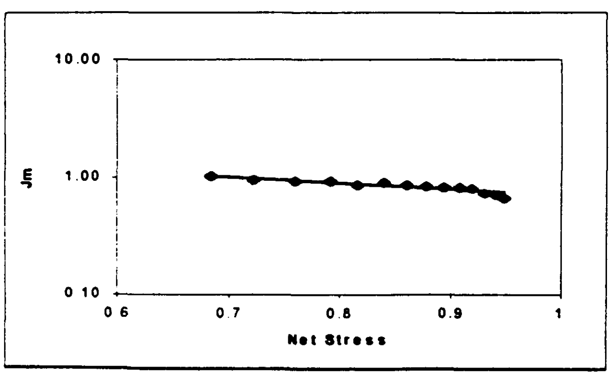

ARTHUR LAKES LIBRARY
COLORADO SCHOOL OF MINES
GOLDEN, CO 80401

3) Plot Jm vs. pore compressibility

Usually three or more compressibility points are recommended to plot against Jm.

4) Fit the data with a power law equation

Y = aX^b
Y=3E-5*X^(-0.812)
where Y = pore compressibility, and X = Jm

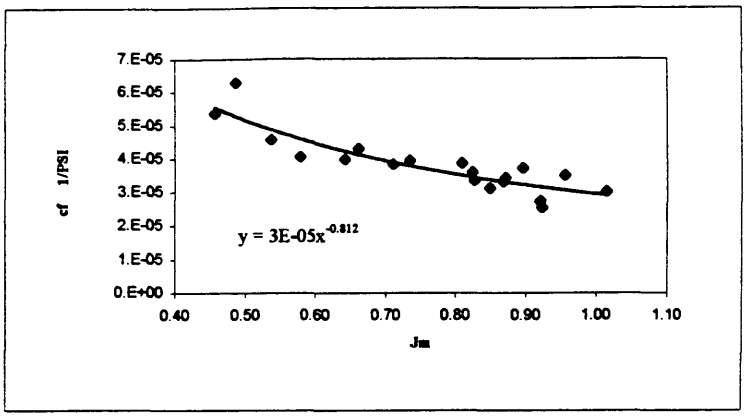

5) From the power law equation, compressibility data can be smoothed, and values at higher stress can be predicted. Only four compressibility points were used to smooth data.

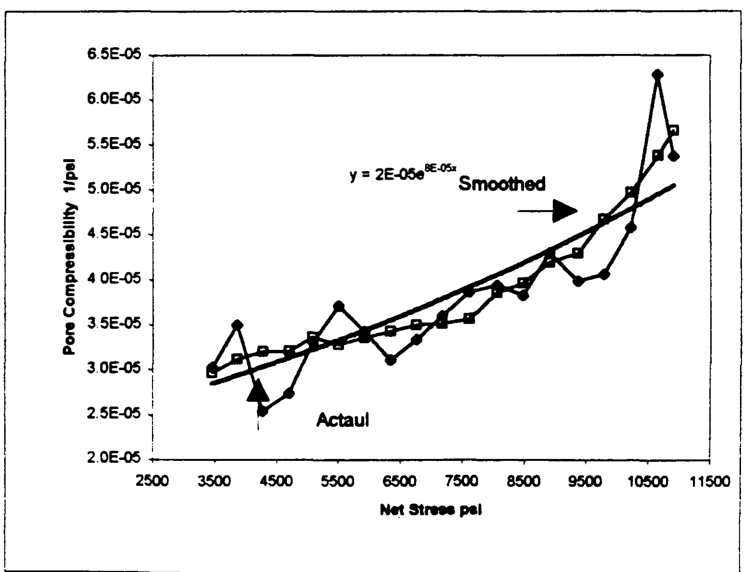

APPENDIX E-5

Sample Calculations - Jones' Method

APPENDIX E-5

SAMPLE CALCULATIONS

Jones' Method

STUDY NO. 1, SAMPLE 2 IS USED FOR SAMPLE CALCULATIONS

VP cc	1-EXP(-STRS/3000)	Vp(1+C*STRS)	Cf 1/PSI MEASURED	Cf 1/PSI PREDICTED	% DIFFERENCE
3.08	0.23	3.085	***		
2.89	0.70	2.920	2.53E-05	2.56E-05	-1%
2.85	0.76	2.888	2.29E-05	2.14E-05	7%
2.85	0.78	2.889	1.76E-05	1.96E-05	-10%
2.83	0.80	2.873	1.96E-05	1.79E-05	9%
2.81	0.82	2.856	1.44E-05	1.65E-05	-12%
2.79	0.86	2.842	1.17E-05	1.39E-05	-16%

Calculation Procedure:

1) Plot Vp(1+C*strs) vs. 1-exp(-strs/3000) in a semi-log plot, where strs = net stress
2) Calculate the slope of the line av

av = - (SLOPE = -0.2292) = 0.2292

3) Calculate pore compressibility from Jone' @ 4890 psi

cf = [av*EXP(-STRS/3000)]/3000 + 3E-6/(1 + STRS*3E-6)

cf (4890) =(0.2292*exp(-4890/3000))/3000 + 3E-6/(1+ 4890 * 3E-6)

cf (4890) = 1.79E-05